

CA.2.142-1886

C.2

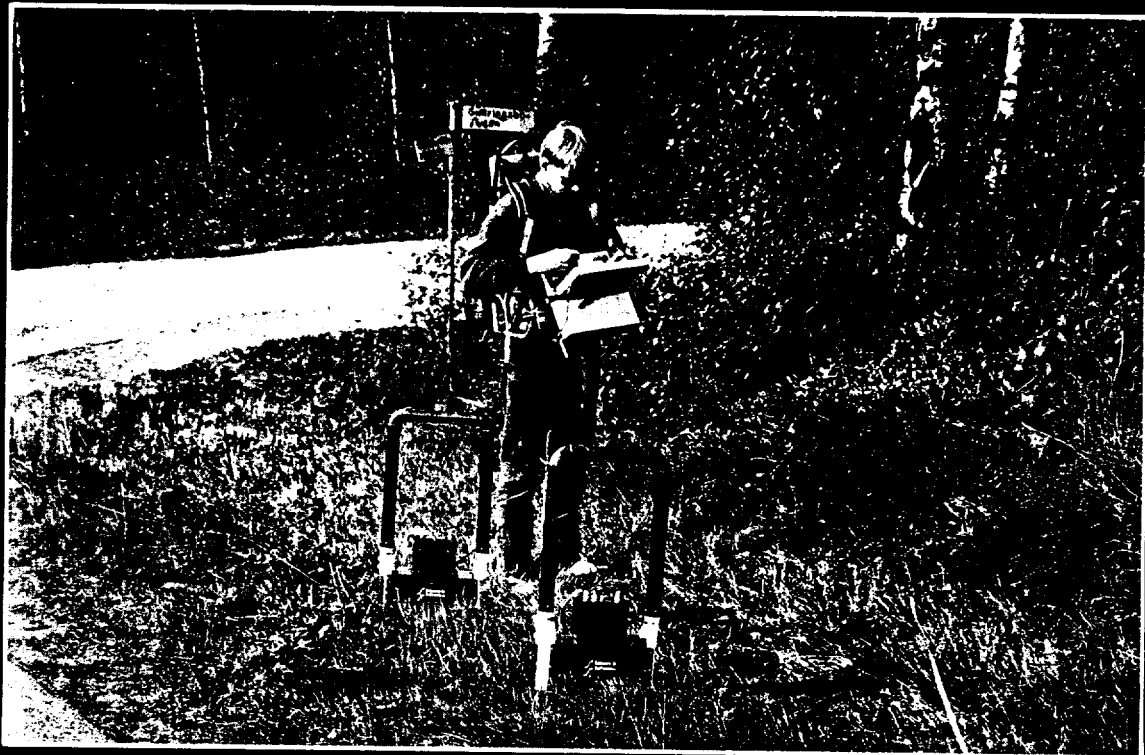


GEOLOGICAL SURVEY OF CANADA
PAPER 90-4

GROUND PENETRATING RADAR

edited by

J.A. Pilon



1992



Energy, Mines and
Resources Canada

Énergie, Mines et
Ressources Canada



Canada

THE ENERGY OF OUR RESOURCES

THE POWER OF OUR IDEAS

©Minister of Supply and Services Canada 1992

Available in Canada through authorized
bookstore agents and other bookstores

or by mail from

Canada Communication Group — Publishing
Ottawa, Canada K1A 0S9

and from

Geological Survey of Canada offices:

601 Booth Street
Ottawa, Canada K1A 0E8

3303-33rd Street N.W.,
Calgary, Alberta T2L 2A7

100 West Pender Street
Vancouver, B.C. V6B 1R8

A deposit copy of this publication is also available for
reference in public libraries across Canada

Cat. No. M44-90/4E
ISBN 0-660-14538-3

Price subject to change without notice

Cover description

Ground Penetrating Radar survey in Sweden to
determine depth to bedrock. (Photo courtesy Sensors
and Software Inc.)

Original manuscript received: 1990 - 12
Final version approved for publication: 1991 - 09

CONTENTS

- 1 J.A. PILON, M.J. BERRY, and L.S. COLLETT
Introductory remarks
- 5 A.P. ANNAN and L.T. CHUA
Ground penetrating radar performance predictions
- 15 A.P. ANNAN and J.L. DAVIS
Design and development of a digital ground penetrating radar system
- 25 S.A. ARNONE, A.J. DELANEY, and R.H. WILLS
Helicopter-borne alpine glacier surveys using short pulse radar
- 33 C.R. CARTER, T. CHUNG, T. MASLIWEC, and D.G. MANNING
Analysis of radar reflections from asphalt covered bridge deck structures
- 41 S.R. DALLIMORE and J.L. DAVIS
Ground penetrating radar investigations of massive ground ice
- 49 J.L. DAVIS and A.P. ANNAN
Applications of ground penetrating radar to mining, groundwater, and geotechnical projects:
selected case histories
- 57 A.W. ENGLAND
The fractal dimension of diverse topographies and the effect of spatial windowing
- 63 J.M. GLOVER
Void detection using standing wave analysis
- 75 J.M. GLOVER and H.V. REES
Radar investigations of firm structures and crevasses
- 85 A.L. HOLLOWAY
Fracture mapping in granite rock using ground probing radar
- 101 R.W. JACOBEL, S.K. ANDERSON, and D.F. RIOUX
A microprocessor based ice-radar system for surface profiling
- 107 K.C. JEZEK, S.A. ARNONE, S. DALY, and R.H. WILLS
Impulse radar studies of interface roughness
- 117 A. KOVACS and R.M. MOREY
Estimating sea ice thickness from impulse radar sounding time of flight data
- 125 S. LEE, E. MILIOS, R. GREINER, and J. ROSSITER
An expert system for automated interpretation of ground penetrating radar data
- 133 D.C. NOBES and B.G. WARNER
Application of ground penetrating radar to a study of peat stratigraphy: preliminary results
- 139 O. OLSSON, P. ANDERSON, S. CARLSTEN, L. FALK, B. NIVA, and E. SANDBERG
Fracture characterization in crystalline rock by borehole radar
- 151 G.K.A. OSWALD
Radar design for geophysical sounding

- 165 | J.A. PILON, M. ALLARD, and M.K. SÉGUIN
Ground probing radar in the investigation of permafrost and subsurface characteristics of surficial deposits in Kangiqsualujjuaq, northern Quebec
- 177 | J.A. PILON, R.A.F. GRIEVE, V. SHARPTON, J. CODERRE, and J. KENNEDY
Reconnaissance ground penetrating radar survey of the interior of Meteor Crater, Arizona
- 187 | H.V. REES and J.M. GLOVER
Digital enhancement of ground probing radar data
- 193 | D. RODDY
Cepstral analysis of subsurface data
- 199 | J.R. ROSSITER, E.M. REIMER, L. LALUMIERE, and D.R. INKSTER
Radar cross-section of fish at VHF
- 203 | K.B. STRONGMAN
Forensic applications of ground penetrating radar
- 213 | L.G. THOMPSON
Interpretation of short-pulse radar soundings from low latitude, high altitude glaciers of Peru and China
- 227 | J.P. TODOESCHUCK, P.T. LAFLÈCHE, O.G. JENSEN, A.S. JUDGE, and J.A. PILON
Deconvolution of ground probing radar data
- 231 | R.H. WILLS
A digital phase coded ground probing radar
- 236 | List of participants

Design and development of a digital ground penetrating radar system

A.P. Annan¹ and J.L. Davis²

Annan, A.P. and Davis, J.L., 1992: *Design and development of a digital ground penetrating radar system*; in *Ground penetrating radar*, ed. J. Pilon; Geological Survey of Canada, Paper 90-4, p. 15-23.

Abstract

Extensive evaluation of the potential applications for ground penetrating radar (GPR) during the 1970s by the Geological Survey of Canada led to the conclusions that the expansion of the GPR method was limited by

- *instrument portability,*
- *instrument sensitivity, and*
- *inability to apply seismic-like processing.*

In 1981, A-Cubed Inc. embarked on a program to develop technology to put in place a GPR system that would overcome these limitations. A joint project between the Geological Survey of Canada and A-Cubed Inc. began in 1983 and led to the introduction of the pulseEKKO III system in 1986. In this paper, we present the design philosophy and principles underlying discrete measurement techniques accompanied by examples of field results.

Résumé

L'évaluation importante des applications potentielles du géoradar à laquelle s'est livrée la Commission géologique du Canada au cours des années 1970 a permis d'établir que l'adoption accrue des méthodes liées à l'utilisation du géoradar était limitée par :

- *la portabilité de l'instrument*
- *la sensibilité de l'instrument, et*
- *l'incapacité d'appliquer un traitement de type sismique.*

En 1981, la société A-Cubed Inc. a entrepris un programme technologique pour mettre en place un système géoradar qui permettrait de surmonter ces limites. Un projet mis en oeuvre conjointement par la Commission géologique du Canada et A-Cubed Inc. en 1983 a mené à l'introduction du système pulseEKKO III en 1986. Dans le présent document, la philosophie et les principes de conception sous-jacents à certaines techniques de mesure sont présentés, appuyés par des résultats recueillis sur le terrain.

¹ Sensors & Software Inc., 5566 Tomken Road, Mississauga, Ontario L4W 1P4

² Formerly A-Cubed Inc., now at Canpolar Inc., 265 Rimrock Rd., Toronto, Ont. M3J 3C6

INTRODUCTION

The pulseEKKO III system developed by A-Cubed Inc. represents the culmination of a decade of effort in developing a precision instrument for ground penetrating radar (GPR) applications. Initial work in ground penetrating radar, which was carried out by the Geological Survey of Canada from 1974 to 1980 (Annan and Davis, 1976), was conducted in a wide variety of environments. The primary application was geological sounding to look for relatively deep structure. Structure that was near surface (1-3 m) was felt to be of little significance in the early stages of the work simply because such structure could be easily excavated. The objective was to develop a system that could penetrate to tens of metres in a favourable environment with 1-2 m resolution.

The initial conceptual work for the pulseEKKO III system evolved from use of a GSSI-SIR system (Morey, 1974) in a wide variety of geological settings. The weight, bulk, and power requirements of that system precluded the use of radar being viable in some applications. Quantitative interpretation was not usually possible given the data format. Considerable effort was expended to define an optimal configuration for a geological sounding radar system. A primary goal was to design the system to collect data digitally and thus to exploit existing seismic processing and computer technologies.

A team and the resources to achieve this objective were assembled in 1983. The pulseEKKO III system was subsequently developed by A-Cubed Inc. with the first prototype being delivered to the Geological Survey of Canada in 1986. This paper provides insight into the development of the system and design trade-offs.

DESIGN SPECIFICATIONS

As general goals, the radar system being developed had provide the following capabilities:

1. It had to be lightweight, battery powered, and ve portable.

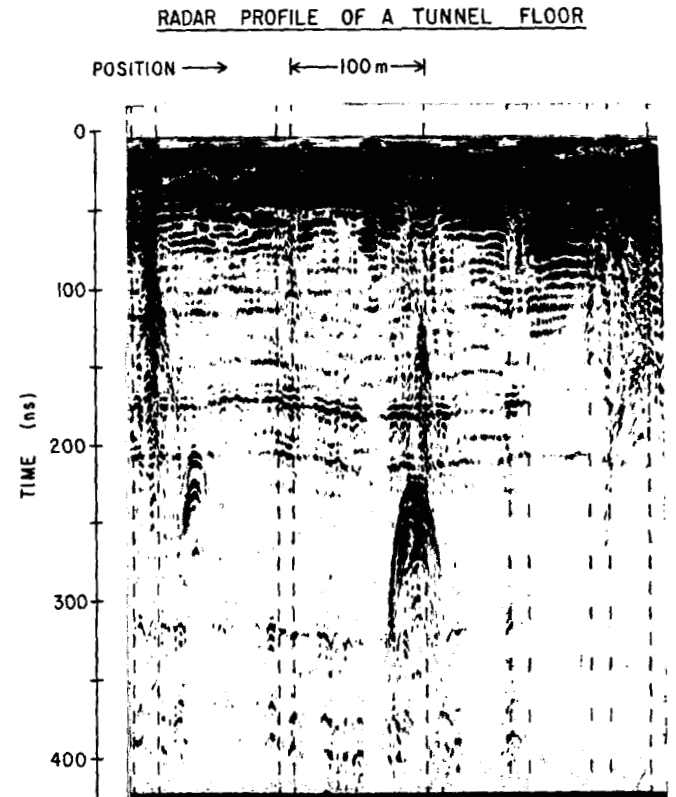


Figure 1. Example of continuous mode radar profiling section obtained in a potash mine.

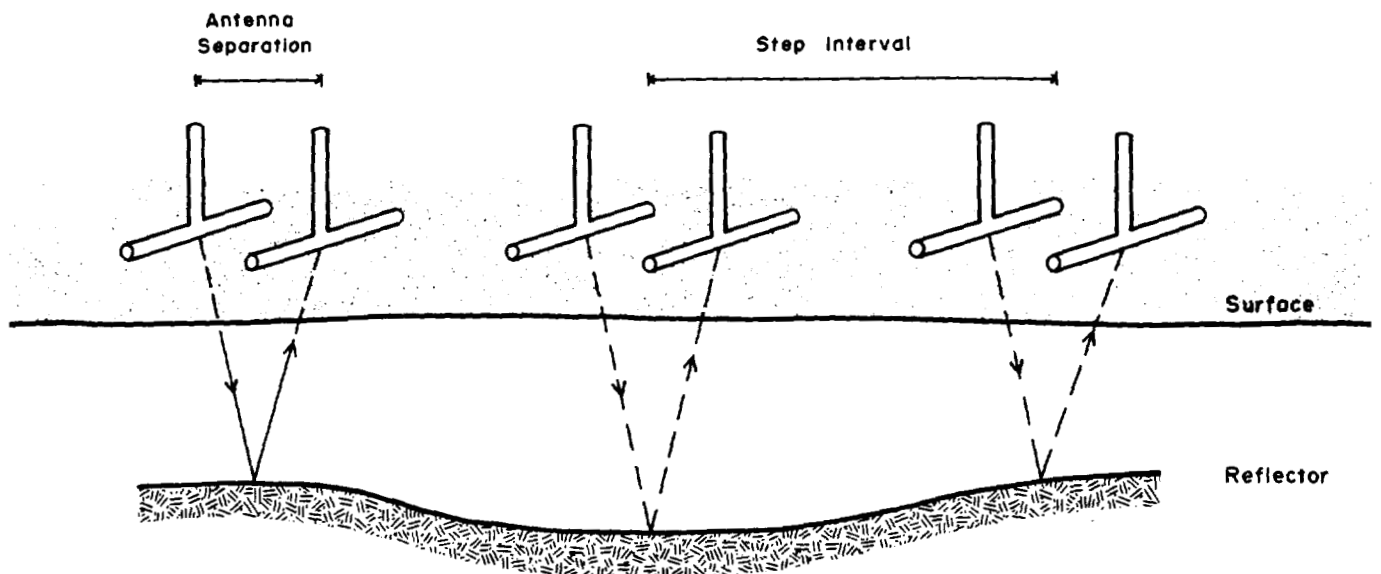


Figure 2. Step mode radar profiling.

2. It had to be user friendly to permit operation by unskilled personnel with a minimum of training.
3. It had to acquire digital data in a wide dynamic range to permit realistic use of seismic-style digital processing.
4. It had to achieve a performance factor or figure of merit of 130-180 dB depending on the operating frequency and bandwidth.
5. It had to be as free of intrinsic component artifacts as possible to allow sensible use of the available dynamic range.
6. It had to have the capability for calibrated amplitude measurement to provide the opportunity to determine quantitatively subsurface radar reflectivities.
7. It had to operate over as wide a frequency range as possible with 10-1000 MHz being the ultimate objective.

One fundamental factor that entered into the analysis was how should the radar be operated. The most successful type of GPR, in fact the only one really available at the time we began this work, was the GSSI-SIR. The SIR systems are continuous profilers, which have data acquisition tied into the data display time base and which require the system to be transported in a manner that is correlated with the display output. The primary display is a facsimile style, grey scale hardcopy. An excellent example record of this type acquired in a potash mine (Annan et al., 1988) is shown in Figure 1. Because the interface between the data acquisition and the display timebase lock had limited many of our geological sounding applications in arduous terrain, we had to eliminate this characteristic from the system for deep geological sounding in environments that are hard to access.

The ability to stack multiple records in the field is particularly important when there are external noise sources such as radio or TV transmissions in the local area. The reasons for stacking are many and are well known. To stack we need signals from the ground that are constant (time invariant), whereas external noise sources are incoherent (time varying). The simplest way to achieve this constancy is to measure with the antenna system in a static position rather than being constantly moved.

The concept of making measurements at a discrete point as opposed to continuously moving the antennas was not new as evidenced by many of the radio echo sounders developed for glacier sounding; it was felt to have many advantages. This mode of operation was a fundamental aspect of the design of the pulseEKKO III system. With this design concept in mind, a number of field tests were carried out using a modified SIR system (named the pulseEKKO I) to acquire data in various formats, which would allow us to assess this type of survey operation and to find how effective it would be.

The discrete step mode of operation is depicted in Figure 2. Figure 3 shows a sample of a pulseEKKO I record where, instead of moving continuously, the antennas were moved in discrete steps. This record looks very similar to the standard continuous profile record (such as shown in Fig. 1) except that the events appear to move in staircase-like steps rather than continuously. One thing that we noticed immediately was that the reflectors were much stronger and much more coherent than those observed with continuous profiling where the antenna coupling with the ground varied continuously.

We conducted a further experiment in very rough terrain where we made measurements at discrete intervals. The data were digitized and processed after the field survey (Davis et al., 1985b). An example data set is shown in Figure 4. The

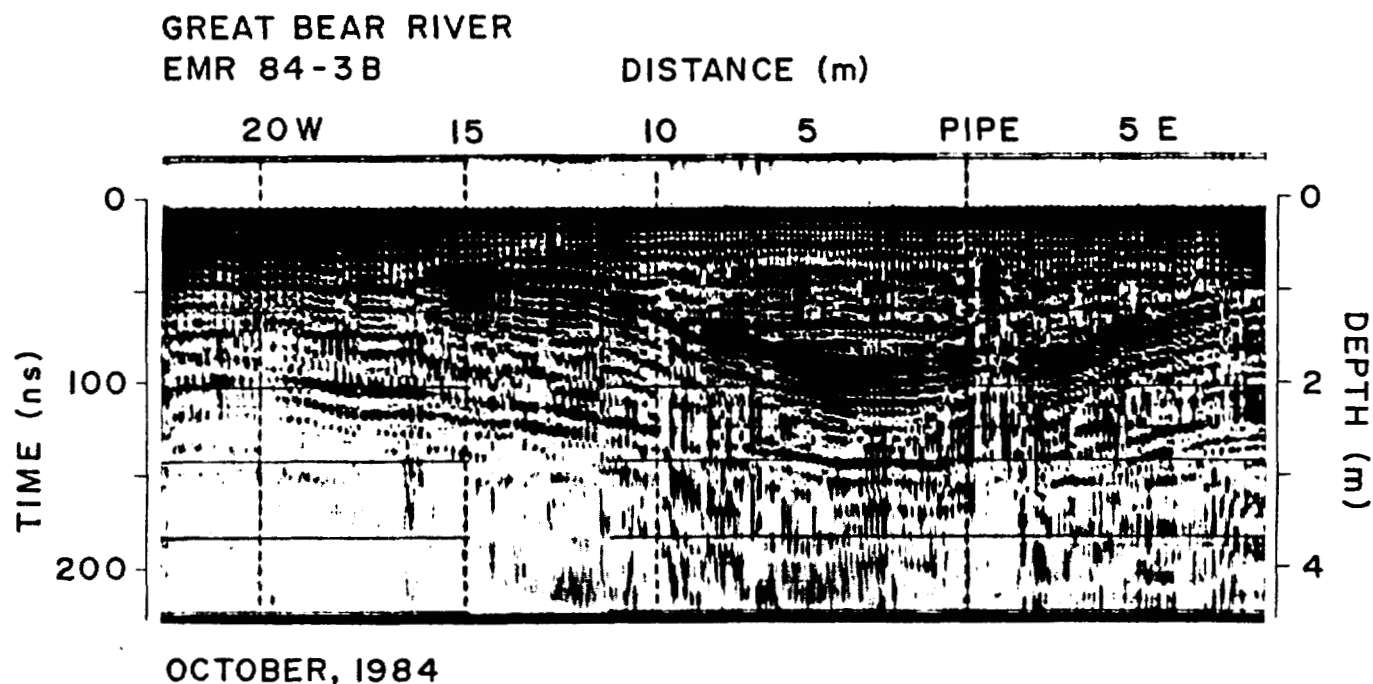


Figure 3. Example of pulseEKKO I discrete step profiling results.

data look rather jumbled; however, by applying topographic correction, the much more coherent section was obtained (Fig. 5). The geological section as inferred from geological mapping, radar, and seismic data are displayed in Figure 6. This example demonstrates one benefit of acquiring discrete step, digital data. Applying topographic corrections can transform a rather distorted image of the ground into one that is much more understandable.

With these design concepts in mind, we hardened the specifications for the pulseEKKO III system and began the development work.

SYSTEM IMPLEMENTATION

System implementation was carried out in two phases. In the first phase, the first totally digital radar (named the pulseEKKO II system (Davis et al., 1985a)) was designed and constructed. With the pulseEKKO I and II systems it was possible to acquire high frequency and low frequency data in digital form and to systematically evaluate the details necessary to implement pulseEKKO III in a second phase.

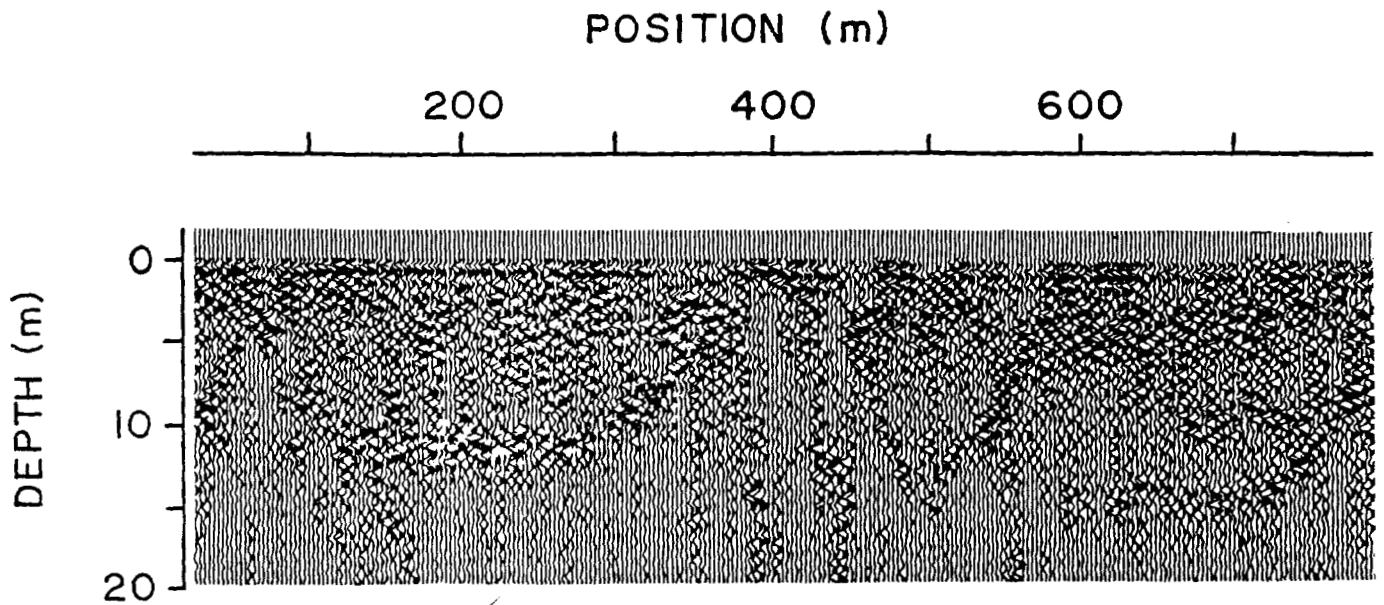


Figure 4. Example of digitized discrete step profiling results using variable area seismic-like display.

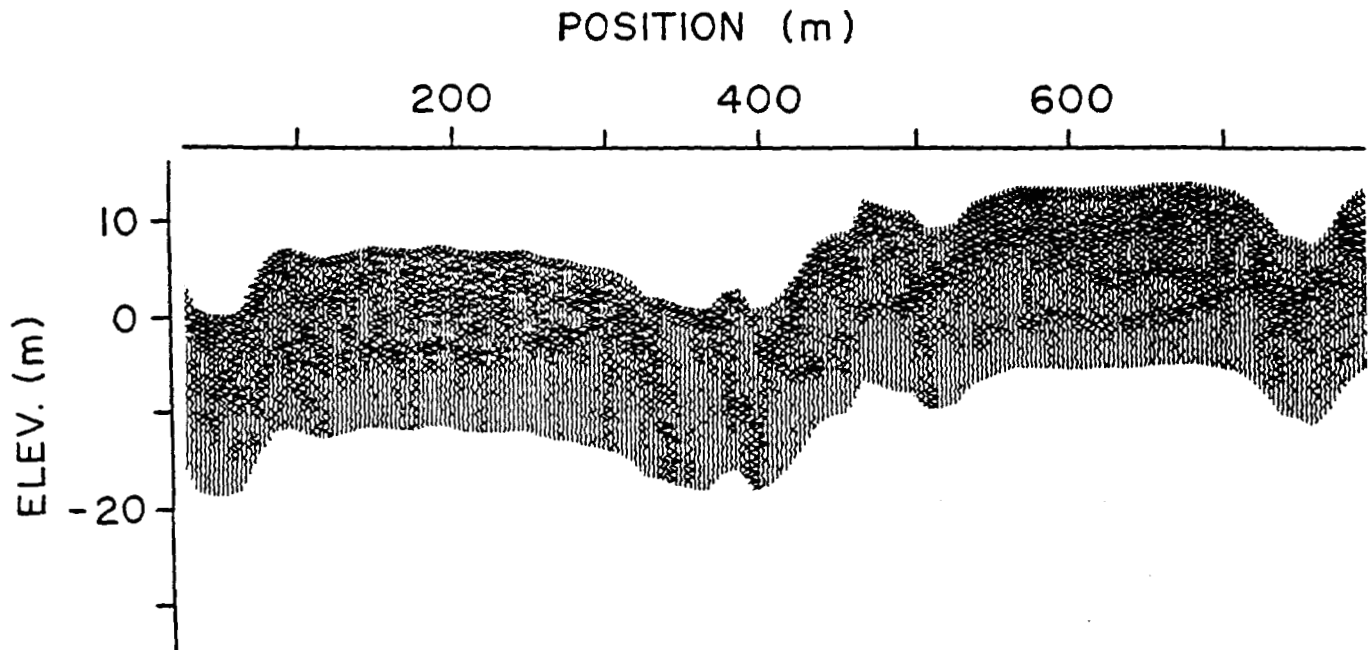


Figure 5. Data presented in Figure 4 compensated for topography.

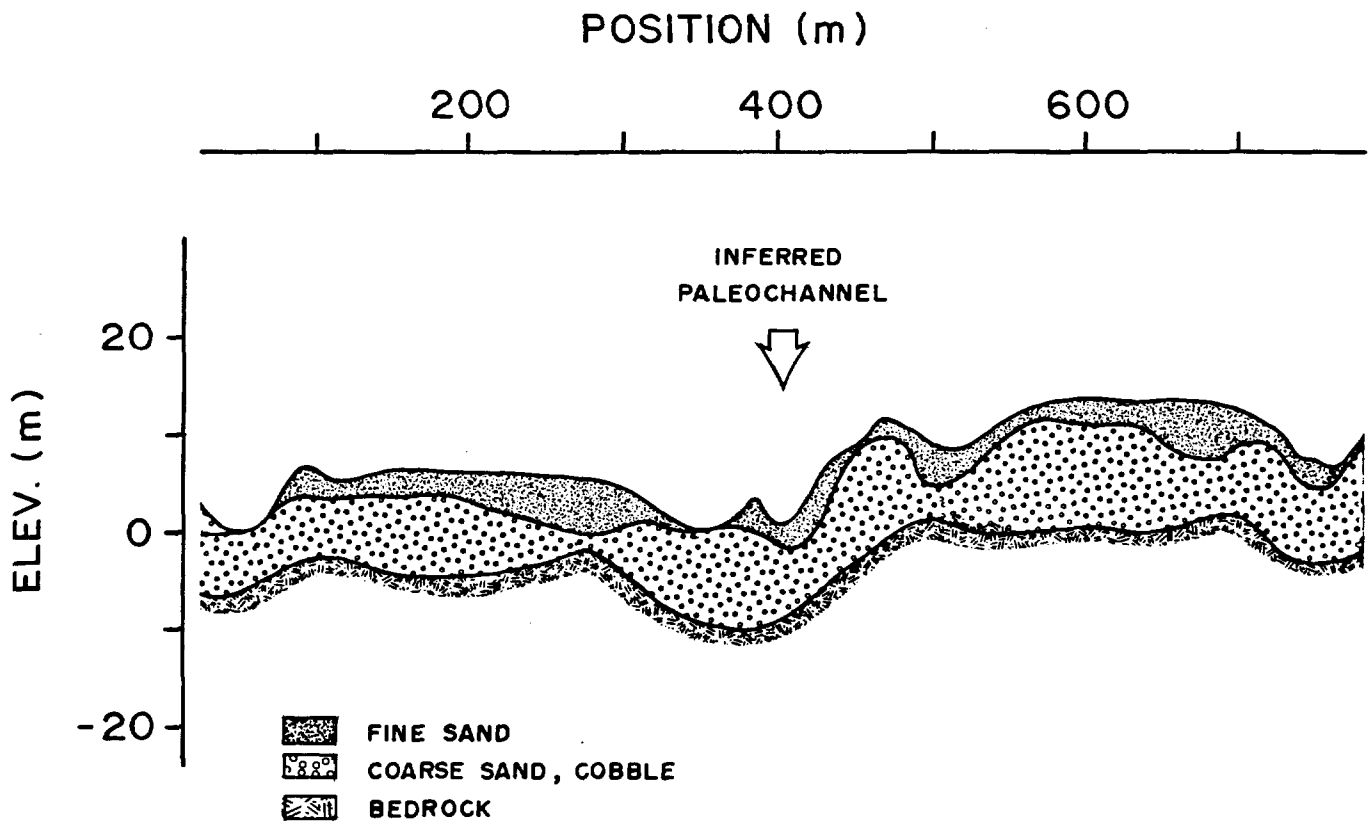


Figure 6. Geological interpretation of data shown in Figures 4 and 5 combined with seismic refraction survey information.

One major development effort was the design and construction of wide bandwidth, lightweight, portable antennas. Although we evaluated and tested many options for building directional antennas, in the end weight and portability became the deciding factor in system design.

To achieve good performance and penetration in most geological situations, operating frequencies had to be 100 MHz or lower. At these frequencies antennas become quite large, especially if a number of elements are included in the construction of the antenna in an attempt to make it directional. Because the design goal was a portable, lightweight system, such a large antenna structure was at odds with the whole design philosophy.

For GPR systems we found that when the antenna is placed in close proximity to the ground, the antenna characteristics change and most of the energy is transmitted into the ground. As a result, design focussed on the use of resistively loaded dipolar antennas that could be kept in very close proximity to the ground. Figure 7 shows how the radiation pattern of a small, electric dipole antenna varies as the electrical properties of the ground vary (Annan et al., 1975). The antenna pattern changes as ground electrical properties change with the peak in the pattern occurring at the critical angle of the air-earth interface.

The other key element of the system is the signal acquisition component or receiver. The state-of-the-art in this area is changing very rapidly. Several very high speed (flash)

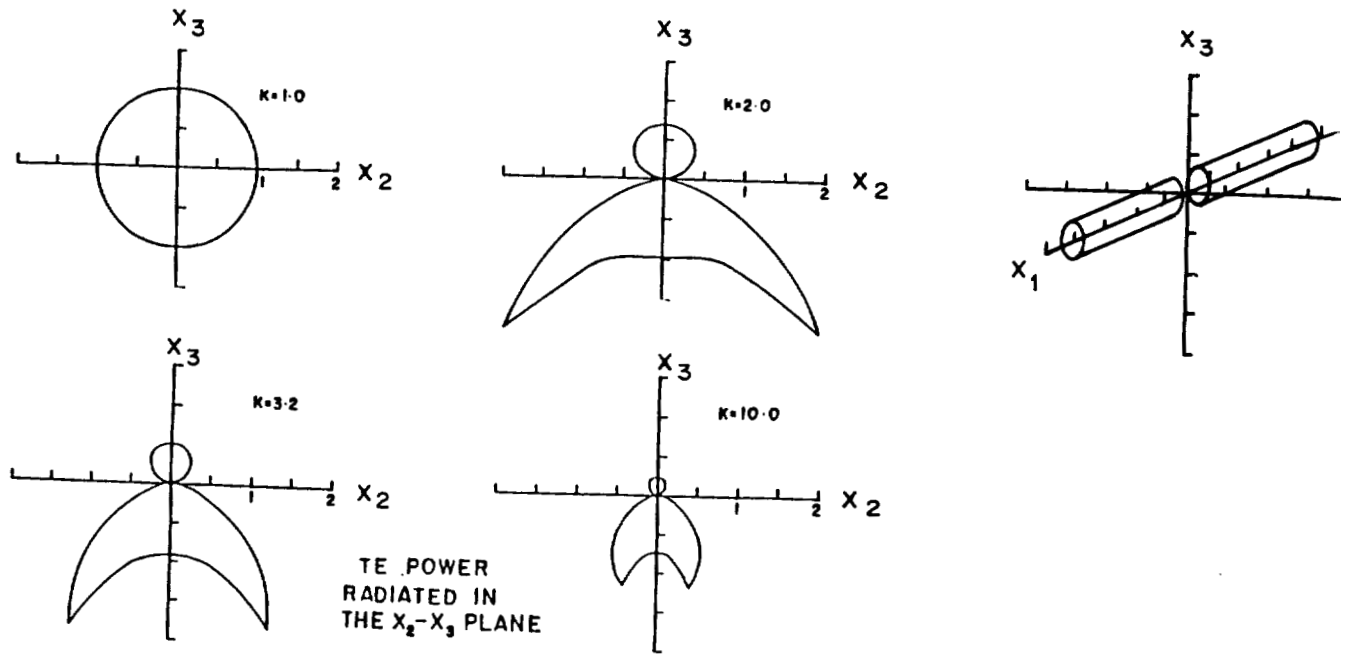
A/D convertors can sample at rates of up to several hundred MHz. These devices generally have limited dynamic range (i.e., 4-6 bit resolution). In the pulseEKKO II system, the unit employed had 8 bit resolution at 50 MHz sampling rate. At that time (in 1983) we decided that use of straight raw sampling was not fast enough for all requirements and was too power hungry for satisfactory operation in a battery powered, portable field instrument. We used synchronous sampling techniques in the pulseEKKO III system such as were used in the SIR system or any of the Tektronix or Hewlett-Packard sampling oscilloscopes.

Probably the most fundamental pulseEKKO development was the use of fibre optics for interconnecting all the components in the system. With the pulseEKKO III system, the transmitter and receiver are separate units and are interconnected into the console by fibre optics cables. Any wire cable in the vicinity of the radar can act as a parasitic antenna or radiator and will generate spurious ringing reflections. By using fibre optics, system artifacts are reduced greatly and the system performance is improved.

The resulting pulseEKKO III system with 100 MHz system antennas is shown in Figure 8. The transmitter and receiver modules, which are isolated by the fibre optics cables, contain their own battery power packs. The pulseEKKO III system is remarkably similar to the borehole radar system developed by the Swedish Geological Company

THEORETICAL

GEOMETRY



SCALE MODEL EXPERIMENT

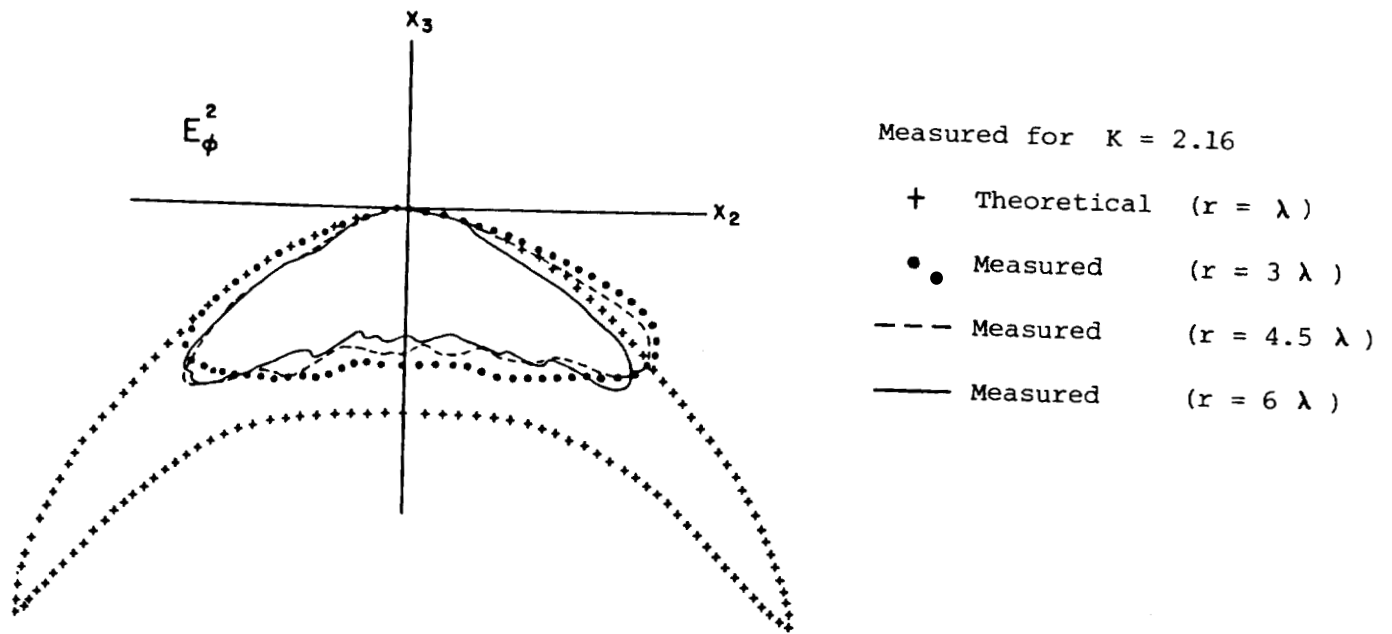


Figure 7. Dipole antenna pattern on soils of varying dielectric constant, K .

(Olsson et al., 1987). The specifications for the pulseEKKO III radar system now commercially available are summarized in Table 1.

EXAMPLE RESULTS

Many results from several case histories are presented in later papers in this proceedings. Here, one example of a set of data collected at a standard test site at Chalk River, Ontario, is presented. The geology at the site consists of fluvial and aeolian deposits of sand underlain by granitic bedrock. Figure 9 shows the system in profile mode operating along a road. Generally a crew of two is used, although in rough terrain a three person crew is beneficial.

The resulting data section is shown in Figure 10. Implicit with the pulseEKKO III system is use of computer processing. All data are recorded on digital tape in the field

and are played back into a field computer. Radar reflection sections such as that shown in Figure 10 are the first stage in data analysis.

A computer facility such as that shown in Figure 11 indicates what is required to support a fully digital GPR operation. At this stage we can edit, process, generate filtered sections, and make topographic corrections. The whole spectrum of seismic processing concepts can be used. With the rapid evolution of computer technology, the sophistication of digital processing will change and expand in the near future. For the section presented in Figure 12, some enhancement processing and automatic gain control (AGC) have been applied to enhance the weak reflections and to make their display amplitude equal to the strong events. This type of processing is common in the seismic industry.

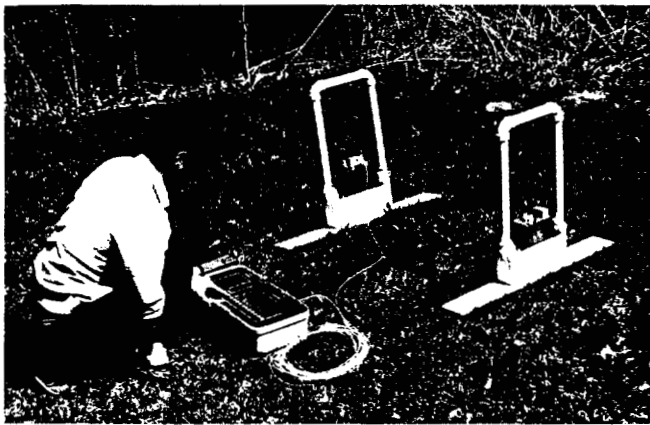


Figure 8. The first pulseEKKO III system.



Figure 9. The pulseEKKO III being used to profile along a road at a test site.

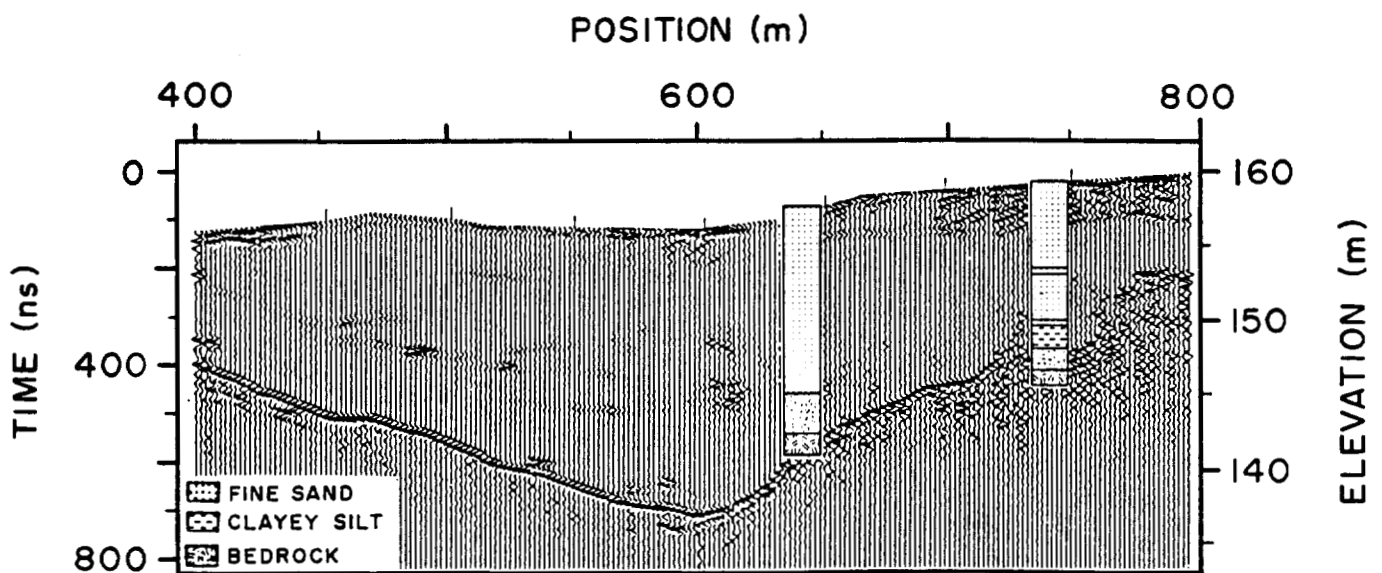


Figure 10. The pulseEKKO III data with topographic correction but without a large amount of time-gain applied.

The same data set processed to yield a colour image is shown in Figure 13. These figures show some different ways of displaying the same information. The important point is that, when we have 100 dB of dynamic range in data, several display techniques may be needed to see the various features

in the data. In some situations, the signal being sought considered to be a nuisance (geological noise is the term applied) in another application.

In many instances, since the pulseEKKO III system came into being, radar investigations have become clutter limited. The wealth of detailed subsurface information surpasses the ability to interpret and exploit in a timely fashion.

Table 1. Specifications for pulseEKKO III system

| RADAR PARAMETERS | | | |
|---------------------------|---|--------------------|--------------------|
| Centre Frequencies | 50 MHz, 100 MHz, (200 MHz - optional extra) | | |
| System Performance | 155 dB | | |
| Programmable Range Window | 1-3200 ns | | |
| Minimum Sampling Interval | 800 ps | | |
| Programmable Stacking | 1-4096 | | |
| ANTENNAS | | | |
| | 50 MHz | 100 MHz | 200 MHz |
| Size | 10.5 x 184 x 0.8 cm | 10.5 x 92 x 0.8 cm | 10.5 x 46 x 0.8 cm |
| Weight | 4 kg | 3.2 kg | 2.8 kg |
| TRANSMITTER ELECTRONICS | | | |
| Output Voltage | 400 Volts (standard equipment) 1000 Volts (optional extra - for 50 and 100 MHz only) | | |
| Maximum Repetition Rate | 30 kHz | | |
| Size | 23 x 14 x 7 cm | | |
| Weight | 0.75 kg | | |
| Power | 12V (4 Amp-hour re-chargeable battery) | | |
| RECEIVER ELECTRONICS | | | |
| Size | 23 x 14 x 7 cm | | |
| Weight | 1.5 kg | | |
| Power | 12V (4 Amp-hour re-chargeable battery) | | |
| CONTROL CONSOLE | | | |
| Size | 47 x 27 x 23 cm | | |
| Weight | 10 kg (with lid) | | |
| Power | 12VDC (3 Amps) | | |
| Recording | Digital Cassette | | |
| Display | LCD Graphic (240 x 640 pixel) | | |
| Data port | 8 bit parallel I/O | | |
| CABLES | | | |
| Control Console Power | 1.5 m power cable | | |
| Transmitter Trigger | 20 m fiber optic cable | | |
| Receiver Timing & Data | 20 m fiber optic cable | | |
| Computer Interface | 1 m GPIO interface cable | | |

August, 1987

SUMMARY AND CONCLUSIONS

The first pulseEKKO III system was completed in the spring of 1986 and delivered to the Geological Survey of Canada that time. Since then the prototype system has seen continuous field work for more than 2 years. It has been used in the Canadian Arctic, in mines, in wet conditions, and desert areas and has been through the mill in terms of field



Figure 11. Computer processing facility for radar data analysis.

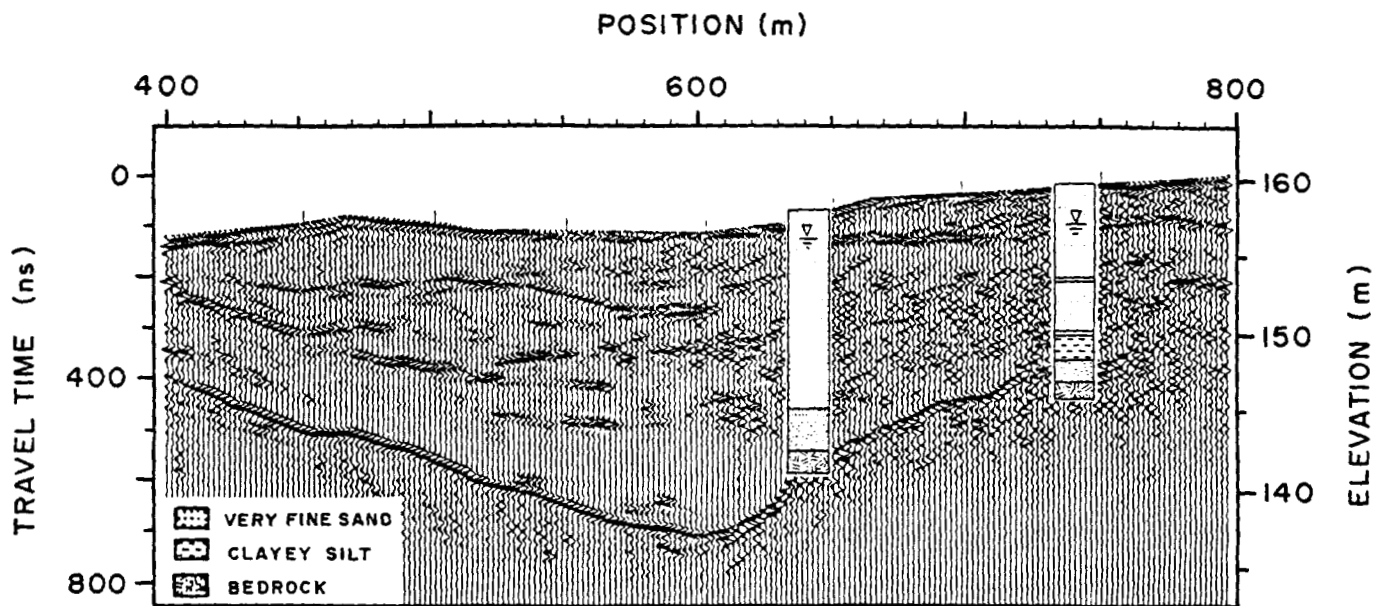


Figure 12. Example of the test site data shown in Figure 10 with AGC applied.

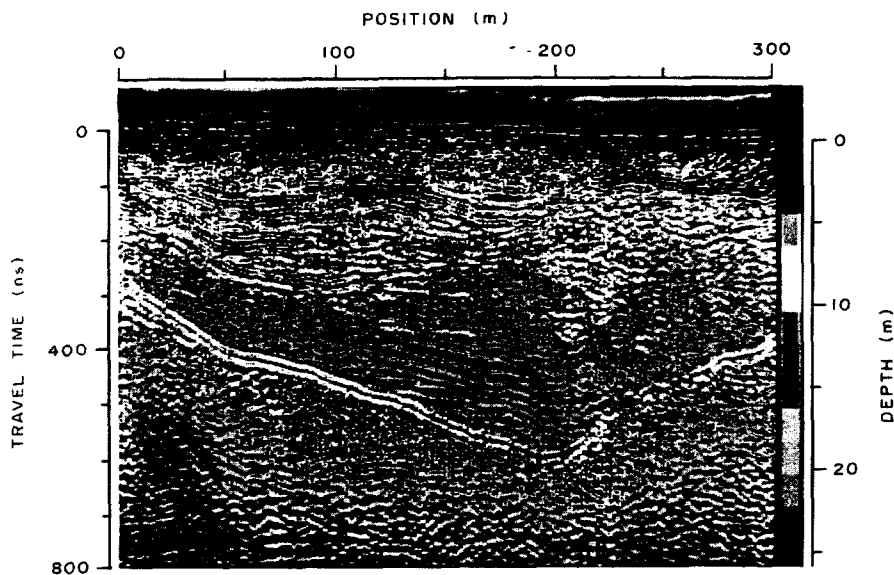


Figure 13.

Example of the test site data shown in Figure 10 or 12 using a colour display.

testing. Results are starting to come forth that demonstrate the benefits of this new generation of GPR system (Davis and Annan, 1992, Pilon et al., 1992).

The benefits of the pulseEKKO III system are many, but the more important are the following:

- high quality, artifact free data
- limits no longer instrumentation but rather ground clutter and attenuation factors
- simple-to-operate, portable system available
- reliable amplitude analysis becoming possible.

In summary, a new era in the GPR area is dawning and the method will see more rapid growth and expanded use as the advances of the seismic processing industry are adopted.

ACKNOWLEDGMENTS

The authors and A-Cubed Inc. would like to acknowledge the enthusiasm and support offered by the GSC personnel over the years of this project development.

REFERENCES

- Annan, A.P. and Davis, J.L.**
1976: Impulse radar soundings in permafrost; *Radio Science*, v. II, p. 383-394.
- Annan, A.P., Davis, J.L., and Gendzwill, D.**
1988: Radar sounding in potash mines, Saskatchewan, Canada; *Geophysics*, v. 53, p. 1556-1564.
- Annan, A.P., Waller, W.M., Strangway, D.W., Rossiter, J.R., Redman, J.D., and Watts, R.D.**
1975: The electromagnetic response of a low-loss, 2 layer dielectric Earth for horizontal electric dipole excitation; *Geophysics*, v. 40, no. 2, p. 286-298.
- Davis, J.L. and Annan, A.P.**
1992: Application of the pulseEKKO III ground penetrating radar system to mining, groundwater and geotechnical projects - selected case histories; in *Ground penetrating radar*, J.A. Pilon (ed.); Geological Survey of Canada, Paper 90-4.
- Davis, J.L. and Annan, A.P.**
1989: Ground penetrating radar for high-resolution mapping of soil and rock stratigraphy; *Geophysical Prospecting*, v. 37, p. 53-551.
- Davis, J.L., Annan, A.P., Black, G., and Leggatt, C.D.**
1985a: Geological sounding with low frequency radar (abstract); *Extended Abstracts of the 55th Annual International Meeting of the Society of Exploration Geophysicists*, Washington, D.C., October, 1985.
- Davis, J.L., Annan, A.P., and Vaughan, C.J.**
1985b: Placer exploration using radar and seismic methods; *Canadian Institute of Mining Bulletin*, v. 80, no. 898, p. 67-72.
- Morey, R.M.**
1974: Continuous subsurface profiling by impulse radar; *Proceedings, Engineering Foundations Conference on Subsurface Explorations for Underground Excavations and Heavy Construction*, Henniker, New Hampshire, p. 213-232.
- Olsson, O., Falk, L., Forslund, O., Lundmark, L., and Sandberg, E.**
1987: Crosshole investigations - results from borehole radar investigations; *Stripa Project TR 87-11*. Swedish Nuclear Fuel and Waste Management Co., Stockholm.
- Pilon, J.A., Allard, M., and Seguin, M.K.**
1992: Ground probing radar in the investigation of permafrost and subsurface characteristics of surficial deposits Kangiqsualujjuag, North Quebec; in *Ground penetrating radar*, J.A. Pilon (ed.); Geological Survey of Canada, Paper 90-4.
- Pilon, J.A., Grieve, R.A.F., Sharpton, V., Coderre, J., and Kennedy, J.**
1992: Reconnaissance ground penetrating radar survey of the interior of meteor crater, Arizona; in *Ground penetrating radar*, J.A. Pilon (ed.); Geological Survey of Canada, Paper 90-4.

Ground penetrating radar investigations of massive ground ice

S.R. Dallimore¹ and J.L. Davis²

Dallimore, S.R. and Davis, J.L., 1992: Ground penetrating radar investigations of massive ground ice; in *Ground penetrating radar*, ed. J. Pilon; Geological Survey of Canada, Paper 90-4, p. 41-48.

Abstract

A series of field trials have been carried out with newly developed ground penetrating radar systems to evaluate their use for mapping buried ground ice and near surface geology in continuous permafrost. In total, 17.5 line kilometres of surveys were conducted at three sites near Tuktoyaktuk, N.W.T. A modified Geophysical Survey System Inc. radar operating at 100 MHz (pulseEKKO I) was used for continuous near surface profiling, and a 30 MHz digital radar (pulseEKKO II) was used for detailed follow up surveys.

Correlating with subsurface data from geotechnical boreholes proved that the radar instruments used in the surveys were extremely useful for delineating massive ice and subsurface geology in a variety of terrains. In areas underlain by glaciofluvial sediments or with a thin cover of glacial till, continuous reflectors were consistently observed in the range of 100-200 ns (two-way travel time) for the pulseEKKO I and in the range of 200-400 ns for the pulseEKKO II. In areas of ideal signal penetration, reflections were observed to more than 800 ns. The two systems proved complimentary for interpreting subsurface information, enabling delineation of the upper and lower contact of thick massive ice bodies and geological contacts such as glaciofluvial channels. In areas of thick glacial till, the signal penetration was more limited and interpretation of data more difficult; however, continuous reflections to 500 ns were observed even with till thicknesses of 10 m.

Résumé

Une série d'essais sur le terrain ont été réalisés avec de nouveaux géoradars pour déterminer leur utilité à la cartographie de la glace dans le sol et de la géologie à faible profondeur dans le pergélisol continu. À trois endroits près de Tuktoyaktuk (T.N.-O.), on a effectué des levés sur 17,5 kilomètres linéaires au total. Un radar modifié de la Geophysical Survey System Inc. fonctionnant à 100 MHz (pulseEKKO I) a servi à produire des profils continus à faible profondeur, et un radar numérique de 30 MHz (pulseEKKO II) pour effectuer des levés de suivi détaillés.

La corrélation des données radar avec les données de sondage géotechniques montre que les radars utilisés dans les levés ont été très utiles pour délimiter la glace massive et la géologie de subsurface dans divers types de terrains. Dans les zones reposant sur des sédiments fluvioglaciaires et recouvertes d'une mince couche de till, on a observé des réflecteurs continus dans l'intervalle de 100 à 200 ns (temps de parcours double) dans le cas du radar pulseEKKO I et dans l'intervalle de 200 à 400 ns dans le cas du radar pulseEKKO II. Dans les zones où la pénétration du signal est idéale, on a observé des réflexions à plus de 800 ns. Les deux systèmes s'avèrent complémentaires pour interpréter les données de subsurface; elles permettent de délimiter les contacts supérieur et inférieur des massifs de glace épais et les contacts géologiques comme les chenaux fluvioglaciaires. Dans les zones de till épais, la pénétration du signal a été plus limitée et l'interprétation des données plus difficile; cependant, des réflexions pouvant atteindre 500 ns ont été observées même lorsque le till mesurait 10 m d'épaisseur.

¹ Geological Survey of Canada, Terrain Sciences Division, 601 Booth Street, Ottawa, Ontario K1A 0E8

² Formerly A-Cubed Inc., 5566 Tomken Road, Mississauga, Ontario L4W 1P4 now at Canpolar Inc., 265 Rimrock Road, Toronto, Ontario M3J 3C6

INTRODUCTION

In many permafrost areas the presence of massive ground ice poses a significant geological hazard for development related activities such as pipeline construction or extraction of granular materials. Ground ice bodies vary substantially in sediment content and ice petrology depending on their origin and the extent of postdepositional deformation. Detailed drilling studies and mapping of ground ice bodies truncated by erosion have shown that they may have complex configurations with irregular upper and lower contacts. Because permafrost soils generally exhibit low electrical loss, the ground penetrating radar is potentially a practical tool for extending borehole information and establishing the character of ground ice bodies and associated sediments.

This paper presents the results of a series of field trials conducted to evaluate newly developed ground penetrating radar systems for mapping buried ground ice and near surface geology in continuous permafrost. Fieldwork was carried out in the Tuktoyaktuk coastal area of the Canadian Beaufort Sea (Fig. 1). The trials were conducted over a variety of terrains and landform to establish the utility of the radar technology at a field scale.

METHODOLOGY

Geological applications of ground penetrating radar have been well documented in the literature and are described in detail by others contributing to this volume. The radar technique is based on the measurement of the two-way travel time of a transmitted electromagnetic wavelet, which is reflected from various surfaces within the ground. The main

consideration in permafrost materials is related to changes in electrical properties that occur at temperatures below freezing. In general, frozen soils are more resistive than unfrozen materials, with the actual velocity of propagation of an electromagnetic wavelet being effected substantially by the unfrozen water content (Annan and Davis, 1978; Patterson and Smith, 1981) and ice content (Kovacs and Morey, 1978, 1985). These properties are material and temperature dependant. Uncertainty in the velocity of wave propagation through in situ materials requires careful interpretation of radar data. Correlation with borehole data and determinations of the velocity structure in the ground with common depth point (CDP) soundings and wide angle reflection and refraction (WARR) soundings are essential.

Two radar systems with different system sensitivities and frequencies were used in the study to map near surface soils (Dallimore and Davis, 1987). The A-Cubed, pulseEKKO I radar, operating at a frequency of 100 MHz, was used for high resolution, continuous, near surface profiling. This extensively modified Geophysical Survey System Inc.

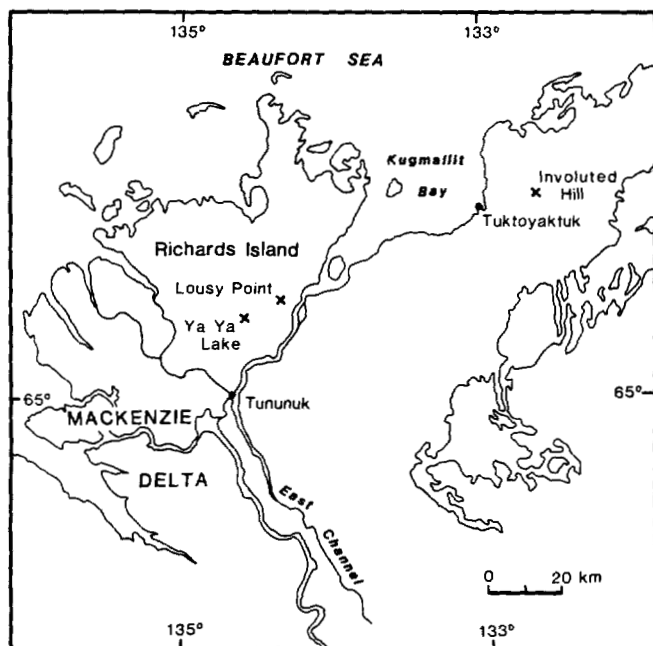


Figure 1. Location of ground probing radar surveys near Tuktoyaktuk.



Figure 2. Involuted Hill test site showing location of radar surveys.

(GSSI) radar was towed slowly (4-6 km/h) on a toboggan behind a snowmobile. The pulseEKKO II radar was designed and constructed by A-Cubed Inc. to operate at the lower frequency of 30 MHz, with similar resolution to the pulseEKKO I system. The pulseEKKO II is a digital radar; it is operated to maximum advantage in a step mode where the signal to noise ratio is improved by averaging many traces at one location before moving to the next position. A step spacing of 4 m was used for most of the surveys reported in this paper.

FIELD WORK

In total, 12.5 km of pulseEKKO I profiling and 5.0 km of pulseEKKO II profiling were conducted along transects at two sites on Richards Island and one site near the village of Tuktoyaktuk on Tuktoyaktuk Peninsula (Fig. 1). The sites were chosen to test the radar equipment in winter field conditions and to establish the performance of the radar in different geological environments. The fieldwork was

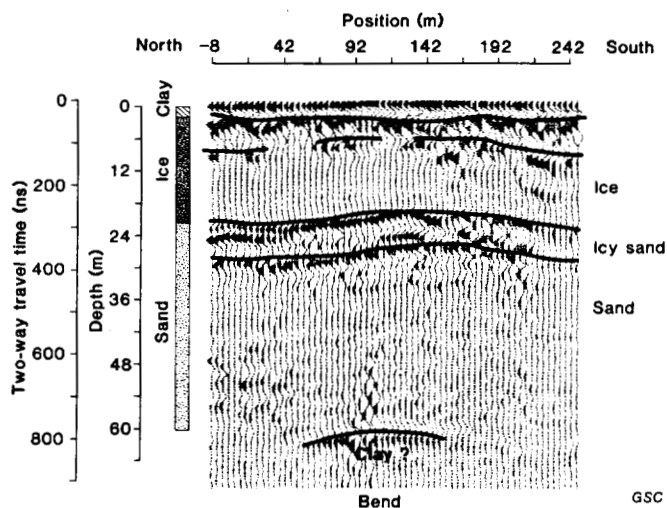


Figure 3. PulseEKKO II data along Involved Hill diagonal showing radar penetration in areas of thin clay till cover.

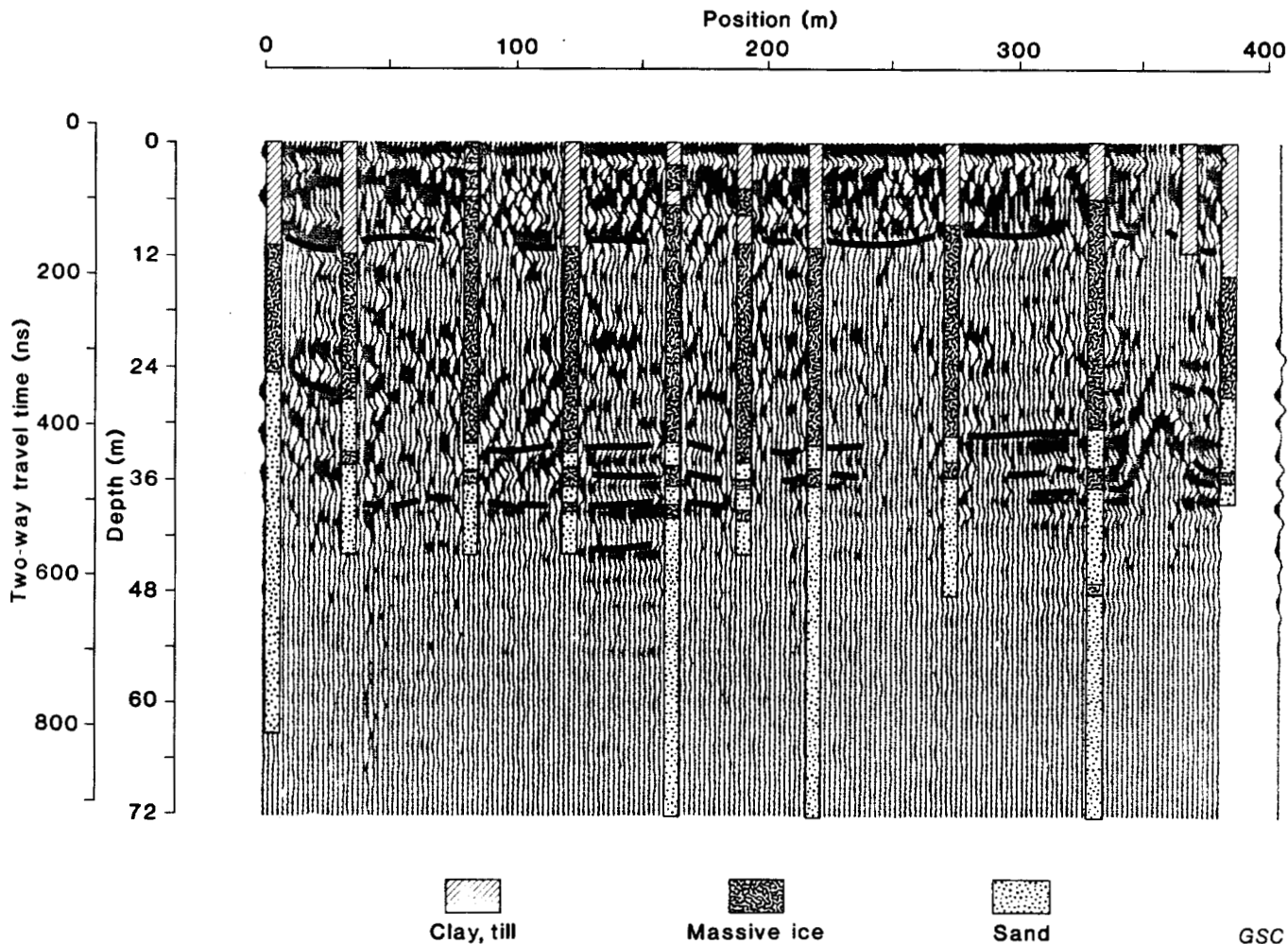


Figure 4. PulseEKKO II data along Involved Hill main line showing radar penetration in areas of thick clay till cover.

conducted during late winter when snowcover over the tundra provided access for snowmobile transportation. A field drilling program was also carried out at the Richards Island sites to provide ground verification for the radar interpretations.

RESULTS

"Involved Hill"

"Involved Hill" (informal name) lies about 15 km northeast of Tuktoyaktuk (Fig. 1). The hill, considered typical of many of the uplands areas in this part of Tuktoyaktuk Peninsula, has a characteristic wrinkled appearance on aerial photographs (Mackay, 1963). The site was established as a test site for various geophysical and drilling investigations carried out during the early seventies by the Geological Survey of Canada. During that time more than 50 boreholes were drilled through the hill to establish the stratigraphy and provide ground verification for geophysical surveys (Annan, 1976; Davis et al., 1976). The drilling investigations established that the main part of the hill consists of a 2-15 m thick mantle of fine grained clay till over a 10-20 m thick body of massive ground ice. A thick unit of sand occurs beneath the ice. The clay till and the ice vary in thickness, with the ice extending close to the surface in some places.



Figure 5. Location of radar transects at Ya Ya Lake.

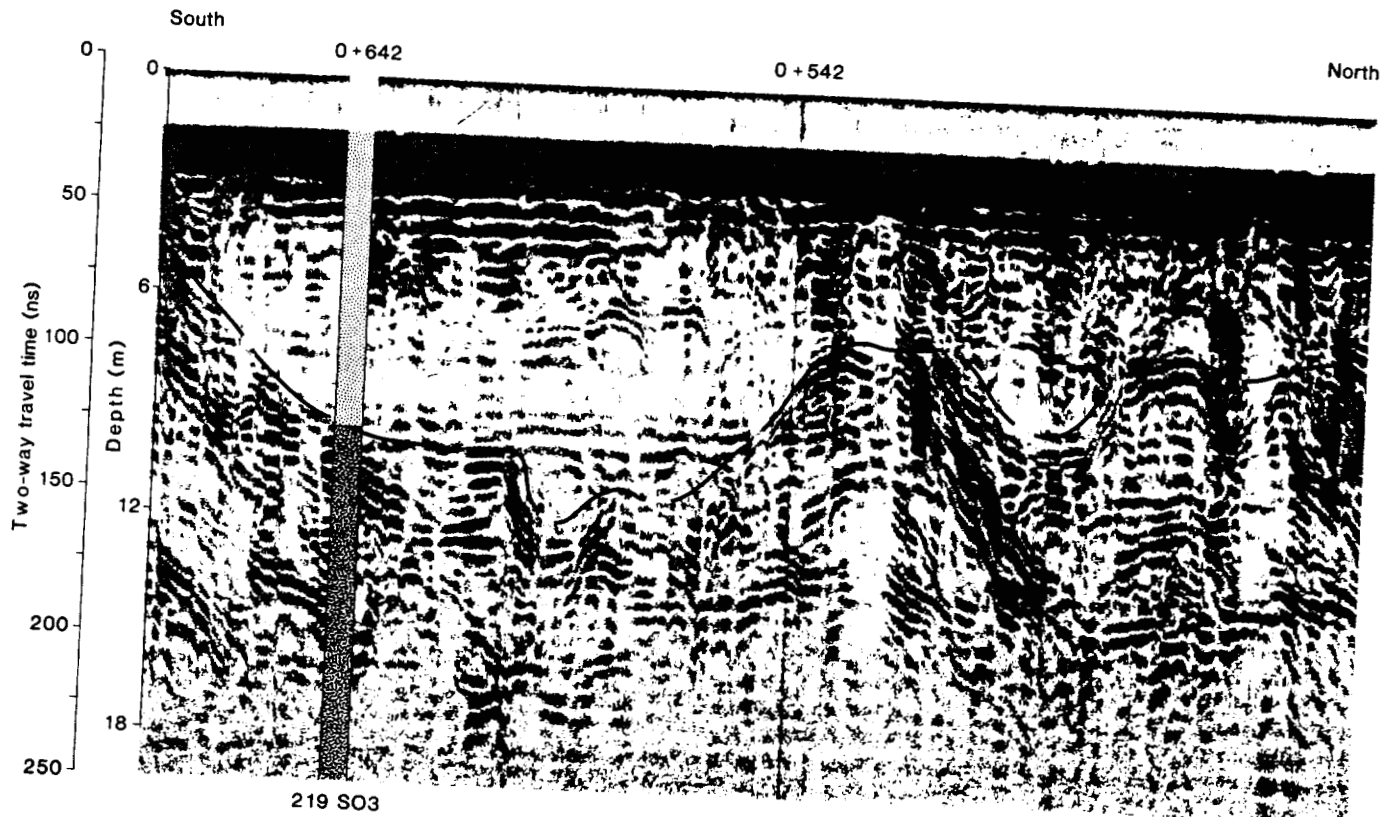


Figure 6. PulseEKKO I data along main transect at Ya Ya Lake showing near-surface channels in glaciofluvial sediments.

Ground penetrating radar studies carried out in the early seventies showed that signal penetration was very limited along the main transect where the clay till was more than a few metres thick (Davis et al., 1976). For the most part deep echoes (>100 ns) were only detected where the ice body came close to the surface and acted as a transparent window for radar transmission (Fig. 2). In these areas reflections were detected to about 300 ns two-way travel time. These deep reflections were interpreted as delineating the contact between the massive ice body and the sand.

The Involved Hill site was revisited during the 1986 field work to compare the capabilities of the newer generation radars with those used previously. Soundings were run along the old base line and along areas of thin till cover where deeper reflections were detected during the early surveys. The pulseEKKO I radar showed similar depth penetration but substantially better resolution and less system noise than the early GSSI radar used in the original survey. However, as observed in the original survey signal penetration was restricted in the areas of thick till cover along the main line.

The pulseEKKO II radar detected deep reflections at nearly all locations where it was tested on the hill. In areas where the massive ice extended close to the surface, reflectors to 800 ns two-way travel time were found where the pulseEKKO I detected reflectors at a maximum of 400 ns travel time (Fig. 3). These data are displayed with a negative variable area shading and a time gain function applied with depth. The depth scale, which is also shown on the figure, has been estimated assuming a constant velocity of 0.14 m/ns. Correlation with borehole data suggests that the reflections shown in Figure 3 may represent the lower contact of the massive ice. A deep reflector at 800 ns may represent a lower clay encountered in a deep borehole drilled along the main line. The pulseEKKO II was measured to have 40 dB greater system performance than the pulseEKKO I.

In the less favourable terrain along the main transect, reflections detected at 550 ns indicate that radar signals were able to penetrate the thick clay till mantle. Figure 4 presents the radar and drilling data along a 400 m long portion of the main line. Correlation with the nine boreholes shown on the figure indicate that the radar is able to delineate the bottom of the till layer and the lower contact with the sand. The multiple reflections near the lower contact of the massive ice correlates with thin ice bands in the upper few metres of the sand.

"Ya Ya Lake"

The radar surveys near "Ya Ya Lake" (Fig. 1) on Richards Island were carried out over an ice-contact ridge composed of glaciofluvial sand and gravel. High quality granular resources in this area are rare. Extraction of gravel is often limited by ground ice, which occurs either as lenses within the gravel or as discrete bodies of ground ice at depth. This study was carried out in conjunction with a granular investigation being conducted by Indian and Northern Affairs (EBA Engineering Consultants Ltd., 1986) along two transects across the ridge (Fig. 5).

The results from the pulseEKKO I and the pulseEKKO II surveys suggest that radar is an ideal tool for investigating the stratigraphy of coarse grained sediments. Penetration with the pulseEKKO I was generally limited to the 100-200 ns range; however, this radar was very effective in detecting both near surface changes in geology and the upper contact of a massive ice body underlying a variable thickness of sand and gravel. Although drilling on the ridge was limited, it appears that the pulseEKKO I detected channel features in the ice (Fig. 6). These channels may be associated with coarser glaciofluvial sediments indicating that radar surveys may be useful in detailed delineation of granular resources.

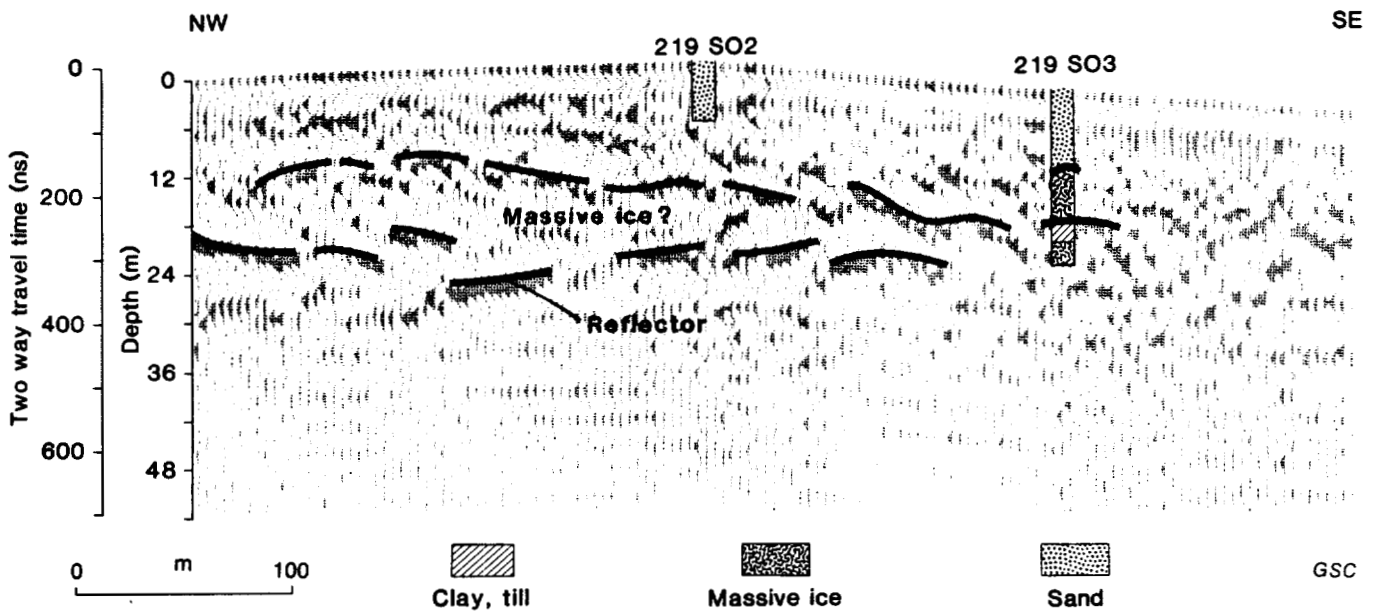


Figure 7. PulseEKKO II data along main transect at Ya Ya Lake.

The pulseEKKO II data suggest that the stratigraphy of the ridge is complex with numerous strong reflectors in the 200-450 ns range. Correlation with drill hole data suggest that some of this layering represents bands of clay till within the massive ice body that underlies the ridge (Fig. 7). Dallimore and Wolfe (1988) discussed the origin of the ice associated with the glaciofluvial deposit at Ya Ya Lake based on stratigraphic and isotopic data. They suggested that the ground ice is most likely of glacial origin. If their interpretation is correct the numerous reflectors within the ice body probably represent englacial and basal debris bands commonly found in active glacial ice.

"Lousy Point"

An 8 km long survey was conducted along a transect which started on the east channel of Mackenzie River near "Lousy Point" (Fig. 8). This transect is in the vicinity of the routes of several overland pipelines, which have been proposed to cross Richard's Island. The transect was chosen to cross a variety of terrain types to test the versatility of the ground penetrating radar systems in different surficial sediments. The transect began on the modern flood plain of Mackenzie River and then passed over an upland area underlain by glaciofluvial outwash material. Low areas along the transect are covered by variable thicknesses of glacial till and lacustrine sediments. The west part of the line crossed an upland area of glaciofluvial sediments. A gravity survey

conducted by Rampton and Walcott (1974) suggests much of the west part of the line is underlain by up to 100 m of massive ground ice.

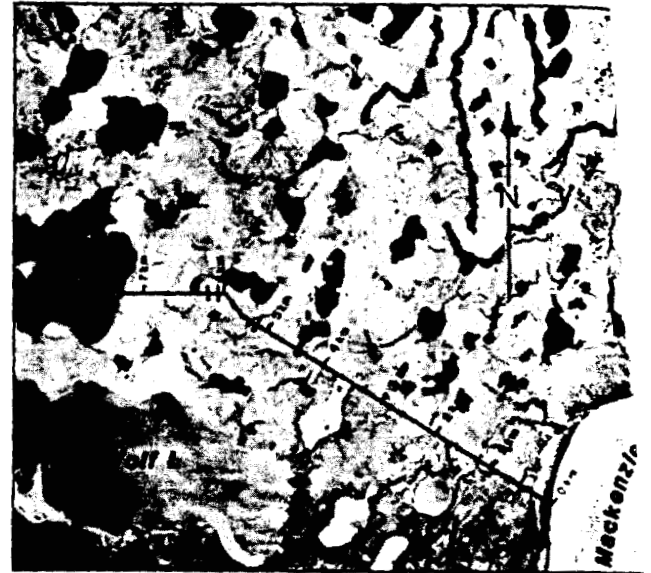


Figure 8. Location of radar transects at Lousy Point.

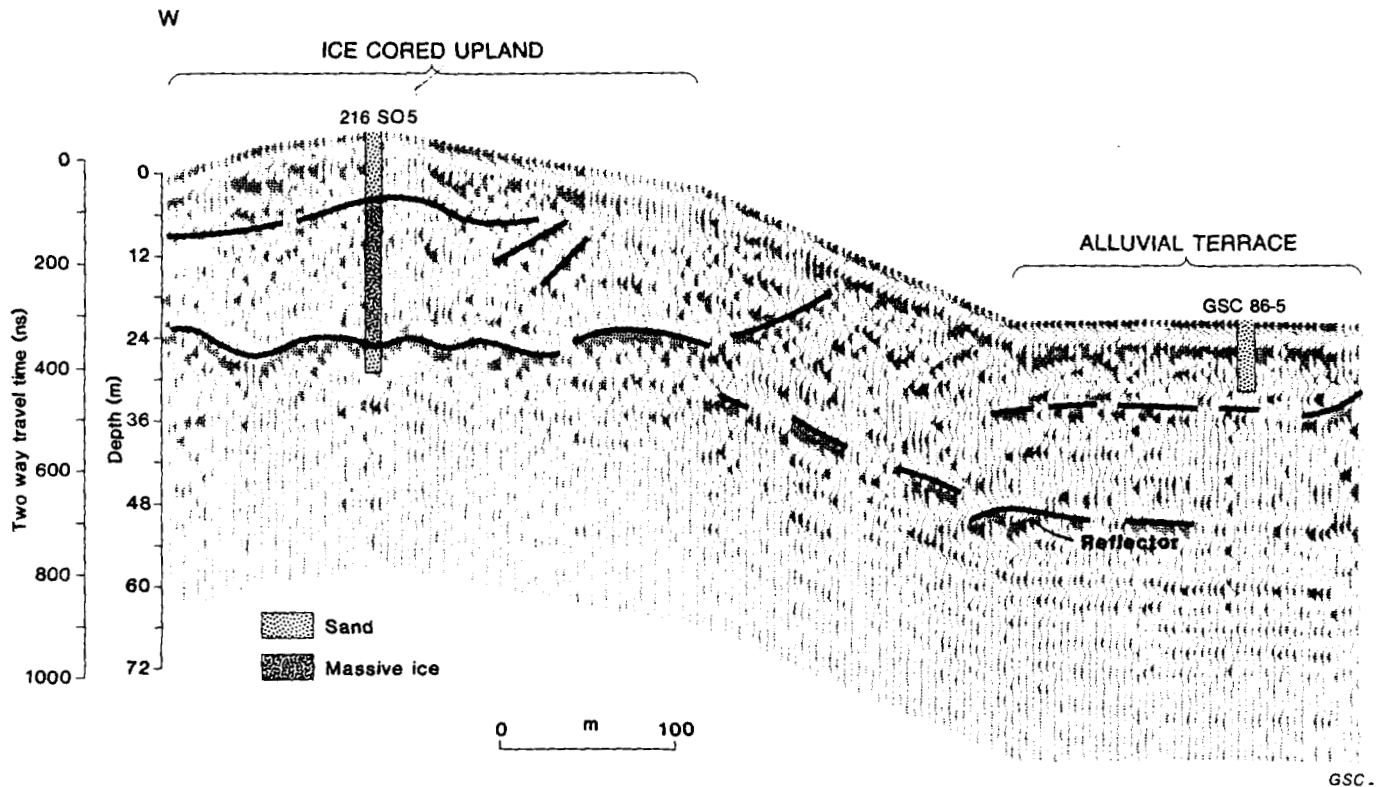


Figure 9. PulseEKKO II data at east end of Lousy Point line showing configuration of massive ice body.

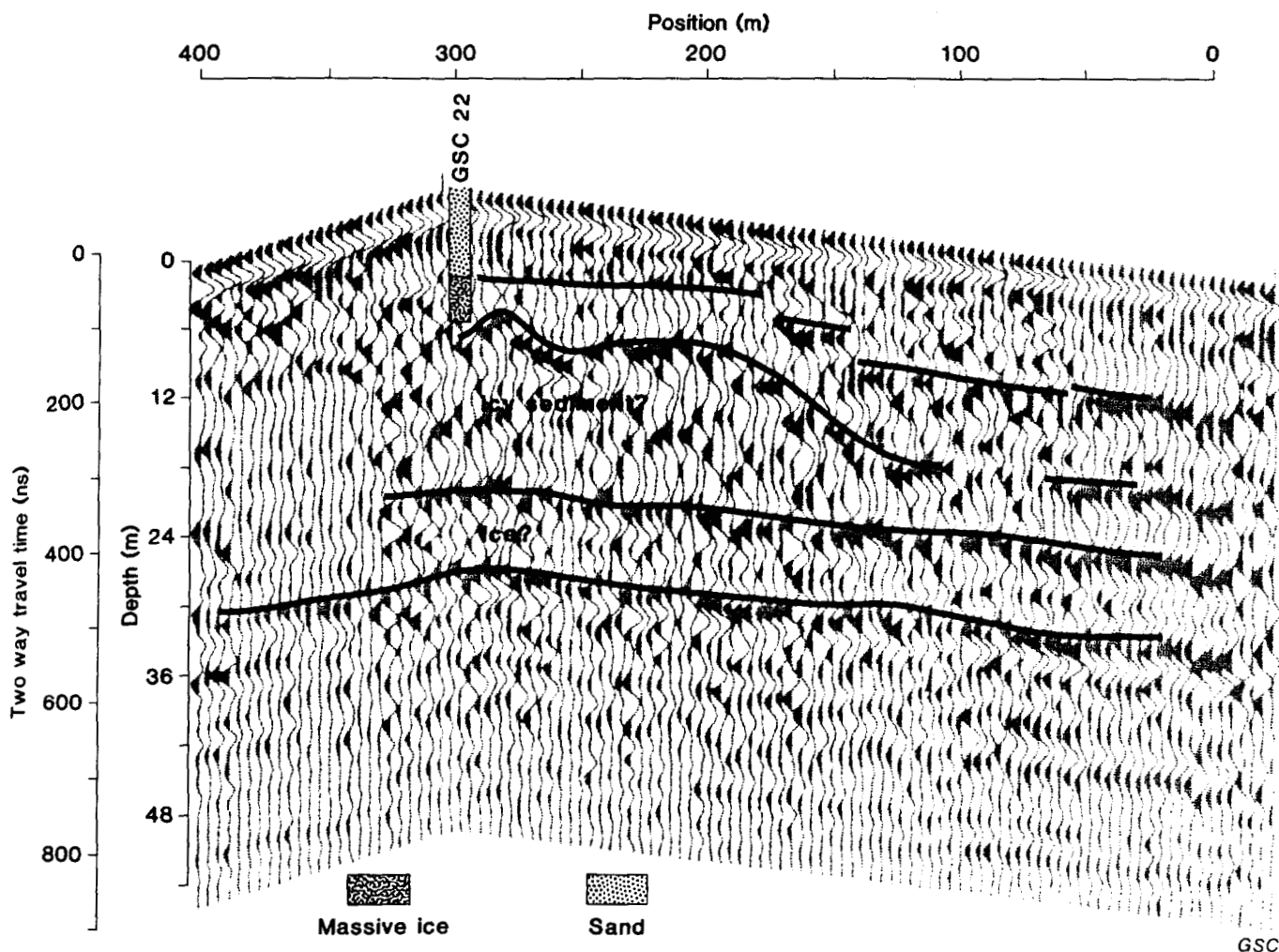


Figure 10. PulseEKKO data along west end of Low Point line.

Radar and drilling data confirm that many of the highland areas along the transect are underlain by substantial amounts of massive ground ice (Fig. 9). At the east end of the transect a 20 m thick ice body occurs beneath 9 m of stratified sand and silt. Radar profiling successfully delineated the morphology of the ice body; the pulseEKKO I was most useful for delineating the upper contact and the pulseEKKO II best delineated the lower contact with a basal sand. Unlike the data from Ya Ya Lake, the pulseEKKO II data suggested that the ice body was relatively clean with few internal reflectors being observed (Fig. 9). This result may be partially due to a different origin for the ice. Dallimore and Wolfe (1988) have suggested a segregated origin for this ice body.

Interpretation of radar data along the remaining part of the line is difficult because of limited data for ground verification. In general the radar systems were found to perform better in the upland areas where coarse sediments are common and where massive ice was encountered at depth. The utility of the radar systems in the low areas of lacustrine sediments and glacial till cover was limited. More drill data and further radar surveys would be required to fully evaluate their performance. The west portion of the radar transect, in

the vicinity of the gravity surveys by Rampton and Walcott (1974), appears to also be underlain by massive ice. The nature of the radar data (Fig. 10) suggests that this ice is perhaps more like the ice at Ya Ya Lake with numerous internal reflectors possibly representing till bands within the ice.

DISCUSSION AND CONCLUSIONS

The studies carried out to date indicate that the ground penetrating radar technique is extremely valuable for detecting massive ground ice and mapping near-surface geology. The radar method is especially useful for correlating between boreholes or for determining the suitable drilling locations. Repeat surveys carried out at Involved Hill indicate that advances in digital radar technology and in system performance have substantially improved depth penetration and resolution when compared to earlier radar system used in the mid-seventies. The successful completion of more than 17.5 km of rigorous field trials also demonstrates that the instruments are sufficiently robust and durable for extensive surveys such as might be conducted along the routes of proposed pipelines or highways.

The two radar systems used for the surveys described in this paper were found to be complimentary for field operations and interpretation of subsurface reflectors. The general pattern for operation used during the survey was to conduct a rapid survey of the entire transect with a 100 MHz continuous profiling radar (pulseEKKO I). This enabled a rapid assessment of the type of terrain expected along the survey line. At Lousy Point, for instance, the 8 km line was surveyed in about 6 h. These data were then reviewed to provide an overview of near-surface geology and the expected radar performance. Areas of particular interest were then chosen for detailed study and were resurveyed with the digital radar operating at a lower frequency of 30 MHz (pulseEKKO II). This survey proved to be the most valuable for delineating deeper ground ice bodies; however, in most instances it was necessary to review the pulseEKKO I data to improve the interpretation in the upper 10 m.

Correlation of radar data with borehole data and velocity soundings indicates that the velocity of propagation of radar signals was in the range of 0.15-0.12 m/ns. In fact for practical purposes an assumed velocity of 0.14 m/ns was considered adequate for nearly all surficial materials. This was true for instance, at Involute Hill, where over 10 m of clay till is present along the main line. The main reason for this relatively high velocity is most likely the extremely cold ground temperatures present in this region during March and April. Temperature records show that ground temperatures in the upper 10 m may vary from -7° to -18°C. It should be noted that depth penetration may be substantially reduced if surveys are conducted at other times of the year when a thawed layer may be present at the surface or ground temperatures are warmer.

ACKNOWLEDGMENTS

The authors would like to acknowledge the field assistance given by F.M. Nixon and J.G. Bisson. Funding for the field work was provided by the Panel for Energy Research and Development, and logistical support was given by the Polar Continental Shelf Project.

REFERENCES

- Annan, A.P.**
1976: Density of ice samples from Involute Hill test site, Dist Mackenzie; Geological Survey of Canada, Paper 76-1C, p. 9.
- Annan, A.P. and Davis, J.L.**
1978: High frequency electrical method for the detection of freeze interfaces; Proceedings, 3rd International Conference Permafrost, Edmonton, Alberta, v. 1, p. 496-500.
- Dallimore, S.R. and Davis, J.L.**
1987: Ground probing radar investigations of massive ground ice and surface geology in continuous permafrost; in Current Research Part A, Geological Survey of Canada, Paper 87-1A, p. 913-9.
- Dallimore, S.R. and Wolfe, S.A.**
1988: Massive ground ice associated with glaciofluvial sediments; Richards Island, N.W.T., Canada; Proceedings, 5th International Conference on Permafrost, Trondheim, Norway.
- Davis, J.L., Scott, W.J., Morey, R.M., and Annan, A.P.**
1976: Impulse radar experiments on permafrost near Tuktoyaktuk Northwest Territories; Canadian Journal of Earth Sciences, v. 13, p. 1584-1590.
- EBA Engineering Consultants Ltd.**
1986: Granular evolution Richards Island, N.W.T.; Contract report prepared for Indian and Northern Affairs Canada, Ottawa, Ontario.
- Kovacs, A. and Morey, R.M.**
1978: Remote detection of massive ice in permafrost along the Alye pipeline and the pump station feeder gas pipeline; Proceedings, ASCE Pipelines Division Specialty Conference, Pipelines in Adverse Environments, New Orleans, p. 268-279.
- 1985: Impulse radar sounding of frozen ground; Proceedings, Workshop on Permafrost Geophysics, US Army Corps of Engineers, Cold Regions Research and Engineering Laboratory, Special Report, 85-5, p. 28-40.
- Mackay, J.R.**
1963: The Mackenzie Delta Area, Northwest Territories; Geological Survey of Canada, Miscellaneous Report 23, 202 p.
- Patterson, D.E. and Smith, M.W.**
1981: The measurement of unfrozen water content by time-domain reflectometry; Canadian Geotechnical Journal, v. 18, p. 131-144.
- Rampton, V.N. and Walcott, R.I.**
1974: Gravity profiles across ice-cored topography; Canadian Journal of Earth Sciences, v. 11, p. 110-121.

Applications of ground penetrating radar to mining, groundwater, and geotechnical projects: selected case histories

J.L. Davis² and A.P. Annan¹

Davis, J.L. and Annan, A.P., 1992: *Applications of ground penetrating radar to mining, groundwater, and geotechnical projects: selected case histories*; in *Ground penetrating radar*, ed. J. Pilon; Geological Survey of Canada, Paper 90-4, p. 49-55.

Abstract

Ground penetrating radar is a technique that offers the capability of high resolution mapping of soil and rock conditions. The need for a better understanding of overburden conditions for activities such as geochemical sampling, geotechnical investigations, and placer exploration, as well as the factors controlling groundwater flow, has increased demand for techniques that can image the subsurface with higher resolution than previously possible.

The basic principles and practices involved in acquiring high quality radar data in the field are illustrated by selected case histories. One case history demonstrates how radar has mapped the bedrock to depths of 20 m and to delineate structure within overburden. Another example shows how the radar has been used to map not only bedrock under a lake but also changes of rock type to a depth of 50 m. Two case histories demonstrate how radar has been used to map fractures and changes of rock type to 40 m depth from inside mines. With the new instruments and field methods, the routine use of radar is becoming economically viable and the method will see greater use in the future.

Résumé

Le géoradar permet d'établir des cartes à haute résolution figurant les conditions du sol et des roches. La nécessité de mieux comprendre les conditions propres aux terrains de couverture dans le cadre de certaines activités comme l'échantillonnage géochimique, les analyses géotechniques et l'exploration des placers ainsi que l'étude des facteurs régissant l'écoulement de l'eau souterraine, a fait accroître la demande pour des techniques permettant de représenter graphiquement les couches profondes à une résolution plus grande qu'auparavant.

Les principes et usages de base mis en oeuvre pour acquérir des données radar de haute qualité sur le terrain sont illustrés par des cas choisis. Un cas sert à présenter la façon dont a été cartographiée le socle jusqu'à des profondeurs de 20 m et comment la structure dans le terrain de couverture a été délimitée. Un autre exemple illustre comment le radar a été utilisé pour cartographier non seulement le socle sous un lac, mais également les changements de type de roche jusqu'à une profondeur de 50 m. Deux autres cas sont donnés pour montrer comment le radar a servi à cartographier les fractures et les changements de lithologie jusqu'à une profondeur de 40 m à partir de l'intérieur de certaines mines. Avec l'apparition de nouveaux instruments et l'élaboration de nouvelles méthodes de terrain, l'utilisation courante du radar est en passe de devenir économiquement viable et ne fera que croître dans l'avenir.

¹ Sensors & Software Inc., 5566 Tomken Road, Mississauga, Ontario L4W 1P4

² Formerly A-Cubed Inc., 5566 Tomken Road, Mississauga, Ont. L4W 1P4, now at Canpolar Inc., 265 Rimrock Road, Toronto, Ont. M3J 3C6

INTRODUCTION

Applications for the use of ground penetrating radar (GPR) are abundant. They include mineral and groundwater exploration, geotechnical and archaeological investigations, as well as rock mechanics and mine development requirements. Some specific examples include mapping bedrock depth, changes of rock type, fractures in bedrock, soil strata, and the water table in coarse grained soils.

The size and depth of features that can be detected with GPR are dictated by the GPR operating frequency and the geological setting. GPR operating at 500-1000 MHz have detected fractures of a few millimetres thick at ranges of several metres. GPR systems operating at 25-50 MHz can sound to depths in excess of 50 m in soils with low conductivity (less than 1 ms/m) such as sand, gravel, and rock, and in fresh water.

EQUIPMENT

Recent developments in GPR technology have increased the ability of the technique to sound to greater depths in geological materials. The newer radar systems, such as the PulseEKKO III (Annan and Davis, 1992) that we use in these case histories (Fig. 1), use state-of-the-art computer technology that allows use of sophisticated digital processing techniques. New instrumentation is portable and easy to use in the field and lends itself well to surveys in difficult conditions. The radar unit (Fig. 1) digitizes the received signal in the receiver at the antenna. The signal is transferred by use of fibre optic cables, which greatly reduce "noise". The digital signal is transferred to the console where it is formatted for display on a graphics liquid crystal display (LCD) and stored on digital magnetic tape. The digital data are transferred to a desk top computer for processing.

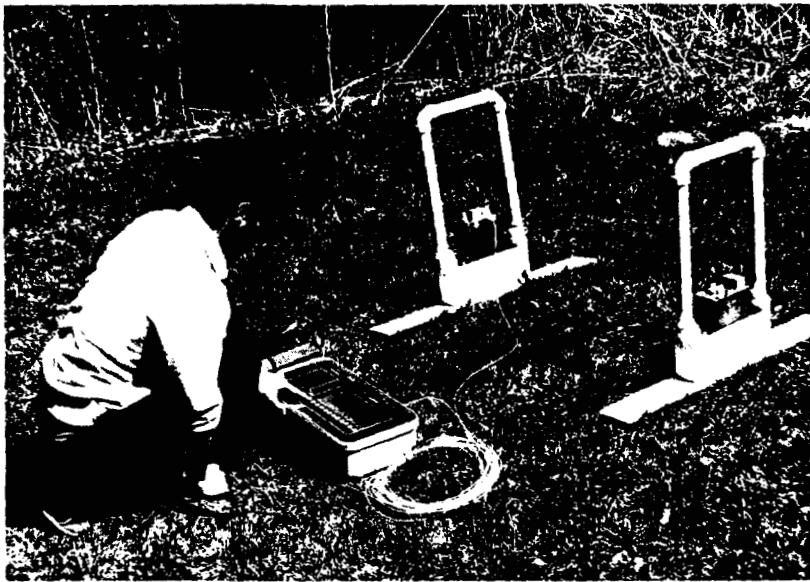


Figure 1. PulseEKKO III radar system with 100 MHz antenna.

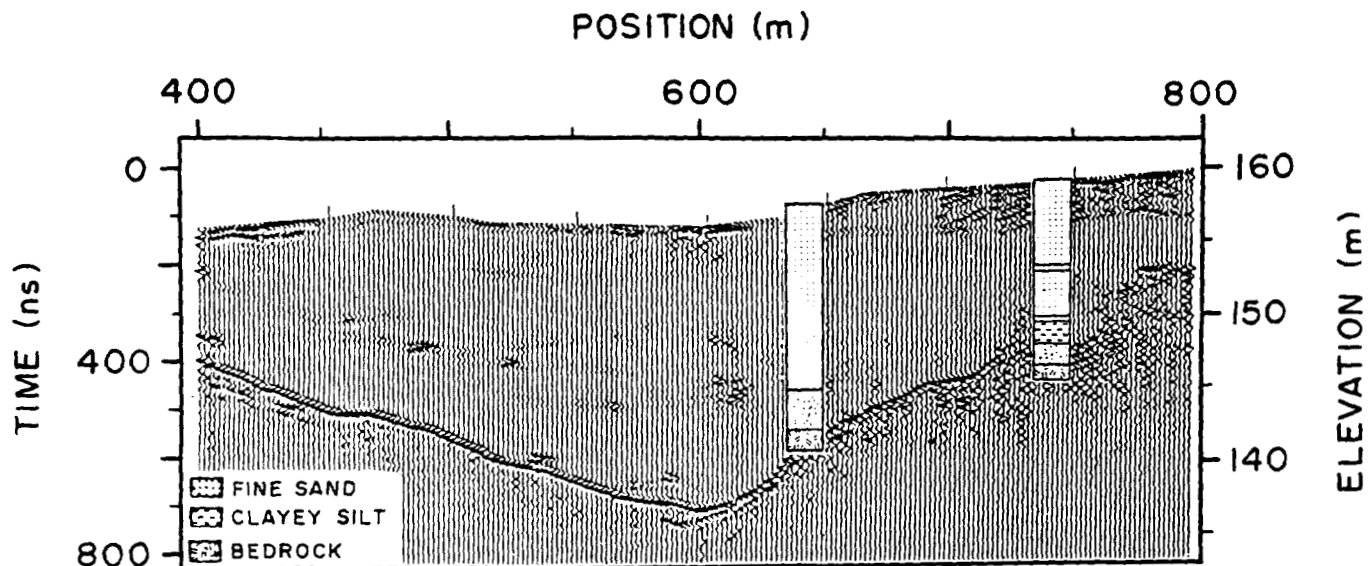


Figure 2. Radar record showing the bedrock topography under a fine sand overburden.

display in hard copy. Digital signal processing techniques commonly employed in the seismic industry are used to produce a high quality data display.

CASE HISTORIES

Five case histories are summarized to show how ground penetrating radar can be used to obtain detailed information of the bedrock topography, soil stratigraphy in the overburden even under a lake, and the extent of a contaminated groundwater plume. Two of the examples demonstrate that the GPR can detect and map features in the rock such as fractures and changes of geology from inside mines.

Soil stratigraphy and bedrock mapping

Figure 2 is a GPR record obtained using 100 MHz centre frequency antennas at 2 m station intervals on the surface at a site in eastern Ontario. The geological setting consists of water saturated fine sand over a granodiorite bedrock. The bedrock depth varies from 5 to 20 m along this 400 m profile. The surface topography was surveyed, and the data were compensated for the topographic variations along the survey line. Two boreholes nearby the survey line show that the radar data agree closely with bedrock depth on the borehole logs.

Figure 3 shows the same profile as Figure 2 but with a time varying gain applied. The weak reflections are caused by thin silt and clay layers as well as erosional unconformities

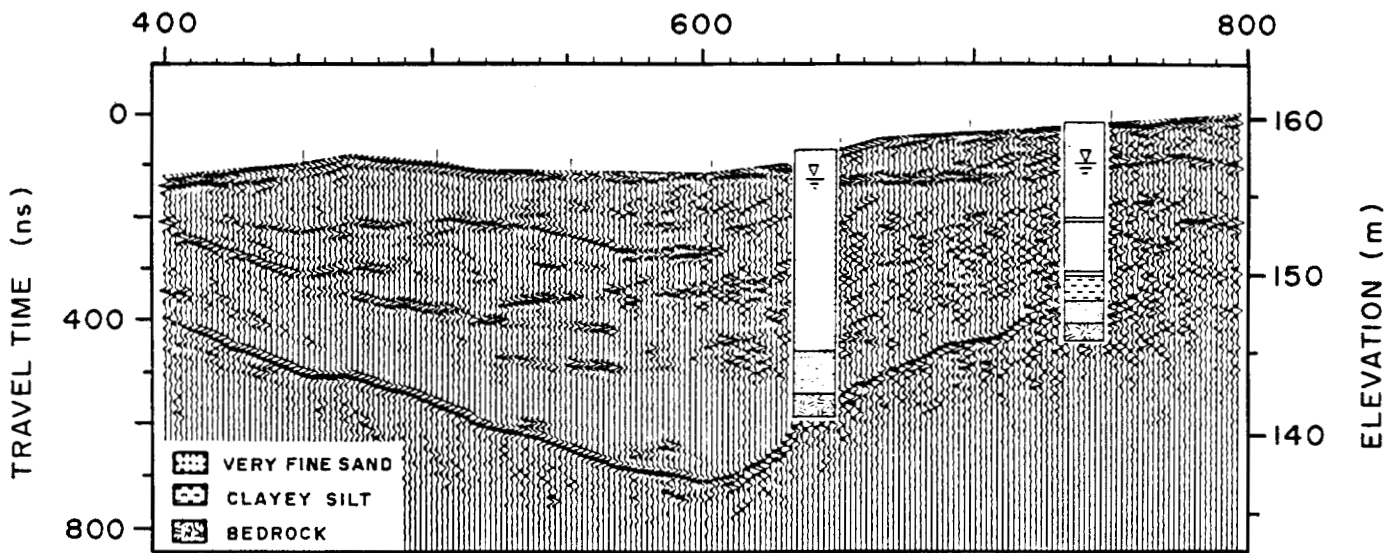


Figure 3. Same profile as Figure 2 but with additional gain applied. Reflections in the overburden are from silt and clay layers in the sand.

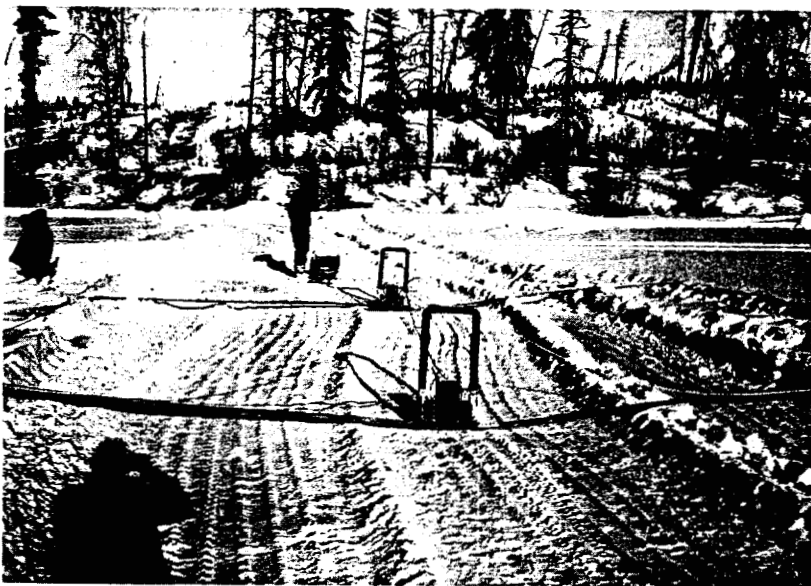


Figure 4. 13 MHz antennas in use on ice-covered lake.

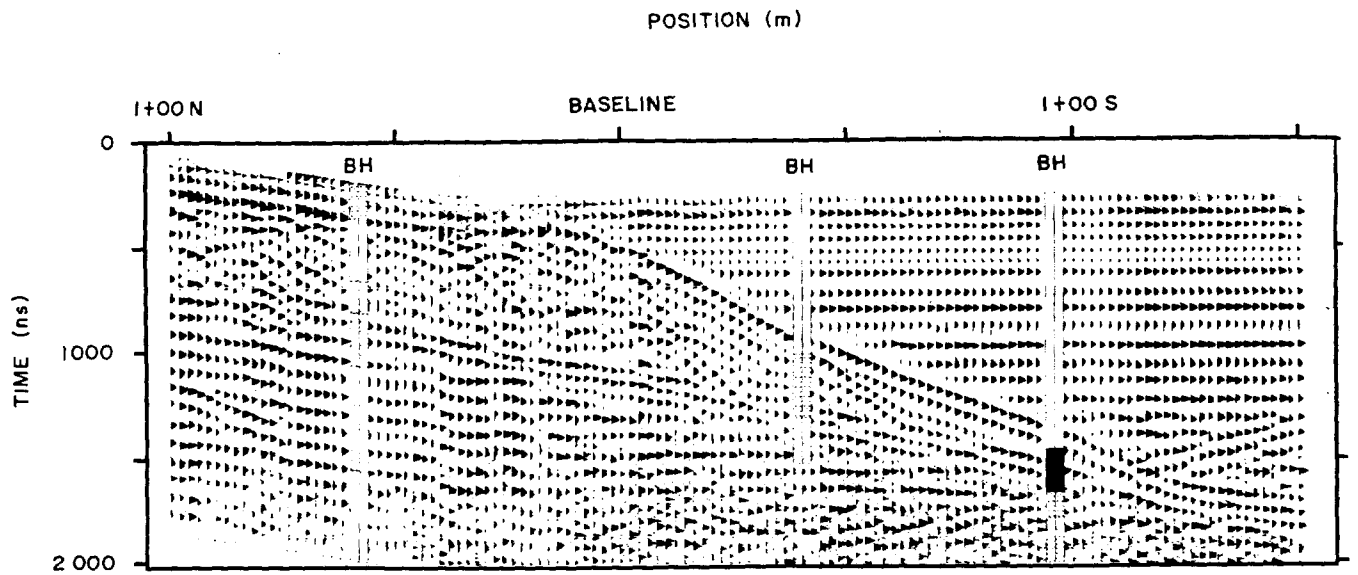


Figure 5. Radar record showing bedrock on shore and under a lake.

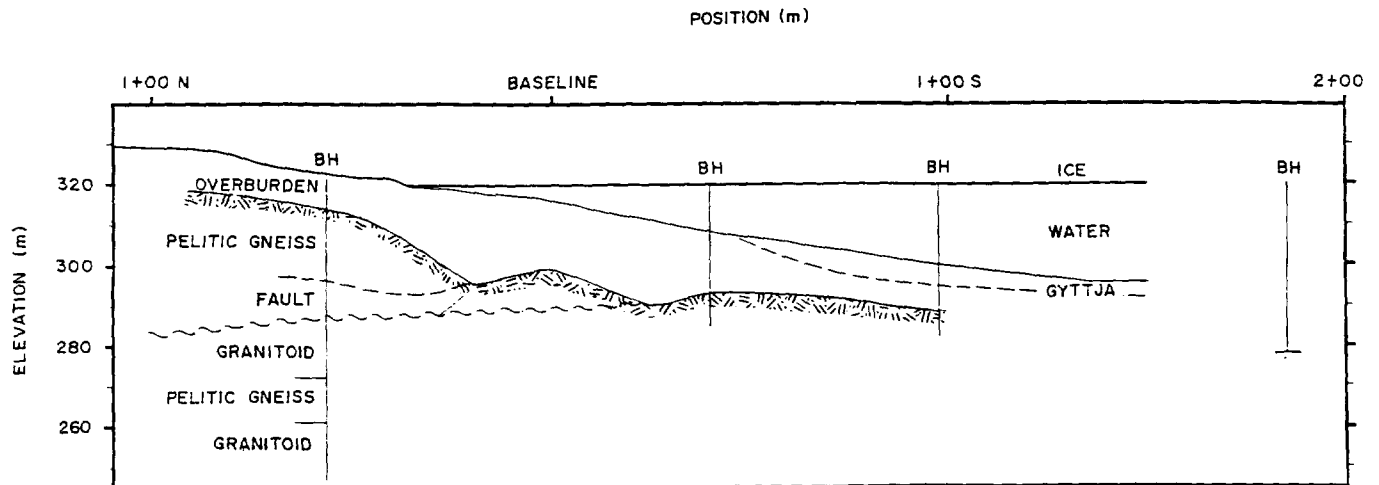


Figure 6. Interpreted geological section based on four borehole (BH) logs and the radar survey data shown in Figure 5.

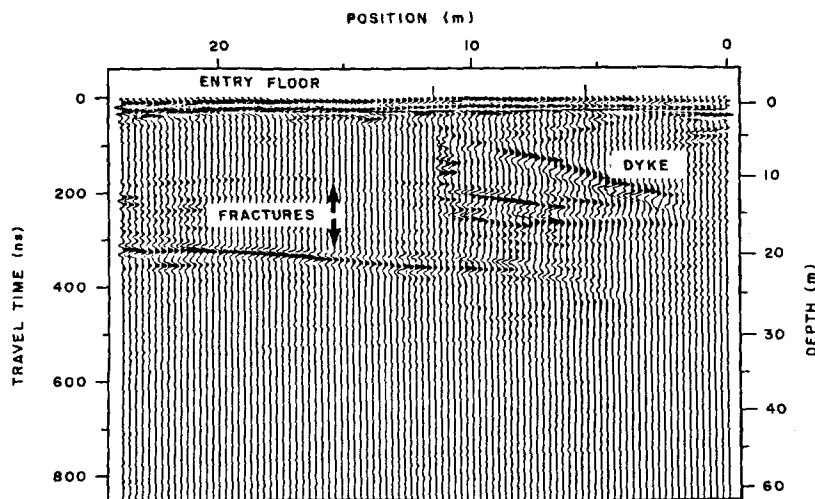


Figure 7. Radar record obtained in a tunnel in granite.

in the fine sand and overburden of eolian and fluvial origin. Because the data are in a form amenable to a wide variety of digital enhancement processing techniques, many other data presentations are possible.

Hydrogeologists have been studying the groundwater flow in this area for many years. A detailed knowledge of the bedrock topography and the soil strata are essential inputs for their groundwater flow model to predict the migration of contaminants. The radar has become an efficient method of extending the borehole information for detailed investigations in the area.

Bedrock mapping under a lake

In many instances knowledge of the bedrock topography under shallow lakes and rivers is required. Construction of dams, placer exploration, and mine engineering of crown pillars are typical examples. In this example, bedrock topographic relief under a lake had to be evaluated to determine the optimum location for a cofferdam to keep the

lake water out of a planned open pit mine. The survey was carried out in the winter and the radar soundings were acquired from the ice covered lake surface (Fig. 4). A low operating frequency (12.5 MHz) was selected to minimize the

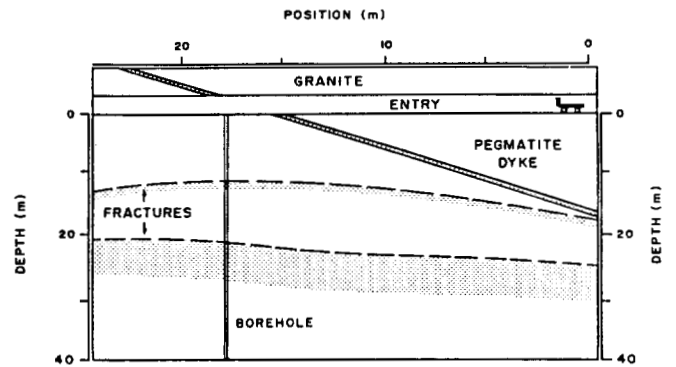


Figure 8. Geological section along the survey line in Figure 7.

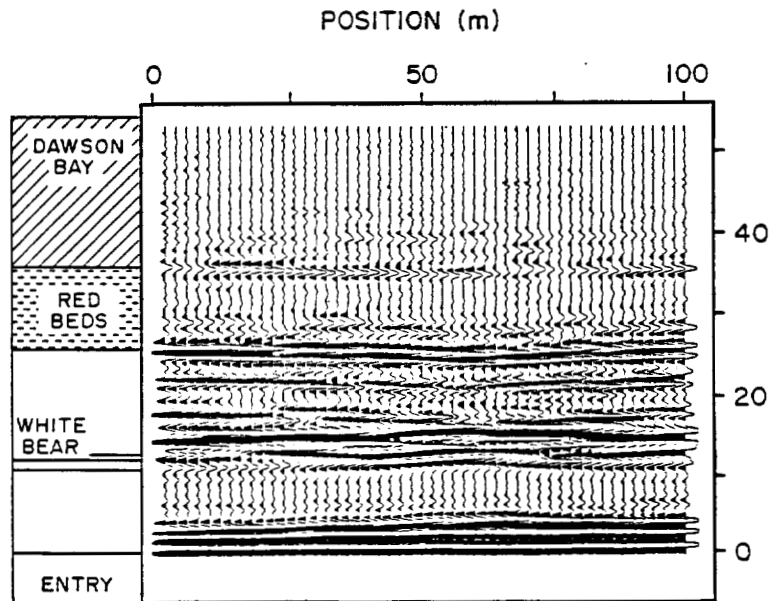
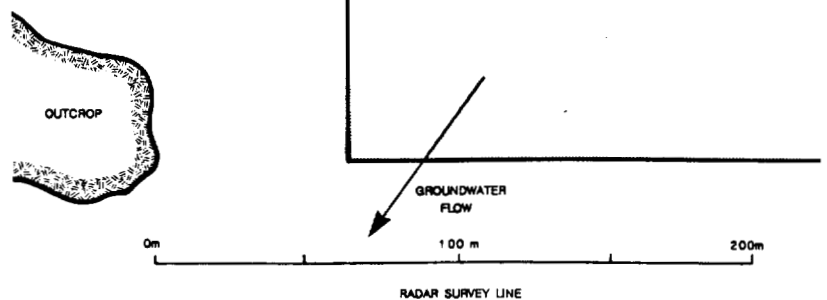


Figure 9. Geological section from potash mines in Saskatchewan beside a radar record obtained in the same mine.

Figure 10. Schematic plan of a landfill site showing a downgradient radar survey line.



attenuation in the clayey muck at the bottom of the lake and to reduce scattering from small scale subbottom stratigraphy (Davis et al., 1985).

Radar data obtained at 2 m station intervals along a survey line extending 150 m from shore are presented in Figure 5. The data have been compensated for the surface topography on shore. There is good correlation with three boreholes drilled near the radar survey line. We have interpreted the section (Fig. 6) using radar signal velocities of 0.1 m/ns in the overburden, 0.12 m/ns in the bedrock, 0.033 m/ns in water, and 0.05 m/ns in the gyttja.

A 2 km by 15 m grid was surveyed at this site and a bedrock knob under the lake defined by the radar data is to provide a base for the proposed dam.

Fracture detection in igneous bedrock

The radar can be used in tunnels to detect and map features such as changes in geology, fractures, and voids around the tunnels. The radar record (Fig. 7) was obtained in a tunnel in a granite pluton located in southeastern Manitoba. Figure 8 shows a geological section along the radar survey line.

The radar data correlate well with the logs from the borehole drilled at position 18 m. A reflection is obtained from a dry fracture zone about 0.5 m thick and 12 m below the floor. A water bearing fracture zone occurs at 22 m depth and a reflection is also detected from this zone. A pegmatite dyke intersects the adit dipping at about 45 degrees. The reflection from the dyke shows up on the data very clearly.

This example gives a good indication of the sensitivity of the radar to geological features in hard rock environments. Reflections from fractures at 50 m range have been routinely mapped by GPR in granitic rock. Further examples of data from this site are presented by Holloway (1992).

Geological mapping in sedimentary rock

The thickness of salt above mining level in potash mines is an important factor in controlling mining operations (Annan et al., 1988). In Saskatchewan potash mines, this information is used to design the mine for maximum safe extraction of potash in the salt which creeps and to assure that water does not enter the mine from the overlying saturated rock. Figure 9 shows the geological section from a potash mine in southwest Saskatchewan beside the radar section obtained from inside the mine at the same location.

The reflections on the radar data correlate well with known geology. A halite rich zone immediately above the mine entry generates a reflection at most masked by the transmission pulse. A sylvite rich zone about 1 m thick, called the White Bear, is located at 16 m. A further halite rich zone at a range of 22 m extends up to the Red Bed shales at 24 m above the mine entry. The radar data also show a reflection that correlates with the contact with the Dawson Bay limestones at a range of 35 m. Reflections from within the Dawson Bay formation are probably from the bedding planes in the limestone.

The GPR data mapped all the major stratigraphic horizons at the site and defined small scale variations that could not be mapped in any other manner. Mapping of the distance to the Red Beds above the mining horizon is important to the mine engineers because of the ever present concern about drilling into a water bearing formation. The radar also offers the potential of detecting anomalies such as brine pickets and solution collapse features prior to mining operations.

Leachate detection and mapping

Fresh, clean groundwater is becoming an increasingly valuable resource worldwide. In some areas careless disposal of wastes has greatly decreased the supply of potable water.

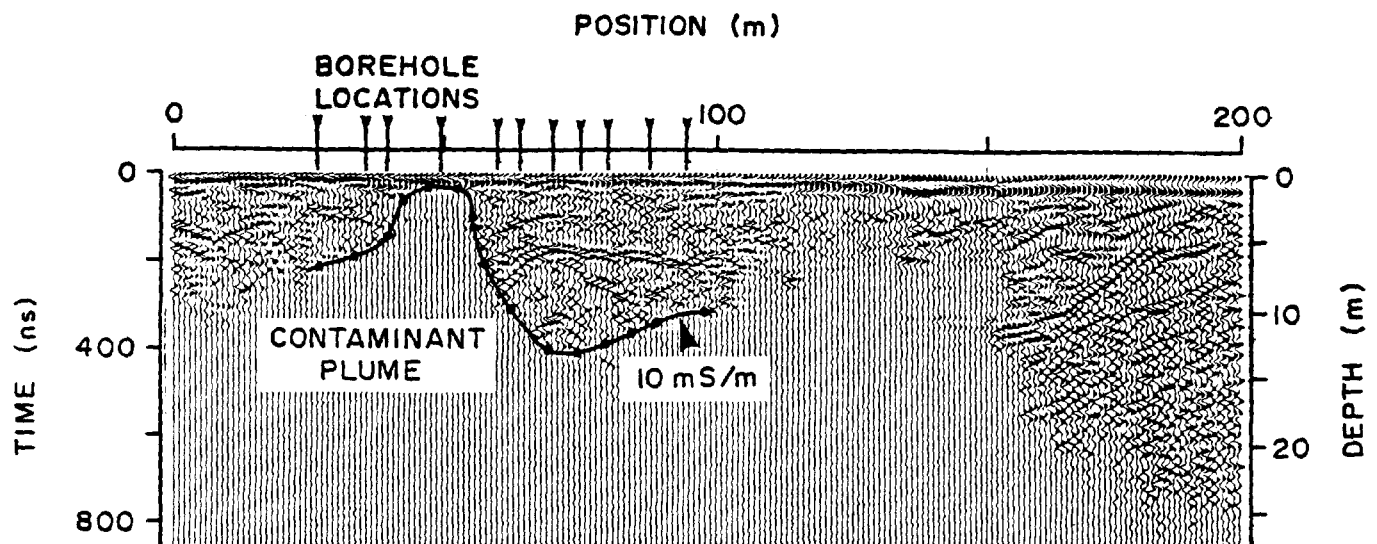


Figure 11. Radar record along the line shown on Figure 10. The area below the 10 mS/m line is interpreted to be in the contaminant plume.

Hydrogeologists frequently require methods to map the soil stratigraphy at waste disposal sites to assist in defining the extent of contamination emanating from the sites.

Figure 10 presents a schematic plan of a landfill site. Figure 11 presents the radar data along the survey line (Fig. 10), which is oriented orthogonal to the general groundwater flow direction. The soil is a fine sand of eolian and fluvial origins. The bedrock is about 20 m deep along most of this survey line but is only detected between stations 150-200 m. Most of the reflections on the data are from variations of grain size and density in the overburden. The zones where the radar reflections are weak or absent indicate the presence of contaminated leachate, which increases the electrical conductivity of the groundwater and strongly attenuates the radar signals.

The electrical conductivities of the groundwater have been measured at a number of boreholes along the survey line. The solid black line (Fig. 11) indicates the position below which the conductivity of the pore water is greater than 10 ms/m. Knowing that the soil type remains essentially the same along the line, the radar data indicate that the contaminant plume comes near the surface between 40 and 60 m as shown by the borehole data; it also extends between 110 and 150 m along the radar survey line at a depth of 6 m below the existing surface. This type of information permits us to monitor the migration of contaminants in coarse grained soils. Radar data such as these are extremely useful for planning where to place monitoring wells around a waste impoundment site.

CONCLUSIONS

We have presented data from case histories representing a wide variety of geological settings and problems, from which we conclude the following:

- Radar can be used in a wide range of environments either on the surface or in mines.
- Radar technique provides high resolution soundings to a range of 50 m in resistive environments.

- Radar can be used to map overburden thickness, soil stratigraphy, changes of geology, fractures in bedrock, and leachate plumes in soils.
- Radar provides a powerful means for developing geological sections and tracing continuity in geological unit defined by limited borehole information.

As with any geophysical method, the GPR method is only effective in geological environments where electrical conductivity is low. The best environments exhibit conductivities less than 1 ms/m.

ACKNOWLEDGMENTS

The authors wish to acknowledge support received from the Geological Survey of Canada, DSS, and NRC PILP program for the development of the A-Cubed Inc. pulseEKKO III radar system. They especially wish to acknowledge the continuing enthusiastic encouragement and support of Len Collett and Jean Pilon of the Geological Survey of Canada. In addition, they thank those clients whose data are used for the case histories.

REFERENCES

- Annan, A.P. and Davis, J.L.
1992: Design and development of a digital ground penetrating radar system; in *Ground penetrating radar*, J.A. Pilon (ed.); Geological Survey of Canada, Paper 90-4.
- Annan, A.P., Davis, J.L., and Gendzwill, D.
1988: Radar sounding in potash mines, Saskatchewan, Canada; *Geophysics*, v. 53, p. 1556-1564.
- Davis, J.L. and Annan, A.P.
1989: Ground penetrating radar for high-resolution mapping of soil and rock stratigraphy; *Geophysical Prospecting*, v. 37, p. 53 - 551.
- Davis, J.L., Annan, A.P., Black, G., and Leggatt, C.D.
1985: Geological sounding with low frequency radar; in *Extended abstracts, 55th Annual International Meeting of the Society of Exploration Geophysicists*, Washington, D.C.
- Holloway, A.L.
1992: Fracture mapping in granite rock using ground probing radar; in *Ground penetrating radar*, J.A. Pilon (ed.); Geological Survey of Canada, Paper 90-4.

Application of ground penetrating radar to a study of peat stratigraphy: preliminary results

D.C. Nobes¹ and B.G. Warner²

Nobes, D.C. and Warner, B.G., 1992: Application of ground penetrating radar to a study of peat stratigraphy: preliminary results; in *Ground penetrating radar*, ed. J. Pilon; Geological Survey of Canada, Paper 90-4, p. 133-138.

Abstract

Previous studies on the utility of ground penetrating radar (GPR) for peat inventories have met with mixed results. In our current study of the correlation of stratigraphy and physical properties of peat with the GPR response, the first site selected was Ellice Swamp, near Stratford, Ontario. A suite of 17 cores were obtained at a spacing of about 100 m. Each core was analyzed for stratigraphy, wet bulk density, water content, organic matter content, and humification at 10 cm intervals. Cross-sections compiled for each of these parameters were compared with the GPR profile. The GPR data were taken at 1 m intervals across the same transect in Ellice Swamp. Preliminary processing of the GPR data reveal some important insights on the utility of GPR in peatland inventories. The base of the peat yields a strong, clear reflection event. The character of the event is simpler where limnic peat and gyttja are lacking above the basal silty clay. Where limnic peat and gyttja are present, the event is more complex. The surface aerobic zone has a number of small events that are obscured in some places by the multiples from the thin snow and ice cover. The GPR response shows a marked transition between the surface aerobic and the underlying anaerobic zones. The anaerobic peat layers contain relatively few internal reflectors and appear to be relatively homogeneous and transparent to GPR.

Résumé

Les études antérieures portant sur l'utilité du géoradar pour inventorier les tourbières ont donné des résultats partagés. Dans la présente étude de la corrélation de la stratigraphie et des propriétés physiques de la tourbe avec la réponse du géoradar, le premier endroit choisi a été le marécage Ellice, près de Stratford (Ontario). On a prélevé une série de 17 carottes selon un espacement d'environ 100 m. Dans chaque carotte, on a analysé la stratigraphie, la masse volumique apparente humide, la teneur en eau, la teneur en matières organiques et l'humidification à des intervalles de 10 cm. Les coupes compilées pour chacun de ces paramètres ont été comparées au profil établi par géoradar. Les données géoradar ont été recueillies à des intervalles de 1 m le long du même transect traversant le marécage Ellice. Le traitement préliminaire des données géoradar donnent quelques indices importants sur l'utilité du géoradar pour inventorier les tourbières. La base de la tourbe produit une réflexion forte et nette. Cette réflexion est plus simple lorsque l'argile silteuse basale n'est pas recouverte de tourbe lacustre ni de gyttja. Lorsque la tourbe lacustre et le gyttja sont présents, l'événement est plus complexe. La zone aérobie en surface donne un certain nombre de petits événements qui sont obscurcis par endroits par les multiples que produit une mince couche de neige et de glace. La réponse du géoradar indique une transition marquée entre les zones aérobies superficielles et anaérobies souterraines. Les couches de tourbe anaérobies contiennent relativement peu de réflecteurs internes et elles semblent être relativement homogènes et transparentes aux signaux émis par le géoradar.

¹ Department of Geology, University of Canterbury, Private Bag 4800, Christchurch, New Zealand. Formerly at the Department of Earth Sciences, University of Waterloo, Waterloo, Ont.

² Department of Geography and Quaternary Science Institute, University of Waterloo, Waterloo, Ontario N2L 3G1

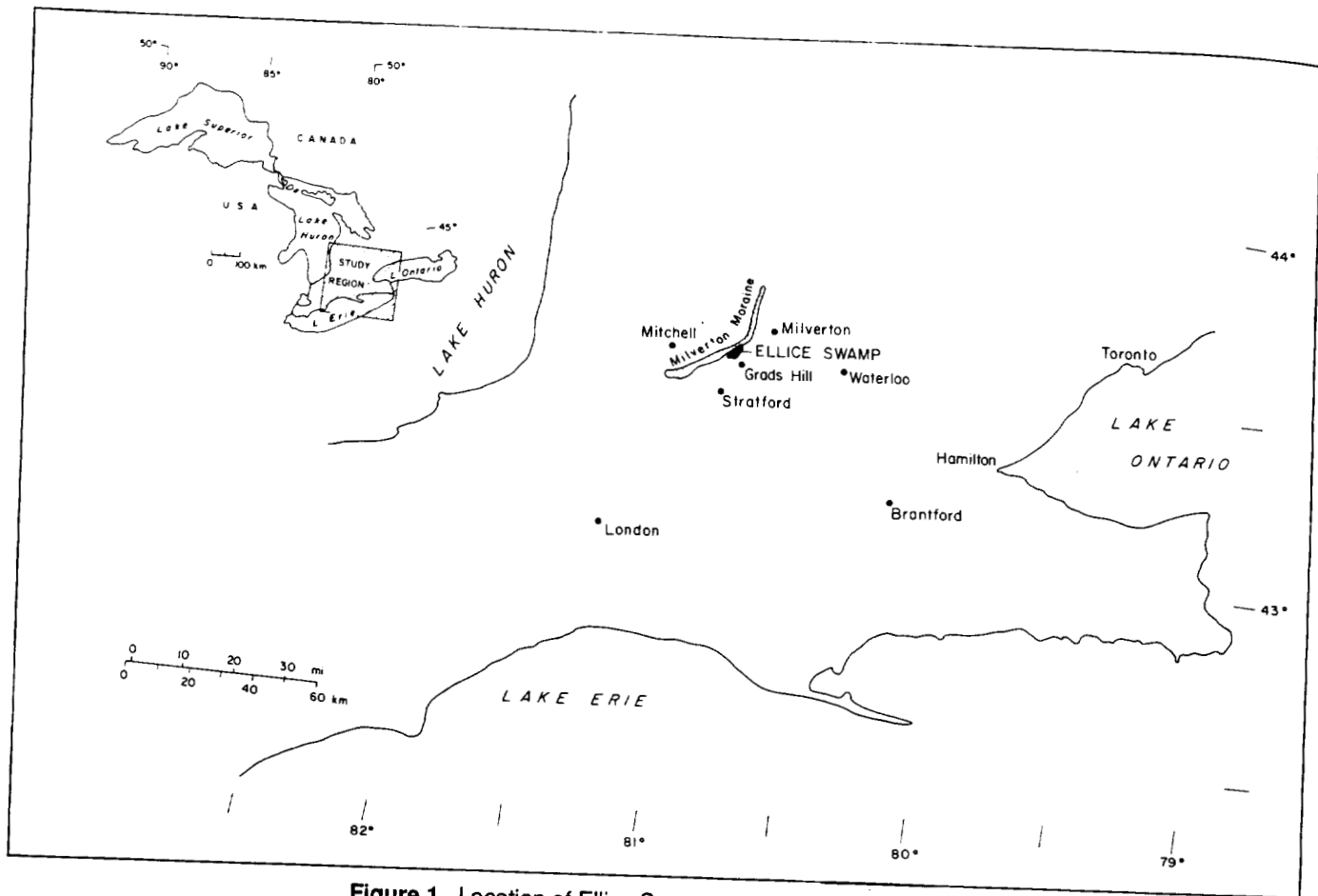


Figure 1. Location of Ellice Swamp, near Stratford, Ontario.

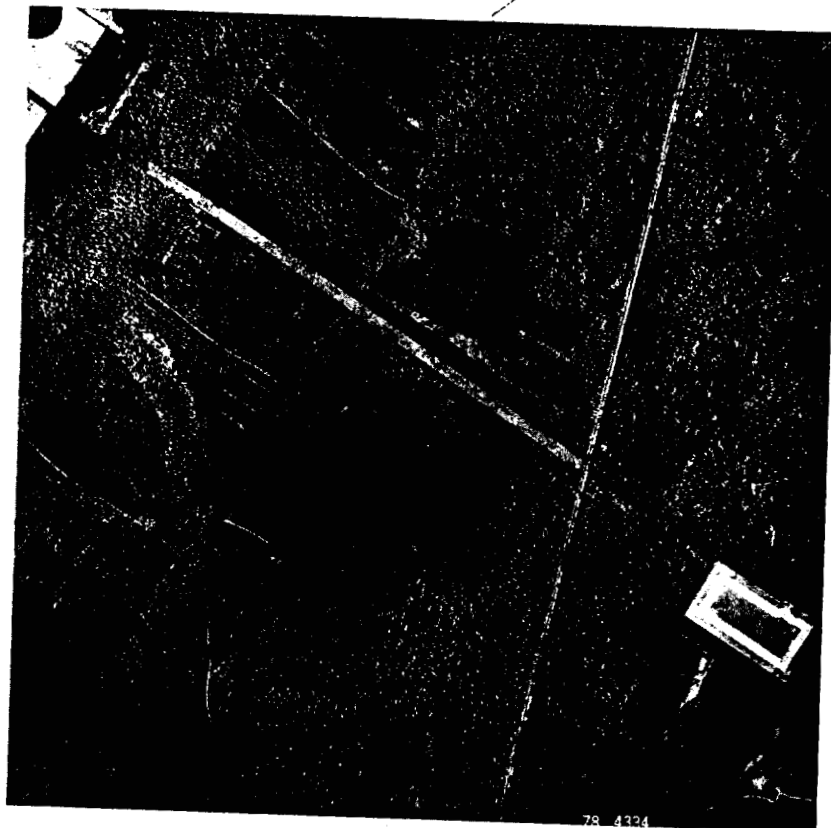


Figure 2. Aerial photograph of Ellice Swamp. The position of the cutline used for the core and GPR profiles is marked (arrows).

INTRODUCTION

Peatlands, common in northern latitudes, constitute a potentially important economic resource. Canada has the second largest peat reserves in the world (Zoltai and Pollett, 1983). Ontario alone ranks third, with an estimated 26 million hectares of peatlands (Korpiljaakko, 1981). Peat inventories are normally conducted by extensive mapping and coring programs that are time consuming. A simple and relatively fast method for mapping peat stratigraphy and estimating peat volumes would aid in peat inventories. We have begun a systematic study to test the utility of ground penetrating radar (GPR) in mapping the areal and stratigraphic extent of peatlands, with the goal of establishing GPR as a simple and effective tool for peat inventories.

Previous studies on the correlation of the GPR response and the peat physical properties have been inconclusive. Some studies found a strong correlation between the permittivity (the dielectric coefficient) and the volume and energy content of the peat (Tolonen et al., 1982; Tiuri et al., 1983, 1984). On the other hand, Ulriksen (1982) found no correlation between the permittivity and the energy content. All researchers noted a correlation with bulk density, which is strongly dependent on the water content. Because GPR responds to changes in the permittivity, then the peat properties could, in principle, be mapped using GPR.

The purpose of our study was to conduct an intensive field program to compare the GPR response with the results of detailed physical analyses of peat cores. Work on the raw GPR field data study is not yet complete, but preliminary results are most encouraging. The GPR section accurately reflects peat stratigraphy, in particular the transition from the surface aerobic to the underlying anaerobic zone; also the basal peat-mineral transition is readily apparent. Further analysis is required, and this work will be extended to other sites and peatland types in the future.

SITE DESCRIPTION AND STUDY METHODOLOGY

The first site selected for the study was Ellice Swamp, near Stratford in southern Ontario (Fig. 1). The bog has developed on the eastern flank of Milverton Moraine (Karrow, 1971). Shortly after deglaciation, drainage was impeded, which led to local ponding during which lacustrine silts and clay were deposited. Silty gyttja, gyttja, and limnic peat represent open-water deposits prior to onset of peatland development. Moss peat with abundant *Scorpidium scorpioides* and sedge remains form the main body of the peat. Overlying this peat, a distinct near surface layer is represented by a well decomposed, amorphous, black detrital peat with abundant wood. Finally, modern *Sphagnum* peat forms a thin layer about 30-50 cm thick at the surface with black spruce and tamarack cover.

The bog is situated on a height of land between the north branches of the Thames and Nith Rivers. Black Creek flows through the bog and drains northward to Nith River. Two artificial drainage ditches form the present western and

eastern boundaries of the bog. The vegetation of the modern bog reflects disturbance by artificial drainage, frequent fires, peat mining activities, recreational sports trails, and red pine plantations. A Canadian National Rail line runs northwards through the bog.

The core and GPR profiles were taken along a cutline running northwest through Ellice Swamp (Fig. 2). The GPR profiles were obtained using the A-Cubed (now Sensors and Software) pulseEKKO III with a nominal signal frequency of 100 kHz. Cores were taken at 100 m intervals; additional cores were taken concurrently with the GPR profile. The stratigraphy of each of the 17 peat cores was recorded. Subsamples, taken every 10 cm along each core were analyzed for wet bulk density, water content, degree of humification, and organic matter content. Cross-sections were compiled for each physical parameter.

The GPR data were gathered at 1 m intervals across the bog, using a common offset technique. The GPR transmitter and receiver antennae were maintained at a constant separation of 40 cm, as the system was stepped across the bog. To date, preliminary filtering of the raw radar records has removed some of the response caused by the snow and ice that covered the bog at the time of the GPR survey. The 20-30 cm thick ice layer caused the GPR signal to reflect numerous times within the ice layer, giving rise to a number of multiples. These multiples appear as banded "events" across the GPR section, which at times obscure the reflected arrivals from the peat. An overall GPR section was constructed by averaging five GPR records to yield an average record every 5 m for the length of the bog. The net presentation thus consists of almost 300 records, rather than almost 1500 raw GPR records. This leads to some loss of detail, but the noise is reduced by averaging adjacent records.

RESULTS AND DISCUSSION

The cross-sections for water content, humification, organic matter content, and wet bulk density are shown in Figures 3A-D. Some correlation exists between the individual parameters, especially humification and organic matter content, and bulk density and stratigraphy (Fig. 4A). The most direct correlation between the preliminary GPR section and the peat properties can be made with the peat stratigraphy and the peat bulk density. The GPR appears to be responding primarily to density changes associated with stratigraphic variations. The GPR section and stratigraphy are shown for comparison in Figures 4A, B. A number of important features can be identified.

The basal silty clay gives rise to a strong clear reflective event on the GPR profile (event "A"). The silty clay is commonly overlain by a thin layer of limnic detritus, limnic peat and gyttja. Where the layer of detritus is present, the reflection from the basal clay is more complex (event "B"); where the detritus is absent, the basal reflection is simpler in character (event "C"). Finally, the transition from the aerobic to the anaerobic zone is well delineated (event "D"). The aerobic zone contains a number of small events. The

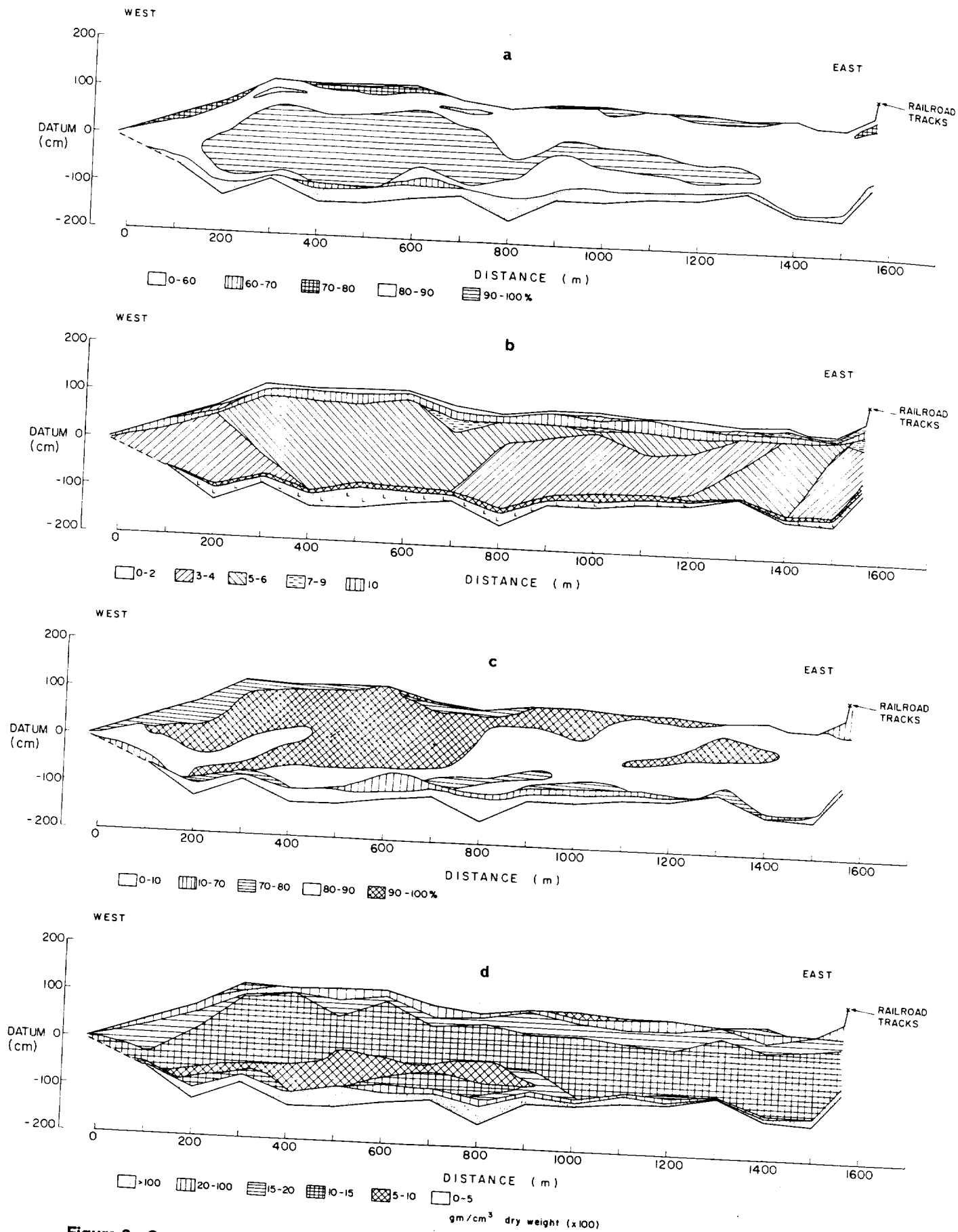


Figure 3. Cross-sections for **A.** percent moisture content from core analyses; **B.** degree of humification; **C.** percent organic matter content; and **D.** wet bulk density.

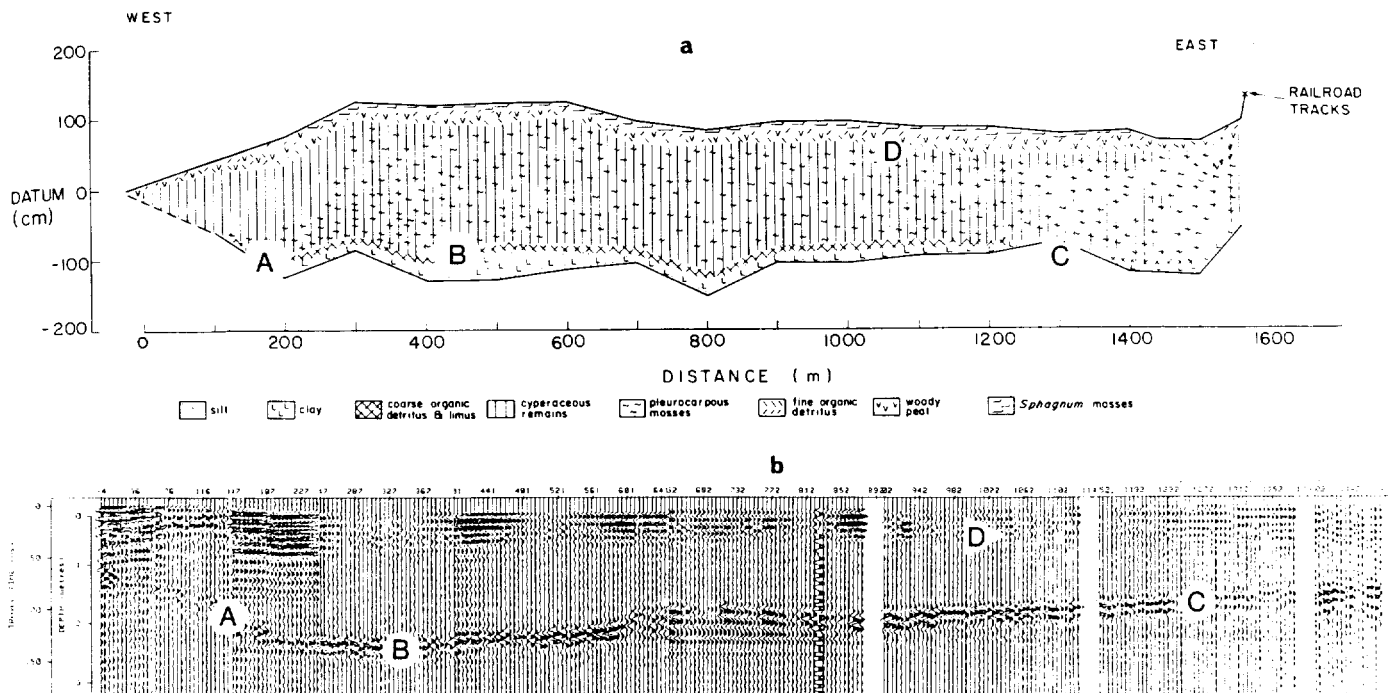


Figure 4. Comparison of the stratigraphy (A) and the GPR response (B) along the Ellice Swamp cutline. The major features are event "a", the transition from the peat to the underlying silty clay; event "b", the more complex reflection which occurs where limnic peat and gyttja are present; event "c", the simpler event where the limnic detritus is absent; and event "d", the transition from the surface aerobic to the underlying anaerobic zone.

underlying anaerobic zone appears to be relatively transparent to GPR signals, and we do not note any events within the anaerobic zone.

CONCLUSIONS

This study represents one of the first serious attempts to compare the physical properties of the peat with the GPR response by compiling cross-sections for each parameter for a single site in southern Ontario. We believe that it would be premature to speculate on wide-ranging applications of the technique. Our tests to date demonstrate great promise for GPR as a tool in assessing both the spatial and vertical extent of peat. However, the real applicability of GPR in peat inventories must await further testing in a much larger suite of peatland types throughout Ontario.

Peatlands are complex ecosystems that vary stratigraphically and areally. Peat has numerous characteristics that depend upon the botanical composition and state of decomposition. These factors in turn can control a variety of other peat parameters. Hence, we cannot assume that GPR will be a viable tool in all peatland types, because a whole spectrum of peat-forming systems exist that differ topographically, hydrologically, and morphologically. However, the real applicability of GPR in peat inventories has been addressed by additional testing both in Ellice Swamp (Warner et al., 1990) and elsewhere (Theimer, 1990).

ACKNOWLEDGMENTS

Our thanks go to R. Balloch, J. Easton, D. Gorling, R. Greenly, K. Hanf, H. Kubiw, and G. Schneider for field and laboratory assistance. Drafting was done by N. Bahar. We acknowledge the support of the Ontario Geological Research Fund.

REFERENCES

- Karrow, P.F.**
1971: Quaternary geology of the Stratford-Conestoga area, Ontario; Geological Survey of Canada, Paper 70-34.
- Korpijaakko, E.**
1981: A preliminary estimate of Ontario's peat resources; in Proceedings, Symposium on Peat, Thunder Bay, Ontario, p. 321-330.
- Theimer, B.D.**
1990: Principles of bog characterization using ground penetrating radar; M.Sc. Thesis, University of Waterloo, Waterloo, Ont.
- Tiuri, M., Toikka, M., Martilla, I., and Tolonen, K.**
1983: The use of radio wave probe and subsurface interface radar in peat resource inventory; a Proceedings, Symposium on Remote Sensing in Peat and Terrain Resource Surveys, Aberdeen, Scotland, p. 131-143.
- Tiuri, M., Toikka, M., Tolonen, K., and Rummukainen, A.**
1984: Capability of new radiowave moisture probe in peat resource inventory; Proceedings, 7th International Peat Congress, Dublin, Ireland, p. 517-525.
- Tolonen, K., Tiuri, M., Toikka, M., and Saarihahti, M.**
1982: Radiowave probe in assessing the yield of peat and energy in peat deposits in Finland; Suo, v. 33, p. 105-112.
- Ulriksen, C.P.F.**
1982: Application of Impulse Radar to Civil Engineering; Ph.D. Thesis, Lund University of Technology, Sweden.

Warner, B.G., Nobes, D.C., and Theimer, B.D.

1990: An application of ground penetrating radar to peat stratigraphy of Ellice Swamp, southwestern Ontario; Canadian Journal of Earth Sciences, v. 27, p. 932-938.

Zoltai, S.C. and Pollett, F.C.

1983: Wetlands in Canada: their classification, distribution, and use; in Ecosystems of the World, v. 4B, Mires: Swamp, Bog, Fen, and Moor, A.J.P. Grove (ed), Elsevier Publ. Co., Amsterdam, p. 245-268.

Ground probing radar in the investigation of permafrost and subsurface characteristics of surficial deposits in Kangiqsualujjuaq, northern Quebec

J.A. Pilon¹, M. Allard², and M.K. Séguin²

Pilon, J.A., Allard, M., and Séguin, M.K., 1992: Ground probing radar in the investigation of permafrost and subsurface characteristics of surficial deposits in Kangiqsualujjuaq, northern Quebec; in Ground penetrating radar, ed. J. Pilon; Geological Survey of Canada, Paper 90-4, p. 165-175.

Abstract

Four geomorphological units were probed with ground penetrating radar (GPR) to investigate the internal structure and composition of surficial deposits near Kangiqsualujjuaq on the east coast of Ungava Bay. The results obtained in the field have furnished information on the active layer, details of the internal stratigraphy, as well as the location of the base of ice-bearing permafrost. These results illustrate that GPR is a useful geophysical tool for the study of surficial deposits in areas of permafrost.

Résumé

Quatre unités géomorphologiques ont été sondées à l'aide d'un géoradar pour en étudier la structure interne et la composition des dépôts de surface près de Kangiqsualujjuaq sur la côte est de la baie d'Ungava. Les résultats obtenus sur le terrain ont donné des renseignements sur le mollisol et des détails sur la stratigraphie interne et la profondeur de la base du pergélisol contenant de la glace. Ces résultats illustrent le fait que le géoradar constitue un outil géophysique utile à l'étude des dépôts de surface dans les zones pergélisolées.

INTRODUCTION

In the Canadian Arctic, detailed studies of permafrost and structure of surficial deposits are limited by the lack of both cores from boreholes and natural sections. In the last decade geophysical methods have increasingly been used to investigate surficial deposits (Séguin and Allard, 1987; Scott et al., 1978). Recently, the availability of a high power, multifrequency, digital ground probing radar (GPR) system to the Geological Survey of Canada has significantly increased our ability to profile and investigate the internal makeup of surficial deposits (LaFlèche et al., 1987). In this paper we present the results of four GPR surveys conducted over different Quaternary substrates during the summer of 1986 in Kangiqsualujjuaq on the east coast of Ungava Bay in

northern Québec. At this location, staff of the Centre d'Etudes Nordiques of Université Laval have conducted detailed studies of permafrost since 1984 (Allard and Séguin, 1987; Fournier et al., 1987; Gahé et al., 1987; Séguin and Allard, 1987). Through these activities, a variety of Quaternary geological deposits have been instrumented with multithermistor cables to study permafrost characteristics and investigated by varied geophysical methods comprising electrical resistivity, induced polarization, self-potential and electromagnetic surveys (Gahé et al., 1987). In addition, both natural and artificial sections through the deposits are also available; the Kangiqsualujjuaq region thus constituted an ideal test site for the GPR because of the substantial body of knowledge available to help with the interpretation of the radar survey results.

¹ Geological Survey of Canada, 601 Booth Street, Ottawa, Ontario, Canada, K1A 0E8

² Université Laval, Centre d'Etudes Nordiques, Québec, Canada, G1K 7P4

REGIONAL SETTING

The Kangiqsualujjuaq region (Fig. 1) is situated on the treeline; black spruce and tamarac occur in sheltered valleys south and up to 40 km northeast of the village. The regional treeline appears to be maintained a few kilometres inland because of the climatic influence of Ungava Bay (Payette, 1983). The climate of the region is characterized by low daily thermal amplitude in summer and large daily thermal amplitude in winter with the frost season carrying well into June (Thériault, 1983). The average annual temperature is estimated at -5.3°C ; that of January at -22°C and that of July

at 9°C (Fournier et al., 1987). The annual total precipitation is estimated to be between 350 and 400 mm, of which 40–45% occurs as snow (Wilson, 1971). Prevailing winds measured at the Centre d'Études Nordiques weather station in Kangiqsualujjuaq are predominantly west-southwest.

The surficial materials are influenced by the history of glacial, periglacial, and marine events and comprise the following major classes: (1) bedrock, usually exposed on moderate to steep slopes below marine limit at about 100 m above mean sea level (asl); (2) till, mantling plateaus and slopes, where it has been subject to modification by solifluction or wave washing, or both; (3) sands and gravels of glaciofluvial and deltaic origin; (4) silty clays of marine origin on valley floors below 100 m asl; (5) sands and gravels forming raised beaches; (6) organic deposits forming peat plateaus, palsas, and peat hummocks; (7) intertidal mud flats strewn with boulders.

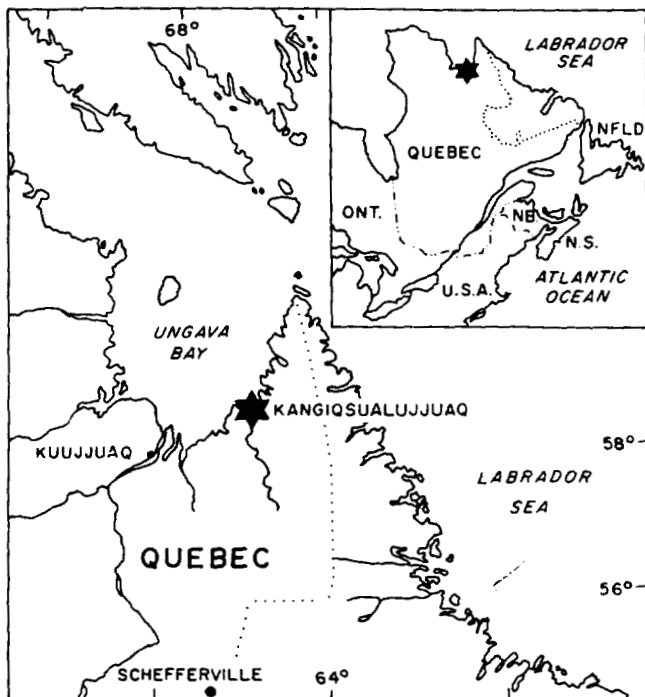


Figure 1. Site location of Kangiqsualujjuaq, northern Québec.

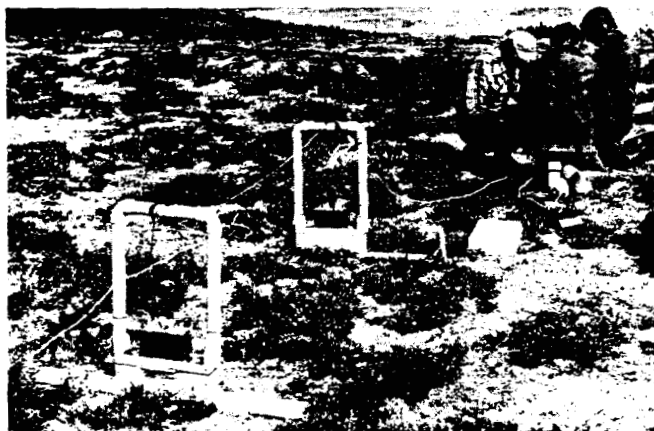


Figure 2. The pulse EKKO III ground probing radar system, on the marine terrace in Kangiqsualujjuaq. The system consists of transmitter and receiver antenna packages and a central control unit. The various units are connected by fibre optic cables.



Figure 3. Photograph of a section at site 1 showing thick, bouldery till overlain by 1 m of fluvial sands, above an unconformity; the radar profile was made on top of this terrace.

Table 1. Typical dielectric constant, electrical conductivity, velocity and attenuation observed in common geologic material ($f = 100 \text{ MHz}$) (after Annan, 1983)

| Material | K | $\sigma(\text{mS.m}^{-1})$ | $v(\text{m.ns}^{-1})$ | $\alpha(\text{dB.m}^{-1})$ |
|----------------------------|-------|----------------------------|-----------------------|----------------------------|
| Air | 1 | 0 | 0.3 | 0 |
| Distilled Water | 80 | 0.01 | 0.033 | 2×10^3 |
| Fresh Water | 80 | 0.5 | 0.033 | 0.1 |
| Sea Water | 80 | 3000 | 0.01 | 10^3 |
| Dry Sand | 3-5 | 0.01 | 0.15 | 0.01 |
| Fresh Water Saturated Sand | 20-30 | 0.1-1.0 | 0.06 | 0.3 |
| Limestone | 4-8 | 0.5-2.0 | 0.12 | 0.7 |
| Shales | 5-15 | 1-100 | 0.09 | 5 |
| Silts | 5-30 | 1-100 | 0.07 | 6 |
| Clays | 5-40 | 2-1000 | 0.06 | 15 |
| Granite | 4-6 | .01-1 | 0.13 | 0.07 |
| Dry Salt | 5-6 | .01-1 | 0.13 | 0.06 |
| Ice | 3-4 | 0.01 | 0.16 | 0.01 |

The study sites discussed in this paper were selected to represent these surficial deposits and include till, wave reworked glaciofluvial deposits, marine clay silt, and peat.

METHOD

Ground probing radar is a relatively new geophysical tool. The first commercial model became available in the mid 1970s. GPR operates on the same principle as conventional radars in that a short pulse of electromagnetic energy is emitted by a transmitter antenna, reflects off a distant electrical boundary, and the reflection is picked up by a receiver antenna. The time taken for the pulse to travel from the transmitter to the receiver antenna via the reflector is measured (Davis and Annan, 1989), and the distance to a reflector can be calculated when the propagation speed of the pulse in the material is known. The propagation velocity can be measured in situ by conducting a common mid point (CMP) or a wide angle reflection and refraction survey. In air, the pulse travels at the speed of light (0.3 m/ns). In the subsurface, the pulse travels slower dependent upon the electrical properties of the material traversed. Table 1 presents typical dielectric constants, electrical conductivities, velocities of propagation, and attenuation factors observed in common geological materials for a frequency of 100 MHz.

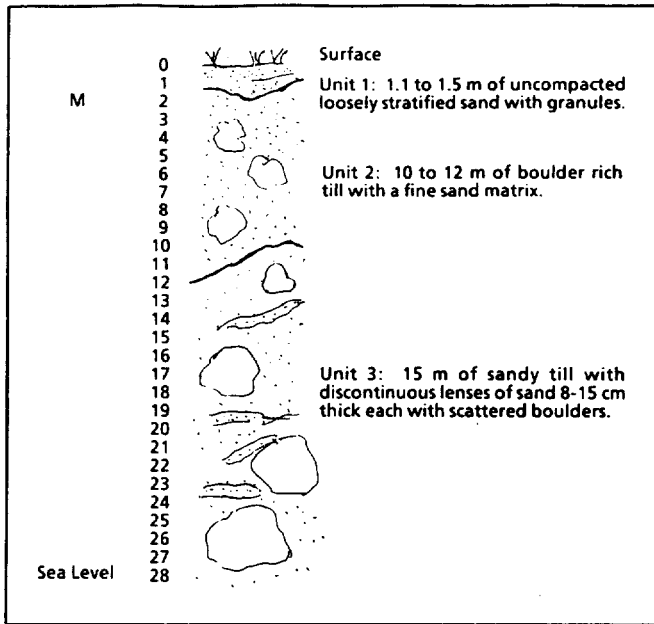


Figure 4. Stratigraphy at site 1, a fluvial terrace cut in a thick, bouldery till deposit as measured in the cliff face.

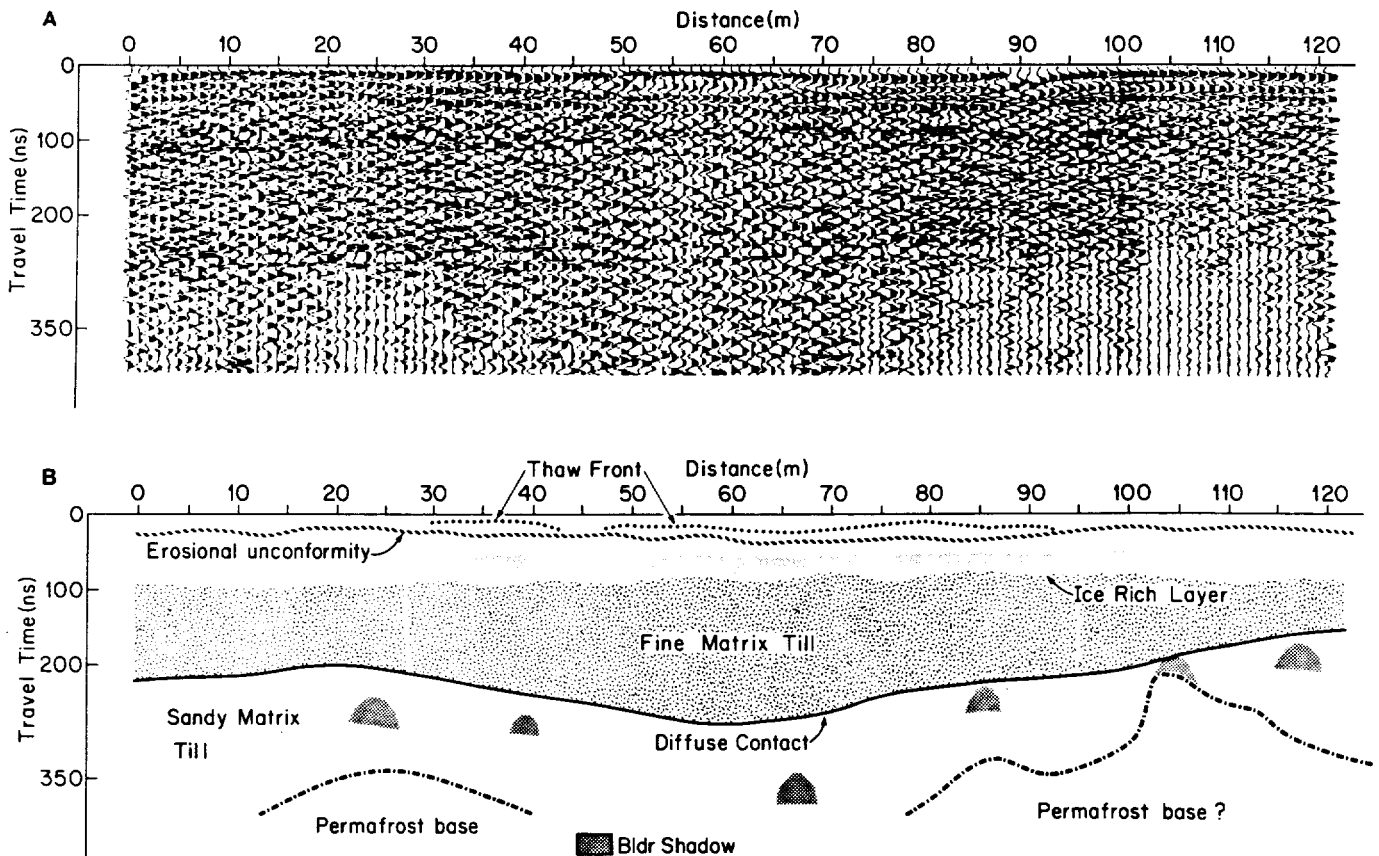


Figure 5A. The 100 MHz ground probing radar profile obtained at site 1 in Kangiqsualujuaq; **B.** The summary interpretation diagram of the same profile.

Reflectors detected with a GPR system are caused by dielectric contrast in the subsurface materials. Common causes of subsurface reflections are material interfaces (overburden-rock, sand-clay, and so on), water table limits, boundaries between frozen and unfrozen water, and ice lenses. A large dielectric contrast exists between water and most geological materials (Table 1). As such, the presence or absence of water controls to a large degree the subsurface propagation characteristics of the radar pulse (see contrast between dry and freshwater saturated sand; Table 1). Thus

the ability of a material to retain water within its pore space is an important factor in the determination of its bulk electrical properties. The depth to which a radar pulse will effectively penetrate depends on the electromagnetic absorption characteristics of the subsurface (see Table 1). The pulseEKKO III system used in this study (Fig. 2) is a fully digital, ground probing radar system with a system performance of 150 dB, which incorporates signal stacking and digital data processing (LaFlèche et al., 1987).

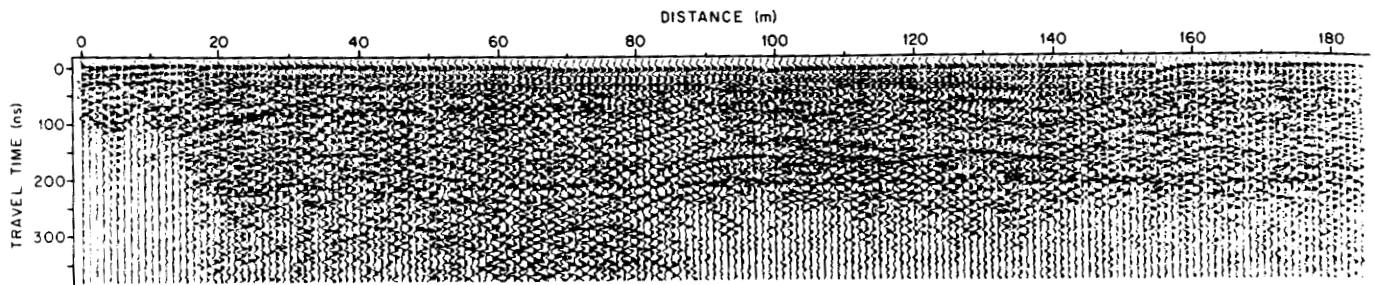


Figure 6. Ground probing radar survey results obtained at site 2, a sandy marine terrace.



Figure 7.

Photographic view of the large borrow pit 200 m southeast of the radar survey line at site 2 in Kangiqsualujuaq; steeply dipping gravel beds can be seen in the centre of the picture.

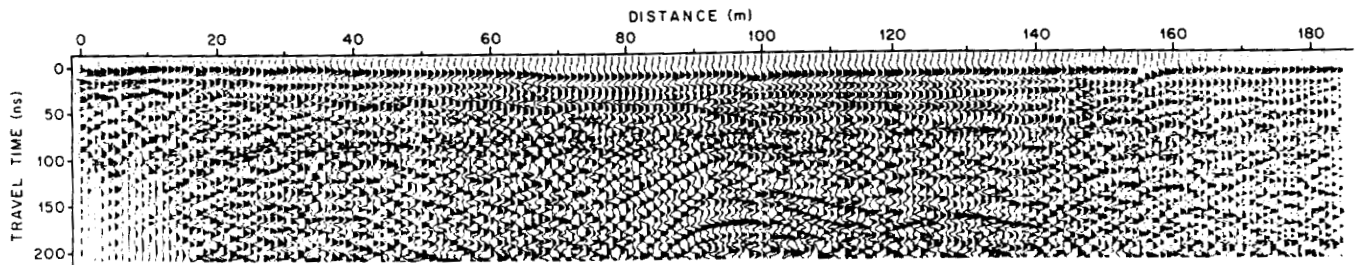


Figure 8. Enlargement of the first 200 ns of radar data in site 2; note the strong reflectors indicating the unconformity around 50-60 ns.

COMMON DEPTH POINT - SOUNDING
ANTENNA SEPARATION (m)

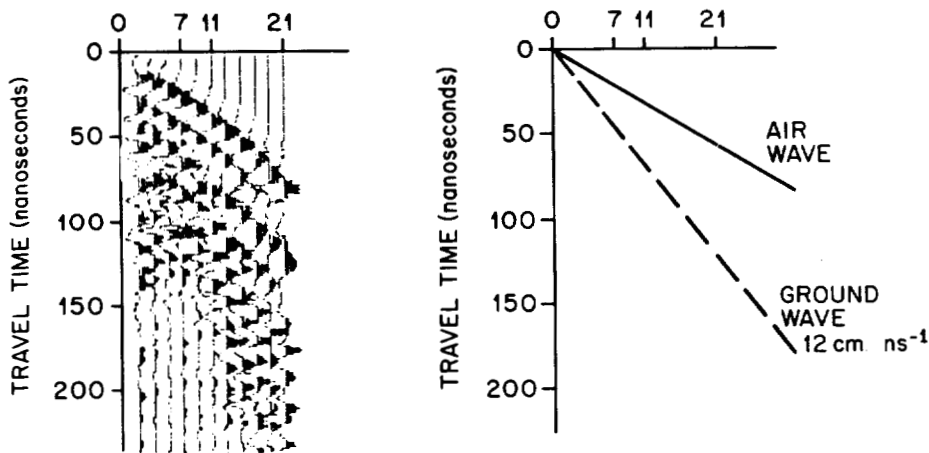


Figure 9.

CMP survey obtained on the marine terrace to determine the ground wave propagation speed at site 2 in Kangiqsualujuaq.

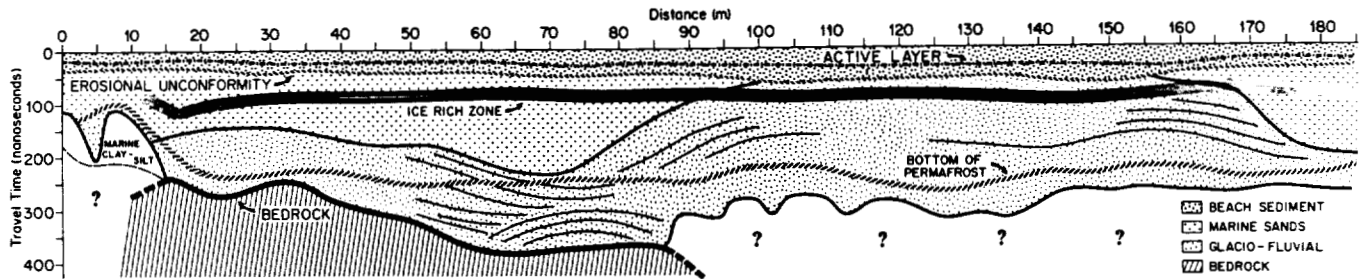


Figure 10. Interpretation sketch of the radar results obtained at site 2.



Figure 11.

Permafrost mounds in clay-silt near the shoreline; near ground is the surface of site 3A. (Arrow points at site 3B.)

SITE INVESTIGATIONS

The Kangiqsualujjuaq site 1 is a fluvial terrace cut in a thick, bouldery till deposit (Fig. 3). The stratigraphy is well known from the numerous sections along George River (Fig. 4). The contact between units 1 and 2 is sharp with a boulder lag, whereas the contact between units 2 and 3 is gradual and diffuse. The GPR survey at site 1 was conducted at a frequency of 100 MHz, along a 121 m transect parallel to the cliff face some 25-30 m inland. A CMP survey carried out at this site yielded a ground wave propagation speed of 12 cm/ns.

As can be seen on the radar profile (Fig. 5A) and its summary interpretation diagram (Fig. 5B), the contact between units 1 and 2 appears at about 30 ns (± 1.5 m) and can be traced for the full length of the transect (Fig. 5A, B). At the time of survey, in August, the initial radar reflector corresponds roughly to the thaw depth. In part of the radar profile, however, between points 30, 45, 50, and 92, a separation indicates divergence of the stratigraphic and thermal contacts. At a depth of about 80 ns (± 5 m) an undulating and irregular reflector most likely indicates an ice rich zone in the upper permafrost layer. Between survey points 75 and 120 the diffuse contact between the upper finer till and the lower sandier till is visible at about 200 ns (± 12 m).

A faint irregular reflector around 350 ns (about 21 m) is tentatively interpreted as the permafrost base. The latter compares favourably with the results of an induced polarization survey carried out on the same line (Gahé, 1988). Large boulders of 2-4 m in diameter, as observed in the geological section, are apparent in the profile at depth as point reflectors shadowing what lies underneath (Fig. 5A, B).

Site 2 is a sandy marine terrace at about 20 m asl composed of glaciofluvial deposits. A 50 m wide section in a large and deep borrow pit 200 m southeast of the transect line lies parallel to the survey axis and contains an erosional contact between wave reworked sand and gravel, and truncated glaciofluvial structures near the surface. The radar survey results discussed here are those obtained at a frequency of 100 MHz along a 185 m traverse using a 2 m antenna separation and an interval between survey points of 1 m (Fig. 6). The borrow pit allows some direct observation of the geological setting (Fig. 7). Beginning at 38 m along the transect, the axis of the radar survey follows a conspicuous beach ridge, which can be clearly seen in Figure 6.

Figure 8 shows an enlargement of the first 200 ns of radar data along this transect. Figure 9 is a CMP survey along this profile indicating that the ground wave propagation speed in this material is 12 cm/ns. Bedrock topography beneath the

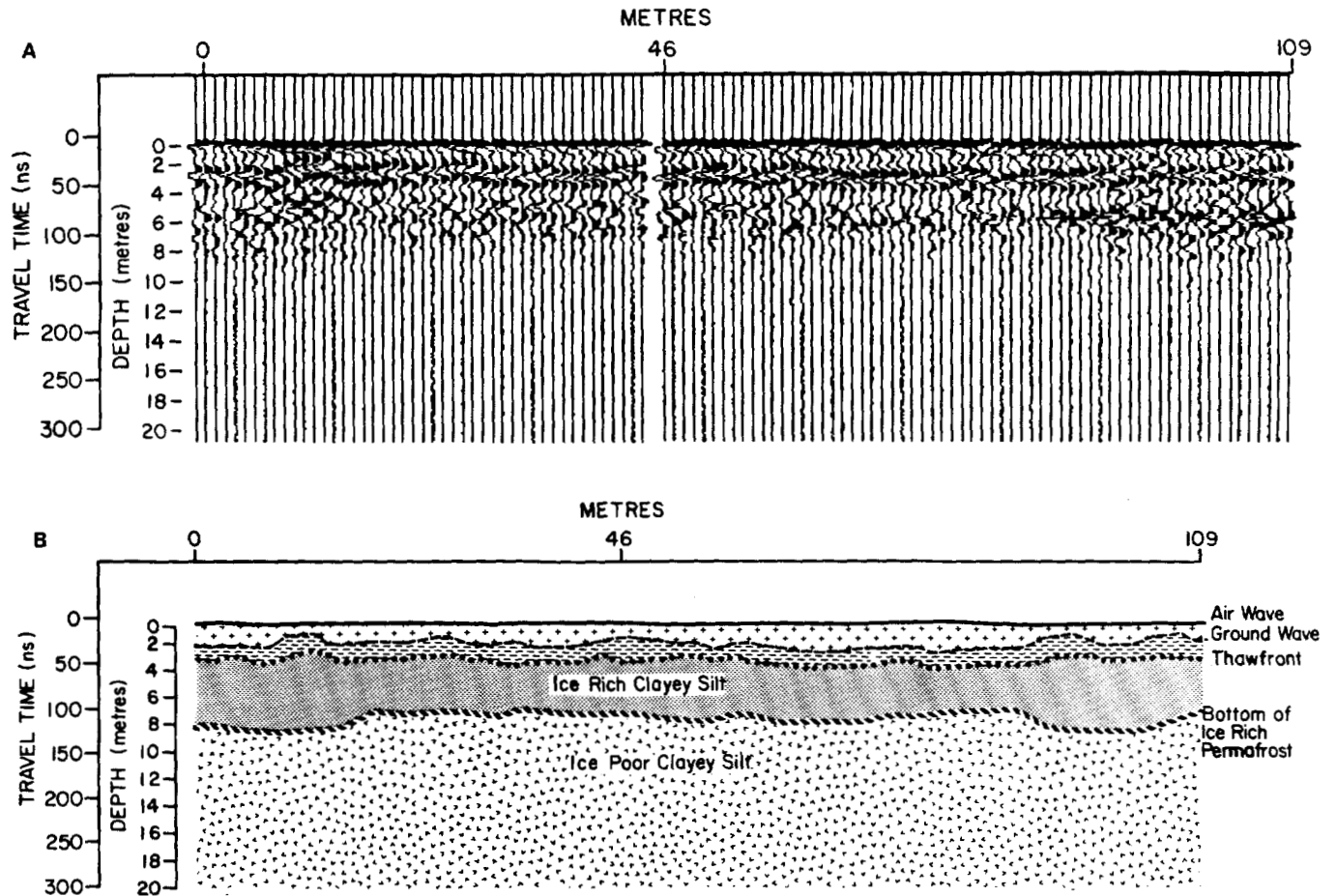


Figure 12A. Ground probing radar profile collected at site 3A in Kangiqsualujjuaq; **B.** Interpretation of the ground probing radar profile at site 3A.

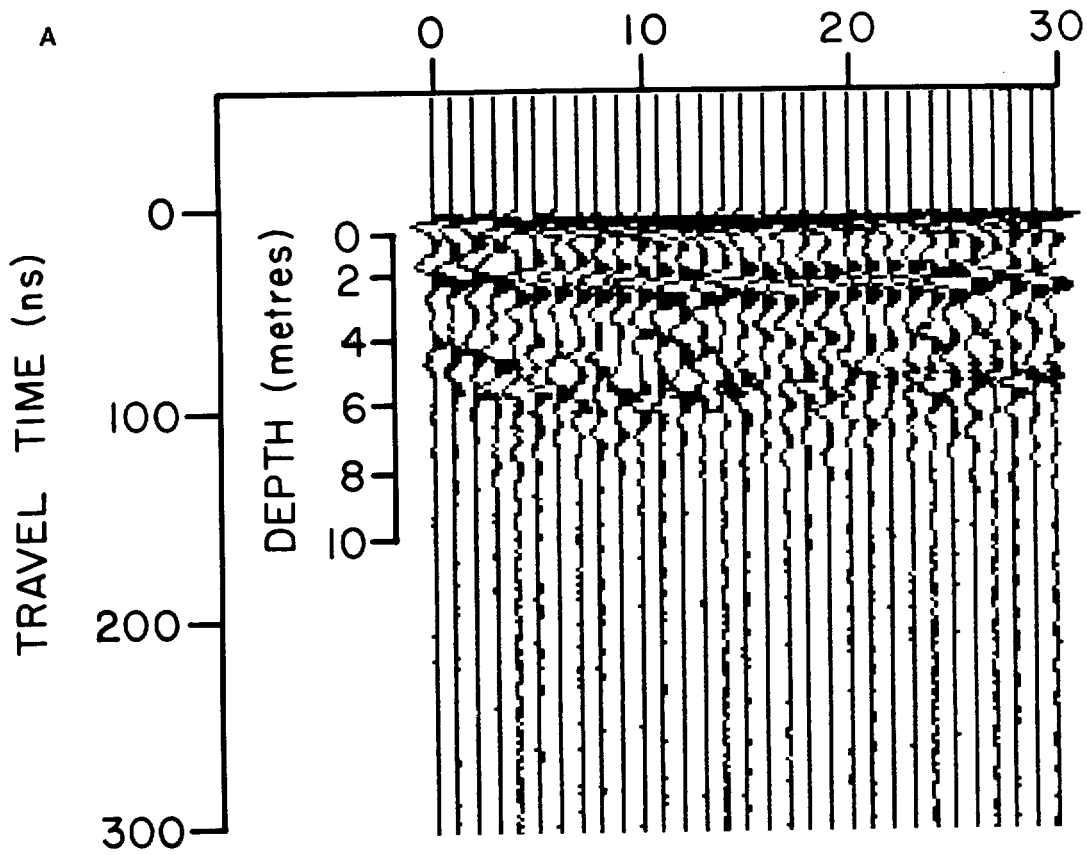


Figure 13.

A. Ground probing radar profile gathered at site 3B in Kangiqsualujjuaq;
 B. Interpretation of the ground probing radar profile at site 3B.

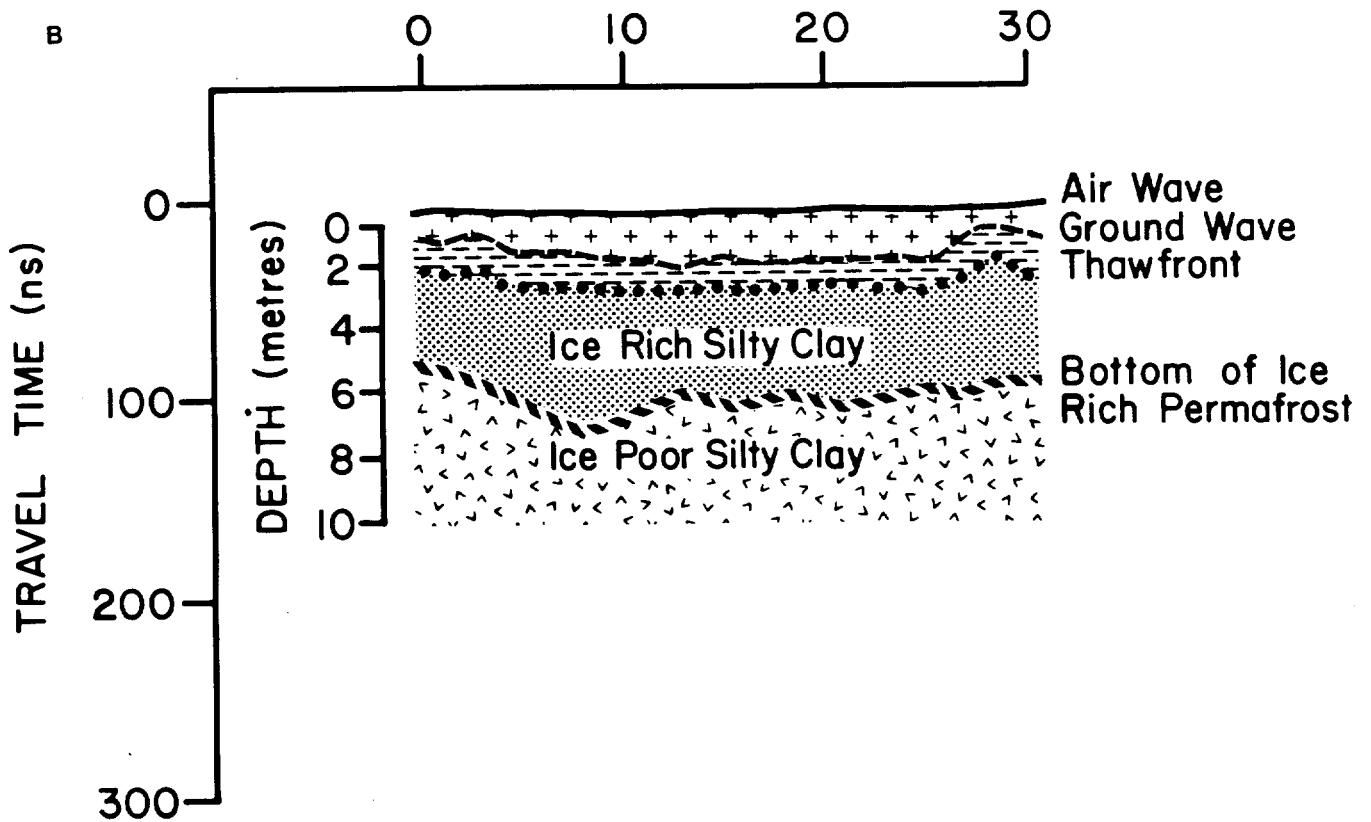




Figure 14. Aerial photograph of Kangiqsualujjuaq bay and surrounding areas. (Sites 3A, 3B and 4 are indicated.)

surficial deposits is irregular and is typical of the stoss and lee topography found in this region as a result of glacial sculpturing. Using the propagation speeds obtained from the CMP survey, Figure 10 shows the interpretation sketch of the results. Between stations 15 and 60, we calculate that bedrock lies on the average beneath 19 m of surficial deposits and reaches 24 m between survey points 60 and 90. The attenuation around 100 ns observed between stations 0 and 15 is caused by a clayey substrate, which masks the underlying material. Elsewhere (90-185 m) along the transect the cause of attenuation beneath the coarse stratified

sediments is uncertain. It could be a fine sediment of unexplained origin, or saline groundwater under the permafrost. The bulk of the unconsolidated deposits consists of stratified glaciofluvial gravelly material and postglacial marine sands and silts with ice rafted boulders. There is a dome-like structure within the glaciofluvial gravel beds interpreted as a buried esker (Fig. 6, 8). The near surface erosional unconformity, created by wave washing during emergence (Fig. 8, 10), occurs between 1.5 and 3 m below the surface. Reworked marine sediments above the unconformity comprise coarse sand and fine gravel.

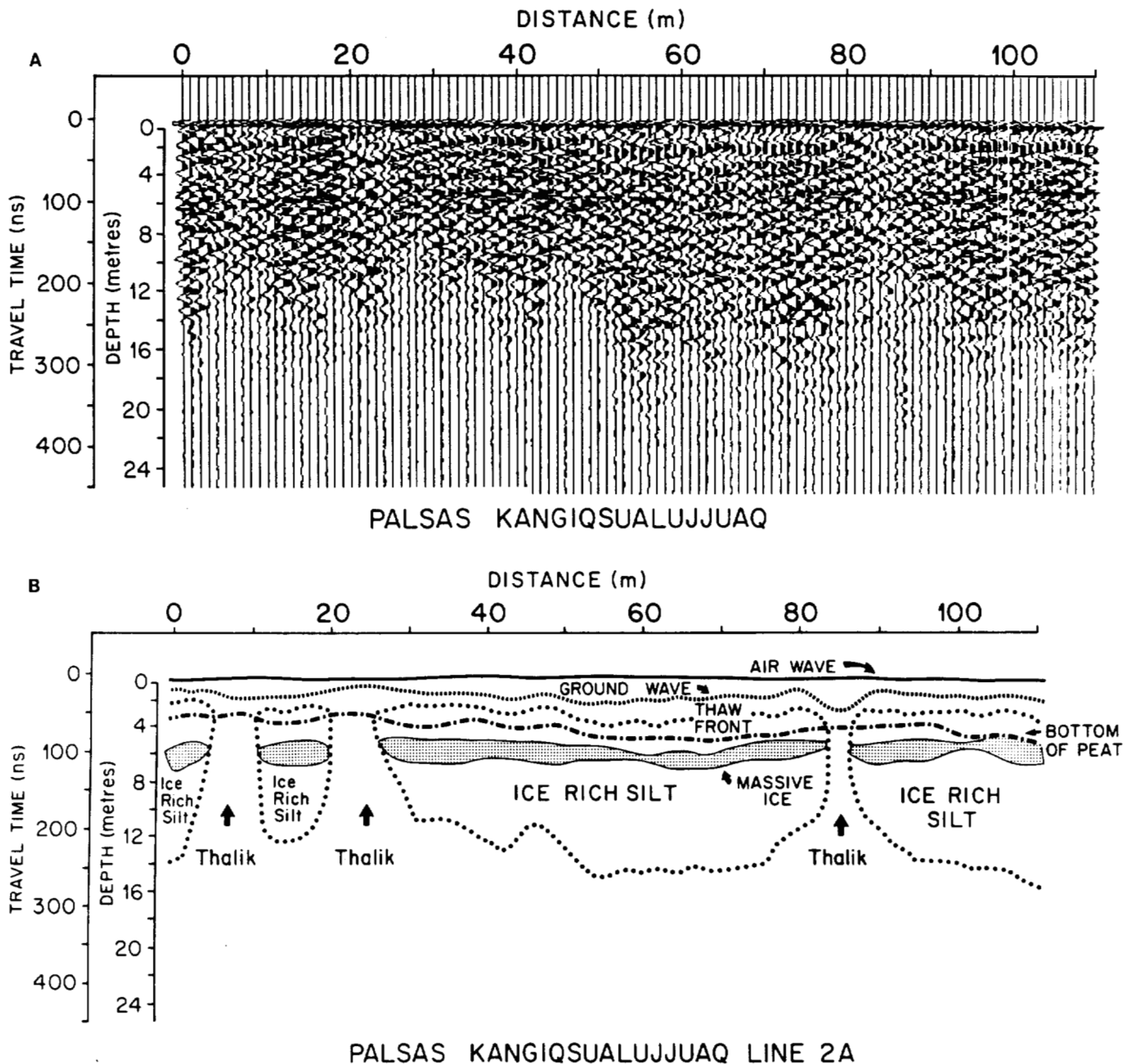


Figure 15A. 100 MHz radar profile of site 4; B. Interpretation of the ground probing radar profile at site 4 in Kangiqsualujjuaq.

The first reflector beneath the surface is the thaw front varying in depth between 1.5 and 2 m (± 50 ns), as confirmed by two thermistor cables along the transect (Bouchard, 1988). An important reflector zone at about 100 ns on (Fig. 6, 8) is interpreted as an ice rich zone corresponding with the coldest permafrost layer observed at about 6 m. An undulating but continuous reflector, which occurs between 200 and 260 ns (12.5 to 15.5 m), cuts stratigraphy and is interpreted to mark the base of permafrost that has been measured with electrical resistivity and induced polarization methods (Séguin and Allard, 1987) to be at about the same depth.

Site 3 consists of two permafrost mounds in marine clay-silt close to the shoreline (Fig. 11): 3A is 2-10 m asl and 3B is less than 5 m asl. Figures 12A and 13A show radar profiles collected on these frost mounds. The clay-silt material is 13-28 m thick as observed in boreholes (Allard et al., 1988). The permafrost thickness, as measured with thermistor cables in the boreholes, is 15 m at site 3A and 9 m at site 3B, which is adjacent to the shoreline. The radar profiles show that radar returns were obtained from the ice rich layers in the upper 3-4 m of the permafrost. Below the ice rich zones, the signal fades away in the saline cryotic clays, as expected from the attenuation coefficients for these materials given in Table 1. Figures 12B and 13B show the interpretation of these two profiles.

Site 4 is a peat plateau located near a lake at 36 m above sea level (Fig. 14). The radar transect, which has been previously used for other geophysical surveys (Gahé and Séguin, 1985; Gahé et al., 1987; Gahé, 1988) cuts across an uneven section of the peat plateau along an axis running southwest. The surface peat varies from a few decimetres to a maximum of 1.1 m in thickness. The peat overlies postglacial marine clays and clay-silt containing ice rafted boulders; a boulder pavement lies at the stratigraphic contact between the peat and the clayey silt. A drillhole in the centre of the plateau a few metres from the survey line revealed a thickness of 24 m of clayey-silt. The near surface layer of the permafrost zone beneath the peat has numerous thick ice lenses adding up to a volumetric ice content of 70% (Gahé et al., 1987). The thickness of frozen ground and the abruptly attenuated radar signal are evident in the unfrozen marine clay sediments in the subpermafrost (Fig. 15A, B). The more massive ice lenses near the surface appear as abundant multilayered reflectors between 50 and 100 ns (4-8 m). From the radar profile, permafrost is interpreted to be thicker beneath the peat mounds and thinner beneath the depressions, and the ice content is lower below the depressions in the peat plateau (e.g., sample points 22-23; 85-86; Fig. 15A, B). The strong reflector around 75 ns represents a thick ice lens. The CMP survey at this site yielded a propagation speed of 8 cm/ns, from which we calculate a maximum permafrost depth of 13 m, which compares favourably with the result of other geophysical surveys along this profile Gahé et al., (1987).

CONCLUSION

As illustrated by the results of the field test conducted in the Kangiqsualujjuaq area, ground probing radar (GPR) is an excellent geophysical tool for the study of permafrost.

GPR has been used successfully to determine the thickness of the thawed zone and of the active layer, to detail the internal stratigraphy of the surficial deposits, and to detect the base of icebearing permafrost. Like all geophysical systems, GPR cannot be used universally and has certain limits imposed on it by the electrical characteristics of fine grained surficial materials, which limit the propagation of a VHF electromagnetic signal. GPR operates most successfully in granular materials, as illustrated by the resolution of sedimentary structures and stratigraphic details at site 2. Even in clayey silts, a material much less favourable for the propagation of the VHF signal, significant geotechnical information can be retrieved on radar profiles, as illustrated at sites 3 and 4 (e.g. the near surface concentration of ground ice). We find that GPR works best in materials less suitable to other geophysical survey systems (e.g., seismic refraction survey method). It is even possible to obtain a general view of the fabric of till layers (site 1). GPR is an important complement to the modern arrays of geophysical methods available to study the internal makeup and permafrost characteristics of unconsolidated materials.

ACKNOWLEDGMENTS

The authors wish to express their gratitude to field assistants: Christian Bouchard, Richard Fortier, Richard Levesque, Jacqueline Bouchard, and Johanne Plourde. They also wish to thank the Inuit community of Kangiqsualujjuaq for their welcome and to Mr. Jean-Guy St-Aubin for his help with recharging and the loan of batteries to power the system. This paper is the result of a collaboration between the Centre d'Études Nordiques of Université Laval and the Geological Survey of Canada. Thank you also to Mrs. J. Barr for typing the manuscript, to A. Rafeek, L. Campbell, and G. MacLeod of the Geophysics Division for drafting the illustrations, and to Richard Delaunais for the photographic work.

REFERENCES

- Allard, M. et Séguin, M.K.
1987: Le pergélisol au Québec Nordique: Bilan et perspectives; *Géographie physique et Quaternaire*, v. XLI, no. 1, p. 141-152.
- Allard, M., Séguin, M.K., and Pelletier, Y.
1988: Shoreline permafrost in Kangiqsualujjuaq Bay, Ungava, Québec; *Proceedings, Fifth International Permafrost Conference*, Trondheim, Norway, v. 1, p. 113-122.
- Annan, A.P.
1983: General state-of-the-art review of ground probing radar; A-Cubed Inc. Report to Earth Physics Branch, Energy, Mines and Resources, March, 1983, 89 p. + Annexes.
- Bouchard, C.
1988: Le régime thermique du pergélisol dans un sol sableux à Kangiqsualujjuaq, Québec Nordique; *Univ. Laval, Dept. Géographie, Mémoire de Baccalauréat*.
- Davis, J.L. and Annan, A.P.
1989: Ground penetrating radar for high-resolution mapping of soil and rock stratigraphy; *Geophysical Prospecting*, v. 37, p. 531-551.
- Fournier, A., Allard, M., et Séguin, M.K.
1987: Typologie morpho-génétique des marelles du marais littoral de la Baie de Kangiqsualujjuaq, estuaire du George, Québec Nordique; *Géographie physique et Quaternaire*, v. XLI, no. 1, p. 47-64.

- Gahé, E.**
1988: Géomorphologie cryogène et géophysique dans la région de Kangiqsualujjuaq; Université Laval, Dept. de Géographie, Thèse de doctorat, 210 p.
- Gahé, E. et Séguin, M.K.**
1985: Géophysique du pergélisol à Kangiqsualujjuaq, Québec Nordique; Annales de l'ACFAS, p. 52-53.
- Gahé, E., Allard, M., et Séguin, M.K.**
1987: Géophysique et dynamique Holocene de plateaux palsiques à Kangiqsualujjuaq, Québec Nordique; Géographie physique et Quaternaire, v. XLI, no. 1, p. 33-46.
- Gahé, E., Allard, M., Séguin, M.K., and Fortier, R.**
1988: Measurements of active layer and permafrost parameters with electrical resistivity, self-potential and induced polarization; Proceedings, Fifth International Permafrost Conference, Trondheim, Norway, v. 1, p. 148-158.
- LaFlèche, P.T., Judge, A.S., and Pilon, J.A.**
1987: Ground probing radar in the investigation of the competency of frozen tailings pond dams; in Current Research, Part A, Geological Survey of Canada, Paper 87-1A, p. 191-197.
- Payette, S.**
1983: The forest tundra and present tree-lines of the northern Quebec-Labrador peninsula; in Tree-line ecology, S. Payette and P. Morisset (ed.); Proceedings, Northern Quebec Tree-line Conference, Nordicana, v. 47, p. 3-24.
- Scott, W.J., Sellmann, P.V., and Hunter, J.A.**
1978: Geophysics in the study of permafrost; Proceedings, Third International Conference on Permafrost, v. 2, p. 93-115.
- Séguin, M.K. and Allard, M.**
1987: La géophysique appliquée au pergélisol du Québec Nordique: historique et développements récents; Géographie physique et Quaternaire, v. XLI, no. 1, p. 127-140.
- Thériault, M.**
1983: Une typologie des régimes climatiques du Québec; Univ. Laval, Ph.D. Thesis, unpublished.
- Wilson, C.**
1971: Le climat du Québec, Atlas climatique du Canada, 1re partie: Ottawa, Service de météorologie.

Deconvolution of ground probing radar data

J.P. Todoeschuck¹, P.T. LaFlèche^{2,3}, O.G. Jensen³,
A.S. Judge⁴, and J.A. Pilon⁴

Todoeschuck, J.P., LaFlèche, P.T., Jensen, O.G., Judge, A.S., and Pilon, J.A., 1992: Deconvolution of ground probing radar data; in Ground penetrating radar, ed. J. Pilon; Geological Survey of Canada, Paper 90-4, p. 227-230.

Abstract

The return signal received in the collection of ground probing radar (GPR) data in layered ground represents the convolution of the emitted wavelet and the reflection sequence for the local geology. Coupling between the transmit and receive antennas and the immediately underlying ground varies considerably from place to place. This variation leads to uncertainty in the precise form of the source wavelet making deterministic deconvolution of the signal impractical. Recent advances in GPR instrumentation have allowed the collection of large volumes of digital data. The close similarity between GPR and reflection seismic data suggests that deconvolution techniques that have been used in the seismic industry could be applied successfully to radar data. Predictive deconvolution allows estimation of the source wavelet from the observed time series. This method involves assuming a model for the reflection sequence. We derive a filter for the scaling noise model, where the power spectrum of the reflection sequence is proportional to some power of the spatial frequency. We show, using recent field data, that deconvolution can enhance the results and resolve additional near surface features.

Résumé

L'écho reçu, selon les données recueillies par géoradar dans un sol stratifié, représente la convolution du signal émis et la séquence de réflexion de la géologie locale. Le couplage des antennes de transmission et de réception avec le sol directement sous-jacent varie considérablement d'un endroit à l'autre. Cette variation crée une incertitude relativement à la forme précise du signal d'origine rendant impossible la déconvolution déterministe du signal. Les perfectionnements récents apportés au géoradar ont permis de recueillir une grande quantité de données numériques. L'étroite similarité entre les données radar et de sismique réflexion indique que les techniques de déconvolution utilisées dans l'industrie sismique pourraient être appliquées avec succès aux données radar. La déconvolution prédictive permet de déterminer le signal source des séries temporelles observées. Cette méthode fait intervenir un modèle de la séquence de réflexion. Un filtre est dérivé pour le modèle du bruit scalant où le spectre de puissance de la séquence de réflexion est proportionnel à une certaine puissance de la fréquence spatiale. À l'aide de données de terrain récentes, on montre que la déconvolution peut améliorer les résultats et permettre de résoudre d'autres éléments proches de la surface.

¹ Defence Research Establishment Pacific, FMO, Victoria, British Columbia V0S 1B0

² Targeted Research Directorate, NSERC, Ottawa, Ontario K1A 1H5

³ Geophysical Research Laboratory, Department of Geology and Geophysics, McGill University, 3450 University Street, Montreal, Québec H3A 2A7

⁴ Geological Survey of Canada, Terrain Sciences Division, 601 Booth Street, Ottawa, Ontario K1A 0E8

INTRODUCTION

Ground probing radar (GPR) has marked similarities to seismic reflection profiling, with electromagnetic replacing acoustic waves. Despite a shallower depth of penetration than seismic methods, GPR has enjoyed wide use in engineering and other applications because of the higher resolution offered by the shorter wavelengths used. The advent of digital data storage has increased the similarities to seismic practice and suggests the use of data processing schemes, which are common there. One of these techniques is deconvolution of the observations. Deconvolution has the effect of removing the character of the emitted pulse or wavelet from the observations, which can allow shaping the pulse for further display. This step is desirable before further processing, such as migration.

The return pulse from an interface is ideally a faithful echo of the transmitted pulse. Additional interfaces will produce additional returns which may very well overlap at the receiver. We can express the returned signal as the convolution of the wavelet with the reflection series representing the reflection coefficients and location of each interface.

If we discretize the wavelet as w_i and the reflection sequence in travel time as r_i then the observations x_i are given by equation (1)

$$x_k = \sum w_i r_{k-i} \quad (1)$$

or

$$x = w * r. \quad (2)$$

We want to use our observations to get the geophysically interesting part of the signal, the reflection sequence. Convolution of the observations with a suitable filter which will remove the effects of the convolution with the wavelet. This process is referred to as deconvolution. An ideal filter would reproduce the reflection sequence exactly. In general our filter will produce an estimate of the reflection sequence, e_i . If the filter is a_i

$$e = x * a. \quad (3)$$

The filter is called the inverse of the wavelet. Now, if we know the wavelet, it is relatively straightforward to calculate its inverse. Use of this inverse can be called deterministic deconvolution. However, if the wavelet is not known, we can still calculate an inverse using the observations and an appropriate statistical model of the reflection sequence by the method of predictive decomposition.

Experience suggests that the waveform in GPR can vary from place to place in both shape and amplitude, perhaps because of the changing coupling with ground of differing electrical properties. This variation suggests

the use of predictive decomposition on GPR traces. Note that this method assumes that the character of the wavelet does not change with depth, for example from dispersion. If dispersion is a problem, it will be necessary to break up the observations into shorter sequences over which the change is small.

PREDICTIVE DECOMPOSITION

The statistical measure that we focus on is the power spectrum of the reflection sequence, which we take to be known a priori. Knowing the power spectrum is equivalent to knowing the autocorrelation function (ACF). If the ACF of the observations is R_m then

$$m = E\{x_k x_{k-m}\} \quad (4)$$

where E denotes the expectation operator.

Assuming for a moment that we have an infinite amount of data, the output of our filter will be

$$e_k = \sum a_n x_{k-n} \quad (5)$$

and the ACF Y_j of the output is

$$Y_j = \sum a_m \sum a_n R_{m+j-n} \quad (6)$$

(Silvia and Robinson, 1979).

Suppose that the reflection sequence has only a few nonzero Y_j 's, say for $0 \leq j \leq J$. (The reason for this will be explained below.) If

$$\sum a_n R_{p-n} = 0, \quad p > J, \quad (7)$$

then from equation 6, the condition on the Y_j 's for $j > J$ will be satisfied, i.e., they will equal zero. Now consider the last nonzero term, Y_J . We will normalize our filter so that $a_0 = 1$. Then, using equation 7, we see from equation 6

$$\sum a_n R_{J-n} = Y_J. \quad (8)$$

Likewise

$$Y_{J-1} = \sum a_n R_{J-1-n} + a_1 \sum a_n R_{J-n} \quad (9)$$

so

$$\sum a_n R_{J-1-n} = Y_{J-1} - a_1 Y_J \quad (10)$$

and so on for the remaining nonzero terms. This process gives us a full set of equations, known as the normal equations, for the filter coefficients based on the ACFs of the observations and the model reflection sequence (Todeschuck and Jensen, 1988).

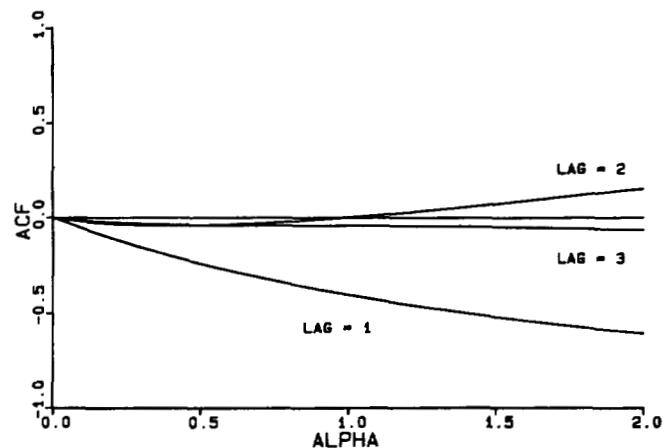


Figure 1. Variation with α of the lag = 1, 2, 3 terms of the autocorrelation function of an f^α process.

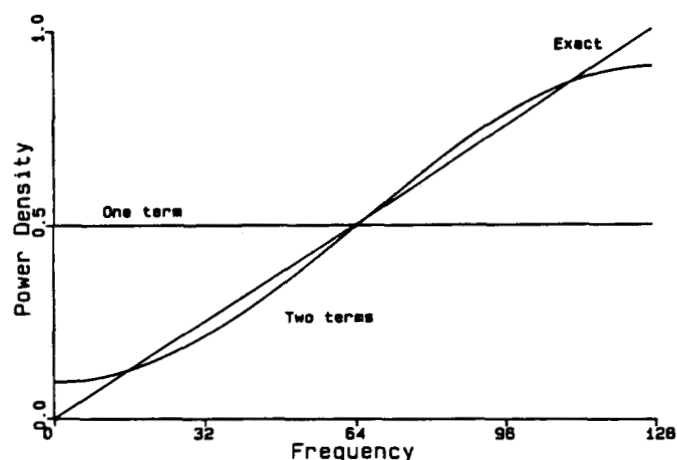


Figure 2. Power spectra obtained by keeping one term and two terms in the autocorrelation function of compared with the exact spectrum for $\alpha = 1$. (Frequency in arbitrary units).

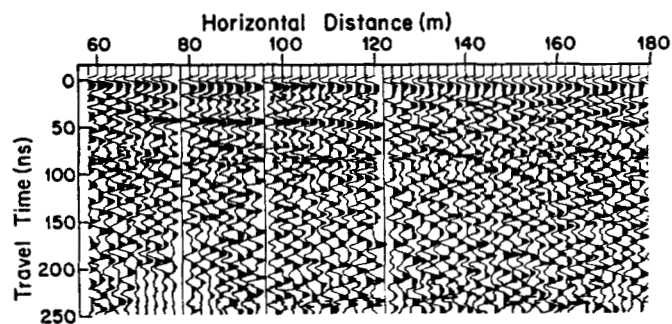


Figure 3. Portion of undeconvolved GPR profile of dam; near surface features are lost in the air and ground waves.

We must now select a model or at least a group of models for our reflection sequence. One class, which has been of great interest for seismic reflection sequences, is that of the scaling noises. A scaling noise is a random sequence with many interesting properties but the important one for us is that its power spectrum P is proportional to some power of frequency f , that is,

$$P \propto f^\alpha \quad (11)$$

where α is a real number. The power spectra of seismic reflection sequences have been found to be well characterized by equation 11 with $\alpha \approx 1$ (Walden and Hosken, 1985; Todeschuck et al., 1989). When $0 \leq \alpha \leq 2$, the ACF dies away quickly for long lags. Figure 1 shows the magnitude of the ACF at the first few lags for this range of α . (Remember that the ACF at lag = 0 is unity.) As can be seen for $\alpha = 0$ (white noise) the ACF = 0 at all nonzero lags. The lag = 1 term grows much more quickly than the others, with the lag = 2 term becoming significant only for $\alpha > 1.5$, which suggests truncating the ACF at two terms. The result in terms of the power spectrum is shown (Fig. 2) for the case $\alpha = 1$. The exact spectrum is the result of Fourier transforming all the terms in the ACF. Taking one term in the ACF corresponds to a white spectrum, the horizontal line through the average. Taking one more term greatly improves the fit, which adding additional terms only slightly improves.

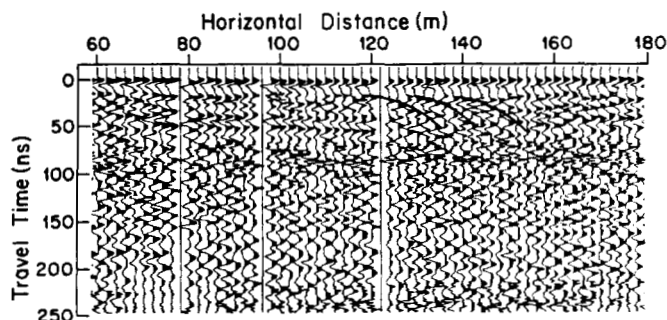


Figure 4. The profile of Figure 3 deconvolved with $\alpha = 0$ and then reconvolved with a half sine for direct comparison; note the near surface layering between 80 and 120 m and the three hyperbolic reflections discussed in the text.

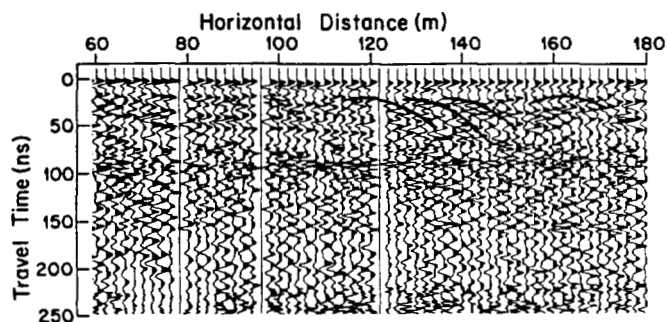


Figure 5. The profile of Figure 3 deconvolved with $\alpha = 1$ and then reconvolved with a half sine for direct comparison; an additional hyperbolic reflector is now discernable.

The normal equations for a two term ACF become

$$\sum a_n R_n = Y_0 - a_1 Y_1,$$

$$\sum a_n R_{1-n} = Y_1,$$

and

$$\sum a_n R_{p-n} = 0, p \geq 2. \quad (12)$$

In all practical cases, we will be interested in obtaining a filter of finite length, $L + 1$, say, so we can write equation 12 in matrix form as

$$\begin{array}{cccccc} R_0 & R_1 & \dots & R_L & a_0 & Y_0 - a_1 Y_1 \\ R_1 & R_0 & \dots & R_{L-1} & a_1 & Y_1 \\ \cdot & \cdot & \cdot & \cdot & \cdot & = 0 \\ \cdot & \cdot & \cdot & \cdot & \cdot & \cdot \\ R_L & R_{L-1} & \dots & R_0 & a_L & 0 \end{array} \quad (13)$$

The matrix is Toeplitz in form, which offers advantages in the solution. Our technique is to assume $Y_1 = 0$, solve for the filter coefficients, use these to calculate Y_0 which, for a given value of α gives us Y_1 , and iterate. A small number of iterations is typically needed.

EXAMPLE

In 1986, a GPR survey was carried out over dam 1A at Lupin Mine near Contwoyto Lake, N.W.T., Canada (LaFlèche et al., 1987). The dam is 250 m long and 7 m high. It was constructed of a silty-sandy fill above graded overburden, with an added 2 m of gravelly sand. Bedrock outcrops at the ends of the dam but is 20 m below the top of the overburden near the centre. The dam leaks, probably because of the presence of unfrozen zones. The survey used an A-Cubed Inc. pulseEKKO III radar with 100 MHz centre frequency. The sampling interval was 800 ps. Figure 3 shows the undeconvolved results from a portion of the survey in a positive-shaded display. The data were filtered to remove any low frequency drift in the traces and automatic gain to a maximum multiplication of 300 was applied trace by trace.

For the deconvolution method outlined above to be fully exploited it is necessary to know the value of parameter α . In the case of seismograms, it was possible to use sonic logs to estimate α . Unfortunately the same has not been done for the variations in dielectric and conductivity properties causing the reflections in the radar case. It is hoped that core logs may indicate of the proper range of α . It may also be possible to determine α directly from the trace. We initially assume $\alpha = 0$ and produce a reflection sequence. We estimate a value of α from its power spectrum and deconvolve the observations using this new value, iterating as necessary. This technique has shown promising results with seismograms. Meanwhile, it is possible to proceed by taking the values $\alpha = 0$ and $\alpha = 1$. The first value gives the well known prediction error filter (Robinson, 1957) and corresponds to assuming a white power

spectrum. There are two ways of looking at this. First, if you know nothing about a spectrum, drawing a horizontal line is the least damaging assumption (Fig. 2). Alternatively, it is equivalent to truncating the ACF at one term. The value $\alpha = 1$ has been found useful in the seismic case.

Figure 4 shows the data deconvolved with the prediction error filter (PEF) trace by trace. Now, the deconvolved reflection sequence consists of a series of numbers and can be transferred to, say, a migration algorithm in that form. They can also be displayed as a series of lines proportional to their value, but we have found this output to be hard to interpret. We have therefore reconvolved the sequence with a half-sine operator of known amplitude and wavelength. This display is comparable to the original. Several features, which were not clearly seen, are now evident in the near surface between 0 and 100 ns. In the interval from 65 to 100 m along the profile, several closely spaced reflecting horizons are now resolved. We interpret these horizons as layering in the uppermost gravelly sand fill. Three shallow hyperbolic reflectors can be seen from 100 to 150 m. They are obscured by the air and ground arrivals in the original data. We know that four culverts were buried 1 m deep between 100 and 168 m. Deconvolution of the data with $\alpha = 1$ yields somewhat improved results (Fig. 5). Four hyperbolic reflectors, which we interpret as the four culverts, can now be seen. It may be that better estimates of α would lead to even better results.

CONCLUSION

In the field of reflection seismology deconvolution has been an important, if not essential step in such things as migration, attenuation, or interpretation of reflection coefficients. The same will probably be true in the processing of digital GPR data. As the example shows, it is also useful for what is in effect shaping the radar pulse. Here we have shortened the pulse and removed any tail. The additional resolution obtained may well be useful, particularly for faint or closely spaced features such as may occur in the nearsurface region.

REFERENCES

- LaFlèche, P.T., Judge, A.S. and Pilon, J.A.
1987: Ground probing radar investigation of the competency of frozen tailings pond dams; in Current Research, Part A, Geological Survey of Canada, Paper 87-1A, p. 191-197.
- Robinson, E.A.
1957: Predictive decomposition of seismic traces; *Geophysics*, v. 22, p. 767-778.
- Silvia, M.T. and Robinson, E.A.
1979: Deconvolution of Geophysical Time Series in the Exploration for Oil and Gas; Elsevier Scientific Publishing Co., Amsterdam, 251 pp.
- Todoeschuck, J.P. and Jensen, O.G.
1988: Joseph geology and seismic deconvolution; *Geophysics*, v. 53, p. 1410-1414.
- Todoeschuck, J.P., Jensen, O.G. and Labonte S.
1989: Gaussian scaling noise models of seismic reflection sequences: evidence from well logs; *Geophysics*, v. 55, p. 480-484.
- Walden, A.T. and Hosken, J.W.J.
1985: An investigation of the spectral properties of primary reflection coefficients. *Geophysical Prospecting*, v. 33, p. 400-435.